pmod wrc

Annual Report
Jahresbericht 2019

Physikalisch-Meteorologisches Observatorium Davos und Weltstrahlungszentrum

Mission

Das PMOD/WRC

- dient als internationales Kalibrierzentrum für meteorologische Strahlungsmessinstrumente
- entwickelt Strahlungsmessinstrumente für den Einsatz am Boden und im Weltraum
- erforscht den Einfluss der Sonnenstrahlung auf das Erdklima.

Auftragerteilung

Das Physikalisch-Meteorologische Observatorium Davos (PMOD) beschäftigt sich seit seiner Gründung im Jahr 1907 mit Fragen des Einflusses der Sonnenstrahlung auf das Erdklima. Das Observatorium schloss sich 1926 dem Schweizerischen Forschungsinstitut für Hochgebirgsklima und Medizin Davos an und ist seither eine Abteilung dieser Stiftung. Auf Ersuchen der Weltmeteorologischen Organisation (WMO) beschloss der Bundesrat im Jahr 1970 die Finanzierung eines Kalibrierzentrums für Strahlungsmessung als Beitrag der Schweiz zum Weltwetterwacht-Programm der WMO. Nach diesem Beschluss wurde das PMOD beauftragt, das Weltstrahlungszentrum (World Radiation Center, WRC) zu errichten und zu betreiben.

Kerntätigkeiten

Das Weltstrahlungszentrum unterhält das Primärnormal für solare Bestrahlungsstärke bestehend aus einer Gruppe von hochpräzisen Absolut-Radiometern. Auf weitere Anfragen der WMO wurden 2004 das Kalibrierzentrum für Messinstrumente der atmosphärischen Langwellenstrahlung eingerichtet und 2008 das Kalibrierzentrum für spektrale Strahlungsmessungen zur Bestimmung der atmosphärischen Trübung. Seit 2013 wird auch das Europäische UV Kalibrierzentrum durch das Weltstrahlungszentrum betrieben. Das Weltstrahlungszentrum besteht heute aus vier Sektionen:

- Solare Radiometrie (WRC-SRS)
- Infrarot Radiometrie (WRC-IRS)
- Atmosphärische Trübungsmessungen (WRC-WORCC)
- UV Kalibrierzentrum (WRC-WCC-UV)

Die Kalibriertätigkeit ist in ein international anerkanntes Qualitätssystem eingebettet (ISO 17025) um eine zuverlässige und nachvollziehbare Einhaltung des Qualitätsstandards zu gewährleisten.

Das PMOD/WRC entwickelt und baut Radiometer, die zu den weltweit genauesten ihrer Art gehören und sowohl am Boden als auch im Weltraum eingesetzt werden. Diese Instrumente werden auch zum Kauf angeboten und kommen seit langem bei Meteorologischen Diensten weltweit zum Einsatz. Ein globales Netzwerk von Stationen zur Überwachung der atmosphärischen Trübung ist mit vom Institut entwickelten Präzisionsfilterradiometern ausgerüstet.

Im Weltraum und mittels Bodenmessungen gewonnene Daten werden in Forschungsprojekten zum Klimawandel und der Sonnenphysik analysiert. Diese Forschungstätigkeit ist in nationale, insbesondere mit der ETH Zürich, und internationale Zusammenarbeit eingebunden.

Das PMOD/WRC ist eine Abteilung der Stiftung
Schweizerisches Forschungsinstitut für
Hochgebirksklima und Medizin in Davos.

Physikalisch-Meteorologisches Observatorium Davos
und World Radiation Center (PMOD/WRC)
Dorfstrasse 33, 7260 Davos Dorf
Schweiz
Tel. +41 (0)81 417 51 11, www.pmodwrc.ch

pmod wrc

Annual Report
Jahresbericht 2019

Table of Contents

Jahresbericht 2019

Louise Harra

Im Jahr 2019 kam es im Physikalisch-Meteorologischen Observatorium Davos und Weltstrahlungszentrum (PMOD/WRC) zu einem Führungswechsel von Prof. Dr. Werner Schmutz zu Prof. Dr. Louise Harra, die am 1. Juni 2019 als neue Direktorin antrat (Figur 1). Werner Schmutz leitete das PMOD/WRC über einen Zeitraum von mehr als 19 Jahren, in dem sich die Mitarbeiterzahl verdoppelte und neue Schlüsseldienste für das World Radiation Center entwickelt wurden.

Im November 2019 wurden die Beiträge von Dr. Werner Schmutz an die Wissenschaft, das PMOD/WRC und die internationale Gemeinschaft mit einem Symposium geehrt. Die Teilnahme am Treffen war hoch, der Seminarraum gut besetzt und in zahlreichen Videobotschaften von überall aus der Welt wurden Werners Leistungen über all die Jahre verdankt.

In der Woche vor diesem Anlass wurde auf der ESA-Ministerkonferenz bekannt gegeben, dass die Weltraummission TRUTHS (Traceable Radiometry Underpinning Terrestrial and Helio Studies) in eine nächste Etappe gehen soll. Das PMOD/WRC ist aufgrund der Zusammenarbeit mit dem britischen National Physical Laboratory (UK) durch den Cryogenic Solar Absolute Radiometer schon seit Jahren in dieses Projekt involviert. Dieses Instrument wird voraussichtlich die neue Weltstrahlungsreferenz für Direktstrahlungsmessungen und wird künftig die aktuelle World Standard Group ersetzen.

In den letzten Jahren fanden verschiedene Gespräche statt, um das PMOD/WRC stärker an die Universität zu binden. Dieses Ziel konnte mit der neuen Direktorin erreicht werden, denn Louise Harra wurde im März 2019 von der Schulleitung der ETH Zürich zur affiliierten Professorin am Institut für Teilchenphysik und Astrophysik (IPA) ernannt. Die neue Zusammenarbeit ist erfreulich angelaufen und die weitere Partnerschaftsplanung ist auf gutem Weg. Der Fokus liegt dabei auf der Zusammenarbeit mit Studenten und im Technologiebereich. Die Zusammenarbeit zwischen dem PMOD/WRC und der ETH Zürich ist auch in der Strategie des PMOD/WRC festgehalten.

Das PMOD/WRC stützt seine künftige Tätigkeit auf folgende Kernbereiche:

- Weltstrahlungszentrum: Internationales Kalibrierungszentrum für meteorologische Strahlungsmessgeräte und Entwicklung von Strahlungsinstrumenten für Messungen am Boden und im Weltraum.
- Weltraumprojekte: Entwicklung von Instrumenten zur Bildgebung und Strahlungsmessung der Sonne.
- Technologie: Mitwirkung bei der Konzeption und Entwicklung von Instrumenten für Boden und Weltraum.
- Klimawissenschaft: Erforschung des Einflusses der Sonnenstrahlung auf das Erdklima.
- Solarwissenschaft: Erforschung der Ursachen der Sonnenaktivität.
- Lehre: Kursangebote auf verschiedenen Stufen der ETH-Zürich.

2019 brachte verschiedene Schlüsselerfolge. Hier ein paar der Höhepunkte:

- Das Weltraum-Instrument JTSIM-DARA wurde nach China ausgeliefert und dort im Dezember 2019 kalibriert.
- Das Pyrheliometer PM06-0401 wurde erfolgreich aktualisiert und in den USA getestet.
- Ein neuer Flachsensor für Solarradiometer wurde mit Davos Instruments entwickelt.
- Drei Präsizionssolarspektroradiometer wurden in Betrieb genommen.
- Das PMOD/WRC wurde zur offiziellen Stelle für den Unterhalt und Betrieb der weltlängsten Ozonzeitreihe (TCO) ernannt.
- Zwei neue «Calibration and Measurement Capabilities» (CMCs) der spektralen Sonneneinstrahlungsempfindlichkeit wurden genehmigt.
- Der Test der Raumsonde «Solar Orbiter» wurde abgeschlossen die Sonde zum Kennedy Space Center transportiert.
- Eine betriebsfertige Version des Atmosphäre-Ozean-Aerosol-Chemie-Klimamodells SOCOLv4 wurde erarbeitet und mit Hilfe des nationalen Hochleistungsrechenzentrums (CSCS) und das Linux-Cluster Euler an der ETH Zürich (mit der Gruppe Atmosphärenchemie der ETH Zürich geteilt) getestet.
- Die Zusammenarbeit mit der ETH ist gestartet, sowohl im Bereich der Lehre als auch der technischen Zusammenarbeit.

Einige der Erfolge sind nachfolgend bildlich in den Figuren 2 und 3 dargestellt.

Werfen wir einen Blick auf unsere künftigen Aufgaben, so werden diese von der Inbetriebnahme des Solar Orbiters und wissenschaftlicher Tätigkeit geprägt sein. Wir sind an mehreren künftigen Weltraummissionen beteiligt: an TRUTHS-Missionen, der japanischen Solar-C Mission und der ESA-Weltraumwettermission Lagrange, deren Start für 2026 geplant ist.

Im Jahr 2020 finden der Internationale Pyrheliometer Vergleich und der damit verbundene Internationale Pyrgeometer Vergleich sowie Filter Radiometer Vergleich statt – internationale Vergleiche, die alle 5 Jahre stattfinden und zu denen über 100 Teilnehmer aus aller Welt nach Davos reisen, um ihre Messgeräte zu kalibrieren. 2020 beginnt auch ein neuer Kurs am Departement Physik der ETH Zürich und die Zusammenarbeit mit der ETH wird weiter ausgebaut. Es gibt vieles, worauf wir uns in den kommenden Jahren freuen können. Wir haben für den Zeitraum 2020 - 2024 eine Strategie erarbeitet, die als separates Dokument erhältlich ist.

Ich möchte die Gelegenheit nutzen, um Werner sowie allen Institutsmitarbeitenden für die freundliche Hilfe und Unterstützung zu danken, die ich für den Start in meiner neuen Funktion und in einem neuen Land erfahren durfte. Bereits vor Arbeitsbeginn konnte ich bei meiner Einarbeitung in ein neues System, mit neuen Geräten, neuen Abläufen und neuen Menschen auf die konstruktive Hilfe und Unterstützung seitens des Stiftungsrates und der Aufsichtskommission zählen. Ich danke meinen neuen Kollegen an der ETH für die geduldige Beantwortung all meiner Fragen und ihre Offenheit zur weiteren Zusammenarbeit.

Figure 1. The handover ceremony of the PMOD/WRC directorshop from Prof. Werner Schmutz (front left) to Prof. Louise Harra (front centre) was marked by the handover of the institute's key on 5 June 2019. Dr. Walter Ammann (front right), President of the Schweizerisches Forschungsinstituts für Hochgebirgsklima und Medizin (SFI), greeted Prof. Harra on behalf of the SFI board.

Introduction

Louise Harra

During the year 2019, the directorship of Physikalisch-Meteorologisches Observatorium Davos and World Radiation Center (PMOD/WRC) went through a transition from the leadership of Prof. Dr. Werner Schmutz to that of Prof. Dr. Louise Harra who started on 1 June 2019 (Figure 1). Werner led PMOD/WRC over a period of more than 19 years, that saw the staff numbers double, and the development of new key services for the World Radiation Center.

In November 2019, a symposium was held to celebrate Werner's contributions to science, PMOD/WRC and the international community. The meeting was well attended with a full seminar room, supplemented by video messages from around the world to thank Werner for his endeavours over the years. At the ESA ministerial, just the week before this event, it was announced that the TRUTHS space mission (Traceable Radiometry Underpinning Terrestrial and Helio studies) was selected to go to the next stage. PMOD/WRC's involvement in this has been over many years of collaboration with the National Physical Laboratory (UK) through the Cryogenic Solar Absolute Radiometer. This instrument will likely become the new World Radiometric Reference for direct normal irradiance measurements and will replace the currently used World Standard Group in the future.

For the previous few years, there have been discussions on how to have a stronger link with PMOD/WRC and a university. This collaboration was successfully achieved with the new directorship being an affiliated professor at ETH-Zürich, Institute for Particle Physics and Astrophysics (IPA). In March 2019, the ETH board approved Louise Harra as an affiliated professor at ETH. This is a new collaboration and has started positively. The planning of the partnership is well underway. The main areas of collaboration are through students and technology. The future strategy of PMOD/WRC includes the cooperation between PMOD/WRC and ETH-Zürich.

The six core areas that PMOD/WRC will undertake are:

- World Radiation Center: serve as an international calibration center for meteorological radiation instruments and develops radiation instruments for use on the ground and in space.
- Space projects: develop instruments for imaging and radiation measurements of the Sun.
- Technology: underpin the design and development of the instruments for ground and space.
- Climate science: Research the influence of solar radiation on Earth's climate.
- Solar Science: research the causes of solar activity.
- Teaching: carry out teaching at different levels at ETH-Zürich.

Figure 2. From top left to bottom right: the development of the new PFR, calibration of the JTSIM-DARA radiometer in China, the TRUTHS mission (UKSA/NPL), the arrival of the Solar Orbiter spacecraft in Kennedy Space Center (NASA/ESA), Proba-3 DARA seeing first light, IR cloud camera being installed in Geneva, a book on the impact of extreme solar particle storms co-authored by Eugene Rozanov and Timofei Sukhodolov, the symposium held for Werner Schmutz, the development of the climate model SOCOLv4, the shipping of the JTSIM-DARA instrument to China.

Figure 3. The Digital Absolute Radiometer (DARA), designed and constructed at PMOD/WRC, is a payload onboard the ESA PROBA-3 satellite mission, which will be launched in the near future. The picture shows the DARA EQM/FS (Engineering Qualification Model/Flight Spare) in the foreground (center right), mounted on the WRC main solar tracker during calibration at PMOD/WRC.

There have been many key successes during 2019. Here are a few highlights:

- The JTSIM-DARA instrument was delivered to China and calibration carried out in China in December 2019.
- The pyrheliometer PM06-0401 was successfully upgraded and tested in the USA.
- A new flat-surface sensor for the Solar Radiometers was developed with Davos Instruments.
- Three precision solar spectroradiometers were put into operation.
- PMOD/WRC became officially responsible for the maintenance and operation of the world's longest total column ozone time-series.
- Two new Calibration and Measurement Capabilities (CMCs) on spectral solar irradiance responsivity were approved.
- The Solar Orbiter spacecraft testing was completed, and it was transported to the Kennedy Space Center.
- An operational version of the ocean-atmosphere-aerosol-chemistry-climate model SOCOLv4 was prepared and tested using the national supercomputer centre (CSCS) and the Euler Linux cluster at ETH Zürich (shared with Atmospheric Chemistry Group at ETH Zürich).
- The collaboration with ETH is underway including teaching and technical collaborations.

A selection of some of the successes is shown in Figures 2 and 3.

Looking to the future, we will be working on commissioning of Solar Orbiter and the science. We are involved in several future space missions: TRUTHS missions, the Japanese Solar-C mission and in the ESA space weather mission Lagrange which is due to be launched in 2026.

In 2020 the International Pyrheliometer Comparison and affiliated International Pyrgeometer comparison and Filter radiometer comparison campaigns take place. This happens every 5 years and has more than 100 international attendees calibrating their instruments here. A new course at ETH-physics will begin in 2020, and the collaboration with ETH will develop. There is a lot to look forward to in the coming years. We have developed a strategy for 2020-2024 which is available as a separate document.

I would like to take this opportunity to thank Werner and all the staff at the institute for their friendly support and help in settling into a new job, and a new country. It was also clear from even before I started the job that the board of trustees and the supervisory commission would provide constructive and supportive advice as I learn about a different system, new instruments, new procedures and new people. I would like to thank my new colleagues at ETH -Zürich for patiently providing answers to many questions, and being open to future collaborations.

Operational Services

Quality Management System, Calibration Services

Ricco Soder, Wolfgang Finsterle, and Julian Gröbner

Calibration and Measurement Capabilities (CMCs)

After acceptance of 2 additional CMCs, PMOD/WRC now has 8 different CMCs which are listed in the KCDB of BIPM. These include:

- Responsivity, solar irradiance pyranometer (1)
- Responsivity, solar irradiance pyrheliometer (1)
- Responsivity, solar irradiance broadband detector (4)
- Responsivity, solar spectral irrad. solar spectroradiometer (2)

Depending on the instrument's wavelength range the CMCs belong to different WRC calibration sections.

Organisation and Human Resources

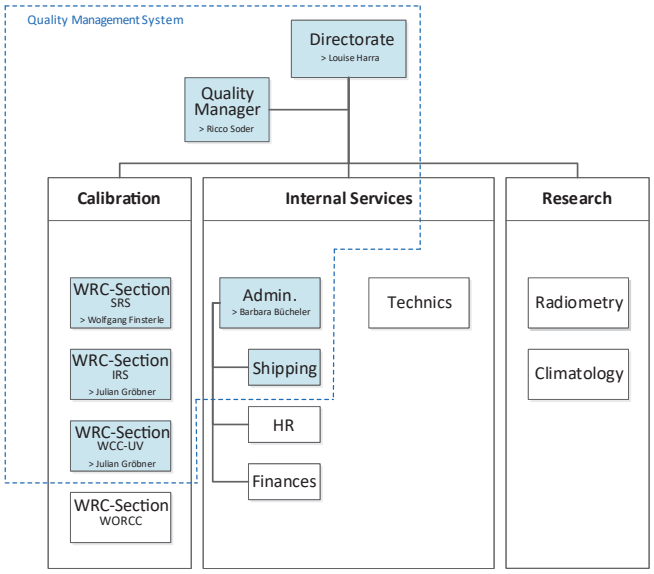

Figure 1. PMOD/WRC Quality Management System (QMS) - Organisational chart. The WRC Solar Radiometry Section (SRS), the WCC-UV and the WRC-IRS sections (in blue), perform calibrations according to EN ISO/IEC standard 17025.

In her role as director of PMOD/WRC, Louise Harra takes over the main responsibility for the Quality Management of all WRC-sections (Figure 1). Ricco Soder was appointed as Quality Manager and Silvio Koller as its deputy in December 2019.

Activities

The transition process which will end with implementation of the revised ISO standard (17025:2018) has started but could not be fully completed in 2019. QM related documentation of all WRC-sections was continuously updated throughout the year. Beside the participation of the mandated inter-laboratory comparisons, two of our WRC-sections were assessed by external experts. The outcome of these audits was very positive and will support the continuous improvement process. Training of staff was performed in accordance to a Section-specific training schedule.

Calibration Services

The overall number of calibrations in 2019 was 208 within the different WRC calibration sections, and is similar to the long-term average shown in Figure 2.

Solar Radiometry Section (WRC-SRS)

The WRC-SRS section calibrated 22 pyrheliometers and 98 pyranometers. Due to a discrepancy regarding the stated level of uncertainty, only 15 pyrheliometer certificates were issued with the CIPM logo. Ricco Soder started in April as a new member of the technical personnel within the science department. The WRC-IRS participated in the National Pyrheliometer Comparison, NPC-2019, at the National Renewable Energy Laboratory (NREL) in Golden, Colorado, USA (Figure 3).

Infrared Radiometry Section (WRC-IRS)

The WRC-IRS section performed 25 pyrgeometer calibrations in 2019. IRIS radiometers and the Absolute Cavity Pyrgeometer (ACP) performed simultaneous measurements alongside the WISG on 20 cloud-free nights between March and September 2019 (Figure 4).

Atmospheric Turbidity Section (WRC-WORCC)

The WRC-WORCC calibrated 17 Precision Filter Radiometers (PFR) against the WORCC Triad standard. In addition, five Precision Solar Spectroradiometers (PSR) were calibrated against a reference standard, traceable to the German National Metrology Institute (PTB).

World Calibration Center for UV Section (WRC-WCC-UV)

The WCC-UV section calibrated 18 UVB broadband radiometers and issued 59 certificates. The certificates typically cover different units. Furthermore, this section performed five lamp/diode calibrations and 18 spectrometers were calibrated against the QASUME travelling reference. These calibrations resulted in 23 certificates, 18 of them with the CIPM logo.

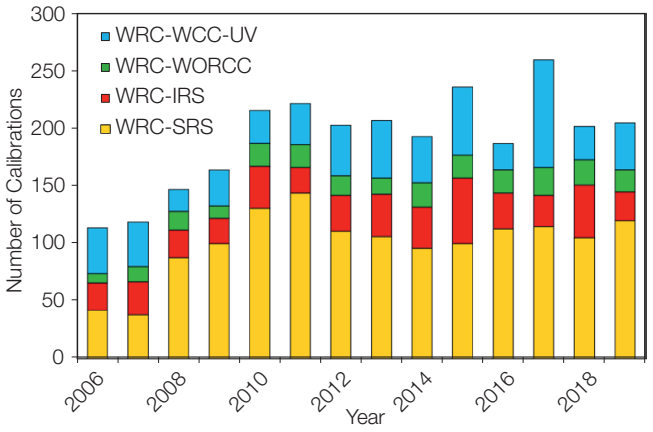

Figure 2. Statistics of instrument calibrations at PMOD/WRC for the 2006 - 2019 period. Remark: One instrument can result in more than one calibration certificate.

Figure 3. View of the NPC-2019 campaign in Golden, Colorado, USA. Image credit: NREL.

Figure 4. Installation of the NREL ACP (foreground) and three IRIS radiometers on the PMOD/WRC measurement platform by C. Thomann.

Instrument Sales

In 2019, PMOD/WRC sold the following instruments:

- Five PMO6-CC absolute radiometers to:

  Peru
  Japan
  India
  Hungary.

- Five Ventilated Heating Systems (VHS) to Germany.

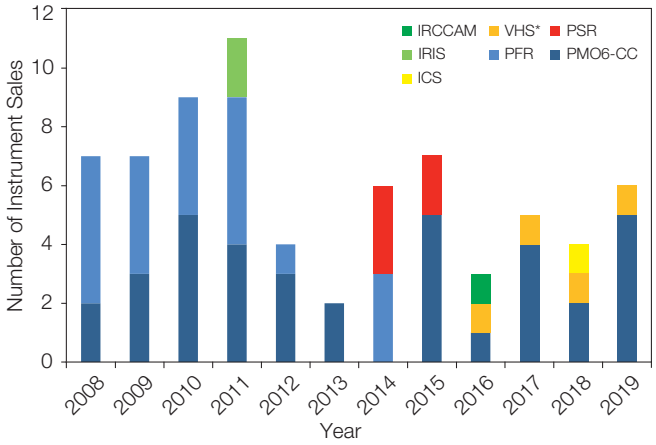

Figure 5. Number of PMOD/WRC instrument sales from 2008 up to and including 2019: i) IRCCAM = Infrared Cloud Camera, ii) VHS = Ventilated Heating Systems, iii) PSR = Precision Spectroradiometer, iv) IRIS = Infrared Integrating Sphere Radiometer, v) PFR = Precision Filter Radiometer, vi) PMO6-CC = absolute cavity pyrheliometer, and vii) ICS = Irradiance Calibration System.

**Note: VHS sales/year shown as a single unit for ease of interpretation. Actual VHS units sold: 2016 = 7; 2017 = 2; 2018 = 36; 2019 = 5.*

Solar Radiometry Section (WRC-SRS)

Wolfgang Finsterle

The Solar Radiometry Section (SRS) of the WRC maintains and operates the World Standard Group (WSG) of Pyrheliometers which represents the World Radiometric Reference (WRR) for ground-based total solar irradiance measurements. The SRS operates the ISO 17025 certified calibration laboratory for solar radiometers (pyrheliometers and pyranometers). During the 2019 calibration season, 110 calibration certificates were issued.

In 2019, the WRC-SRS calibrated 110 radiometers. These consisted of 98 pyranometers, 15 pyrheliometers with a thermopile sensor and 7 absolute cavity radiometers. The WSG was operated on 61 days. Due to staff shortage, the Cryogenic Solar Absolute Radiometer and Monitor for Integrated Transmittance (CSAR/MITRA) could not be operated in 2019.

The vacant position of the SRS laboratory technician was filled in April 2019. Funding was secured in 2020 to fill the vacant position for a CSAR/MITRA instrument scientist. Thanks to the efforts of the new laboratory technician and other involved staff, the 2019 calibration season was completed without major problems. Familiarisation with the CSAR/MITRA has also started although no measurements have yet been possible.

From September to December 2019, the WRC-SRS contributed to the Data Science master's programme of the ETH Zürich by providing Total Solar Irradiance (TSI) time-series and expert advice. Three master students developed and tested several machine learning algorithms to determine the degradation of the TSI radiometers on board VIRGO, which have been measuring TSI from space since December 1995. The results were presented by the students in a poster session at ETH Zürich. PMOD/WRC will continue to improve the machine learning algorithms and plans to implement them to provide operational degradation correction to existing and future solar irradiance measurements (total and spectral) in space.

Table 1. The WRR correction factors for the three transfer standard pyrheliometers determined in the NPC-2018 and NPC-2019 agree well with the results from IPC-XII in 2015. The US standard group maintained by NREL served as the independent reference during both NPCs. The observed relative changes are well below the significance threshold of the comparison and confirm the stability of the WSG. In 2019, the PMO6 0401 was successfully upgraded with the new LINARD control unit by Davos Instruments.

	IPC-XII (2015)	NPC-2018	NPC-2019
PMO6-cc 0401	1.02080	1.02097[a]	1.02134[b]
PMO6-cc 0803	1.00034	1.00005	1.00019
AHF 32455	1.00138	1.00140	1.00061

[a]*Operated with the original "cc"-type control unit.*

[b]*Operated with the new "LINARD" control unit by Davos Instruments.*

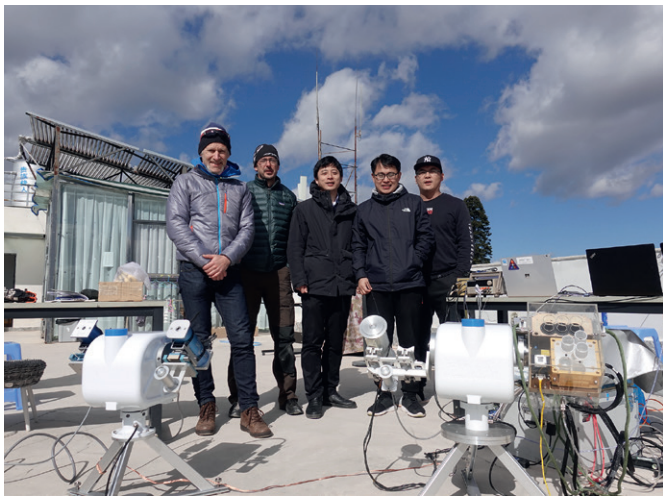

Figure 1. The WRC-SRS participated with two transfer radiometers in the JTSIM cross-calibration campaign which was held in December 2019 at Gemini Observatory near Lijiang, Yunnan province, China. The SRS radiometers are mounted on the tracker on the left-hand side in this picture. The tracker on the right-hand side carries the Chinese reference radiometer (SIAR) and both JTSIM radiometer packages which will fly on the FY-3E space mission by the Chinese Meteorological Administration (CMA).

The WRC-SRS participated in the US National Pyrheliometer Comparison, NPC-2019, which was held in September/October 2019 at NREL in Golden, Colorado, as well as the JTSIM cross-calibration campaign at Gemini Observatory near Lijiang, Yunnan province, China, in December. Two PMO6 radiometers served as the SRS transfer standard, of which one was operated with the new LINARD controller developed by the spin-off company, Davos Instruments. During the NPC-2019, the WRC-SRS operated the AHF32455 absolute cavity radiometer as a third transfer standard. The weather conditions were excellent during both comparisons. The results of the NPC-2019 were published in the NREL technical report NREL/TP-1900-75123. They confirm that the WSG has been stable since the last IPC. (see Table 1). The purpose of the JTSIM cross-calibration campaign was to calibrate both TSI radiometers that will fly on the Chinese Meteorological Administration's (CMA) FY-3E satellite. The WRR was realised by the SRS transfer radiometers and the Chinese SIAR radiometer. Results from the JTSIM cross-calibration campaign will be published in a scientific journal.

Regular confirmation of the stability of the WSG through participation in pyrheliometer comparison is required by ISO 17025 to maintain the Calibration and Measurement Capabilities (CMCs) of the WRC-SRS.

Infrared Radiometry Section (WRC-IRS)

Julian Gröbner, Christian Thomann, and Stephan Nyeki

The Infrared Radiometry Section of the WRC maintains and operates the World Infrared Standard Group of pyrgeometers (WISG) which represents the world-wide reference for atmospheric longwave irradiance measurements.

The WISG serves as an atmospheric longwave irradiance reference for the calibration of pyrgeometers operated by institutes around the world. The WISG has been in continuous operation since 2004, and consists of four pyrgeometers which are installed on the PMOD/WRC roof platform. The measurements of the individual WISG pyrgeometers with respect to their average are shown in Figure 1 for the period 2004 to the end of 2019. As can be seen in the figure, the long-term stability of the WISG is very satisfying, with measurements of the four pyrgeometers within ±1 Wm^{-2} over the whole time period.

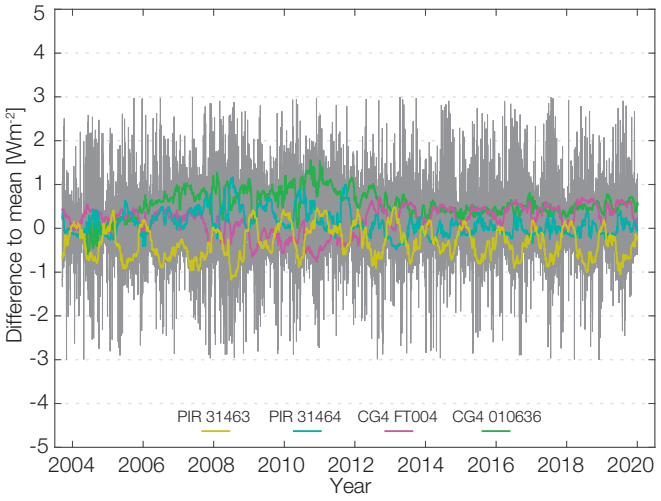

Figure 1. Night-time atmospheric longwave measurements of the WISG pyrgeometers relative to their average. The coloured lines represent a 30-day running mean of each WISG pyrgeometer, while grey-shaded areas represent daily averages.

Simultaneous measurements with the IRIS radiometers and the Absolute Cavity Pyrgeometer (ACP; instrument nos. ACP-96), loaned from NREL, were performed on 20 cloud-free nights between 20 March and 4 September 2019 alongside the WISG. Measurements from ACP-96, IRIS-4 and the WISG are shown in Figure 2, relative to IRIS-2. The data confirm that the WISG underestimates longwave irradiance by about 3 to 5 Wm^{-2} compared to IRIS-4 and ACP-96. The ACP-96 residuals, operated with the default calibration procedure, give a double peaked distribution with a peak in winter/spring centered at about +5 Wm^{-2}, and a second peak in summer of -2 Wm^{-2} with respect to IRIS-2. The standard deviation of the residuals for the 2019 data is 4 Wm^{-2}.

One of the recommendations mentioned in the final report of the WMO CIMO Task Team on Radiation References is to review the ACP physical model. Based on discussions with B. Forgan and I. Reda, several approaches were tested using physical models incorporating a conduction term, resulting in the following ACP instrument equation:

$$E = U/C + k_1\sigma T_r^4 + k_2\sigma T_c^4 + k_3 (T_r - T_c)$$

Where U represents the thermopile voltage, C its responsivity and T_r and T_c the thermopile hot surface and concentrator temperatures, respectively. The parameter k_1 represents the thermopile coating emissivity (assumed to be 0.98), k_2 the gold reflectivity of the concentrator (assumed to be 0.0285) and k_3 the conductance term. Fitting this equation to the measured outdoor data of IRIS-2 and retrieving C and k_3, considerably improved the agreement with the IRIS-2 and IRIS-4 radiometers, where the resulting standard deviation was 0.8 Wm^{-2}. This illustrates that the ACP physical model, with a conductance term, gives consistent results throughout the year, in good agreement with the IRIS radiometers. On the other hand, if the original ACP instrument equation is used, and the responsivity is retrieved from a best fit to the IRIS-2 data, then the residuals do not improve significantly. More data obtained in 2020, with additional ACP radiometers during the upcoming IPgC in Autumn 2020, will hopefully resolve this issue. The data and the report of the ACP-IRIS 2019 comparison is available on request.

References: CIMO, (2017), Final Report, Commission for Instruments and Methods of Observation, Task Team on Radiation References, 15-17 Nov. 2017, www.wmo.int/pages/prog/ www/IMOP/reports/2017/CIMO-TT-RadRef-Mtg_Report.docx.

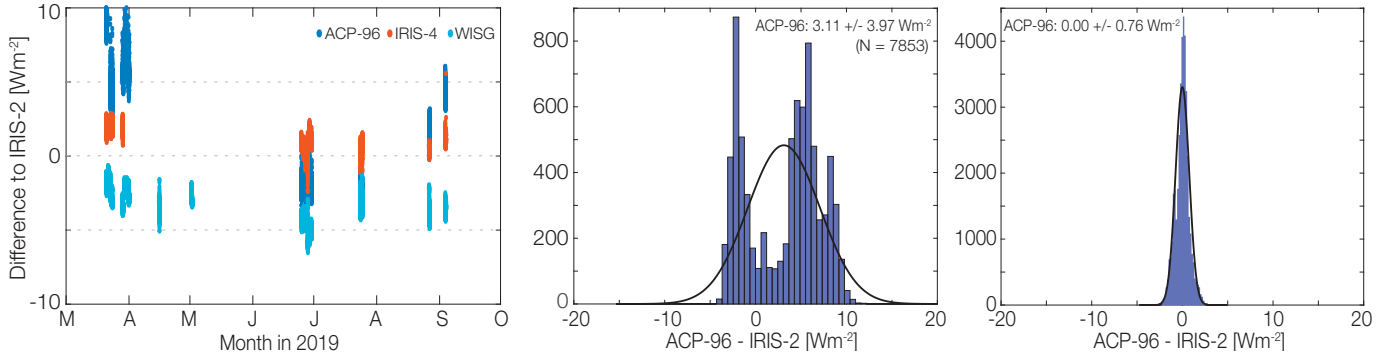

Figure 2. Left-hand figure: Atmospheric longwave measurements from ACP-96 (dark blue), IRIS-4 (red), and WISG (light blue), relative to IRIS-2. Middle and right-hand figures: residuals of ACP-96 to IRIS-2 for: a) using the default ACP equation, and b) equation with conduction term and fitting to IRIS-2.

Atmospheric Turbidity Section (WRC-WORCC)

Stelios Kazadzis, Natalia Kouremeti, and Julian Gröbner

The Atmospheric Turbidity Section of WRC maintains a standard group of three Precision Filter Radiometers (PFR) that serve as a reference for Aerosol Optical Depth (AOD) measurements within WMO. WORCC also operates the global GAW-PFR AOD network.

The World Optical depth Research and Calibration Center (WORCC) calibration hierarchy uses the WORCC reference. This reference is based on the average of three (Triad) well maintained precision filter radiometers (PFRs) that are located at PMOD/WRC, Davos, Switzerland. In addition, instruments operating at high mountain stations such as Mauna Loa (USA) and Izaña (Canary Islands, Spain) perform Langley calibrations which are sent (one instrument every six months) to WORCC in order to check the Triad stability with an independent instrument.

Analysis of these scheduled comparisons has shown differences less than 1% for all cases. In addition, the average differences of each of the Triad instruments compared with the Triad average was less than 0.005 (in AOD) in >99% of cases (1-minute measurements since 2005). This number is well below the WMO-related limits. Hence, no changes have been introduced to the Triad data set. Annual quality assured data sets from seven GAW-PFR stations were updated and submitted to WDCA. In 2019, four instruments of the GAW-PFR network and 10 other instruments, all part of the extended GAW-PFR network, were calibrated against the reference Triad at Davos.

The Lunar-PFR was also deployed at Ny Ålesund from November 2018 - March 2019 and November 2019 - March 2020 for AOD monitoring during the polar winter in the framework of the SIOS project (https://sios-svalbard.org/InfraNor).

WORCC have started a close collaboration with AERONET Europe, and SKYNET Europe and Asia. A PFR instrument participated in the Quatram campaign (http://www.euroskyrad.net/quatram.html) from March to September 2019. The PFR was used as a reference instrument for this campaign with the participation of a number of different instruments. The main objective was the initiation of an AOD traceability study of instruments among already existing federated networks and to promote measurement synergies.

Three new Precision solar Spectroradiometers (PSR) were produced at PMOD/WRC in 2018. They are now fully operational but are still in the testing/measuring phase. The PSRs are operating at PMOD/WRC in parallel to the PFR Triad to investigate their stability and accuracy.

A comprehensive comparison of more than 70,000 synchronous 1-minute AOD data values from three GAW-PFR stations (traceable to the World AOD reference) and 15 AERONET-Cimel radiometers (calibrated individually with the Langley plot technique), was performed for four wavelengths near to 380, 440, 500 and 870 nm for the 2005 - 2015 period. This long-term comparison

Figure 1. The new Precision Filter Radiometer (PFR) series, along with two Precision Spectroradiometers in the background.

(see Table 1) shows an excellent traceability of AERONET-Cimel AOD with the World AOD reference in the 440, 500 and 870 nm channels. Fairly good agreement is found in the more complex 380 nm channel (Cuevas et al., 2019).

Table 1. Percentage of AERONET-Cimel (V3) 1-minute AOD data meeting the WMO criteria for the four interpolated GAW-PFR channels for the 2005-2015 period.

Channel	(%)
380 nm	92.3
440 nm	95.2
500 nm	95.7
870 nm	97.8

The production of a new PFR series (Figure 1) started in 2019. This series is being produced with full compatibility to existing data acquisition systems. Improvements are based on current technology and the 21 years of experience since the first PFR series in 1998. The prototype instrument has been operational since December 2019, and the evaluation of a New-PFR-Triad is foreseen to occur in September - October 2020 during the 5th Filter Radiometer Comparisons (FRC-V).

References: Cuevas E., et al.: 2019, Aerosol optical depth comparison between GAW-PFR and AERONET-Cimel radiometers from long-term (2005-2015) 1 min synchronous measurements, Atmos. Meas. Tech., 12, 4309-4337, doi.org/10.5194/amt-12-4309-2019

World Calibration Centre for UV (WRC-WCC-UV)

Julian Gröbner, Gregor Hülsen, and Luca Egli

The objective of the World Calibration Center for UV (WCC-UV) of WMO GAW is to assess the data quality of the Global GAW UV network and to harmonise the results from monitoring stations and programmes in order to ensure representative and consistent UV radiation data on a global scale.

The WCC-UV portable reference spectroradiometer QASUME was used during four quality assurance site visits. In May 2019, we visited the Norwegian Radiation and Nuclear Safety Authority (DSA) in Oslo, Norway. It was the 3rd audit in Oslo, after 2003 and 2010. In addition to the two Bentham spectroradiometers, operated by DSA, several GUV and NILU broadband radiometers joined the campaign (Figure 1).

In June 2019, we visited the headquarters of the Agencia Estatal de Meteorología (AEMET). It was the 6th audit in Madrid, Spain, after 2009, 2011, 2013, 2015 and 2017. In September 2019, we organised the 8th visit to the Agenzia Regionale per la Protezione dell Ambiente (ARPA) in the Valle d´Aosta, Italy. Reports describing the results of the campaign can be found on the QASUME website (see links further down).

The second main activity during 2019 was the participation in the 14th Regional Brewer Calibration Center - Europe (RBCC-E) campaign. Both global and direct irradiance measurements were carried out in May - June 2019 at the Istituto Nacional de Technica Aeroespacial (INTA), El Arenosillo, Spain (Figure 2). The global UV irradiance spectra recorded by QASUME provided the reference data for the participating 20 Brewer spectrophotometers. Direct solar UV irradiance measurements were used to derive total column ozone values which were compared to the reference data from the reference Brewer #185 operated by the Izaña Atmospheric Research Center of the Spanish Meteorological Agency (AEMET).

Figure 1. The DSA station in Oslo, Norway, showing the QASUME entrance optics (dome with blue cylinder) towards the front of the platform, while the GUV and NILU radiometers, and the local spectroradiometers are at the far end.

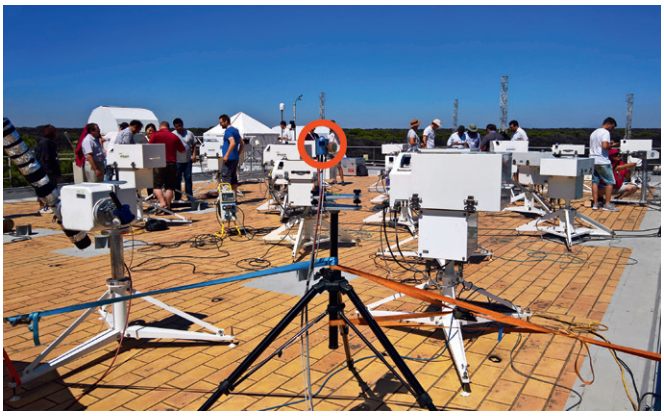

Figure 2. View of the measurement platform at the Istituto Nacional de Technica Aeroespacial (INTA), El Arenosillo, Spain. The QASUME input optic for: i) global irradiance measurements (dome on blue cylinder) is seen in the red circle, and ii) direct irradiance measurements is on the tracker to the left.

Results from all the QASUME site audits and the campaigns can be found on the WCC-UV website at:

www.pmodwrc.ch/en/world-radiation-center-2/wcc-uv/qasume-site-audits/

The 2nd solar UV broadband radiometer comparison campaign (UVC-II) which was organised in 2017 was the largest ever campaign organised so far. Within the overall campaign, nine institutes participated in an inter-laboratory comparison, with PMOD/WRC being the pilot laboratory. The calibrations performed by PMOD/WRC relative to those from the home institutions agreed to within the respective uncertainties for seven out of the eight participants. A publication describing the results of the campaign is now available in the peer-reviewed literature (Hülsen et al., 2020).

References: Hülsen G., Gröbner J., Bais A., Blumthaler M., Diemoz H., Bolsee D., Rodríguez A.D., Fountoulakis I., Naranen E., Schreder J., Stefania F., Vilaplana Guerrero J.M., 2020: Second solar ultraviolet radiometer comparison campaign UVC-II, Metrologia, doi: 10.1088/1681-7575/ab74e5

Section Ozone: Total Column Ozone and Umkehr Measurements

Julian Gröbner, Herbert Schill, Franz Zeilinger, and Luca Egli

Operational Total Column Ozone and Umkehr measurements are performed at PMOD/WRC with two Dobson and three Brewer spectrophotometers to monitor the stratospheric ozone layer, hence extending the world's longest continuous total ozone time-series at Arosa and Davos, Switzerland.

After the agreement between MeteoSwiss and PMOD/WRC Davos in 2018 to continue the Arosa stratospheric ozone measurements in Davos, 2019 was the first full year with direct sun (total ozone) measurements (Figures 1 and 2). These were performed with two Dobsons (D051 and D101) and three Brewers (B072 and B156, Meteoswiss; B163, PMOD/WRC), while the observations at Arosa continued with one Dobson (D062) and one Brewer (B040). However, Dobson 051 is dedicated to Umkehr measurements in the first instance, and is therefore only occasionally used for direct sun observations. Tables 1 and 2 give the monthly data for the Dobson and Brewer direct sun measurements collected at both sites, respectively.

The beginning of the year saw the adaption of data streams and formats for data quality control at the PMOD/WRC, as well as the integration of the datasets into the structure of the institute.

In August 2019, a new air conditioning system was installed in the Dobson container in order to guarantee more efficient heating/cooling.

Due to the retirement of the current operational station head of the Licht-Klimatisches Observatorium (LKO) Arosa at the end of May 2020, a new technician dedicated to the supervision of the operational ozone measurements started at PMOD/WRC in October 2019. The overlap period will be used for extensive knowledge transfer and the relocation of spare parts and tools from the LKO Arosa to Davos.

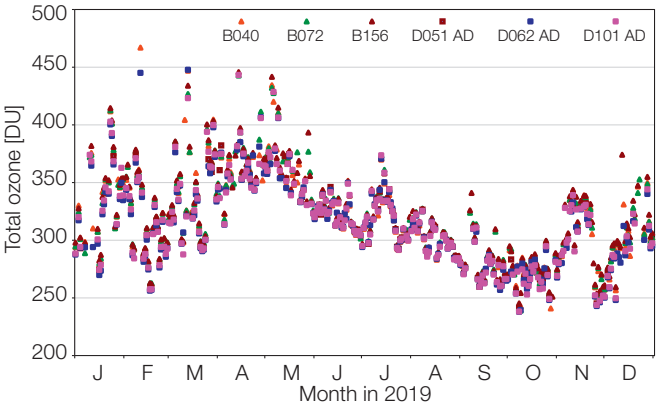

Figure 1. Daily total ozone values in 2019 from direct sun measurements of the Brewer and Dobson spectrophotometers at LKO, Arosa (Brewer B040 and Dobson D062) and PMOD/WRC, Davos (Brewers B072, B156 and Dobsons D051, D101).

In October 2019, the slit geometry of each Dobson was characterised (Figure 3) with a tuneable radiation source (TuPS) by experts of the Czech Metrology Institute. This is a main goal within the framework of the INFO3RS project. Further detailed results on this topic can be found in this report in the article, “The effect of the Dobson spectrophotometer slit characterisations at the PMOD/WRC on the ozone absorption coefficients”.

Tables 1 and 2. Number of monthly direct sun measurements of Dobsons (left) and Brewers (right) at LKO, Arosa and PMOD/WRC, Davos in 2019. Columns include: number of days with measurements, number of all measurements ("all") , and the number of unflagged ("unflag."; i.e. reliable) measurements.

Dobson direct sun measurements at Arosa and Davos in 2019

	D062 (Arosa)			D101 (Davos)			D051 (Davos)		
month	days	all	unflag.	days	all	unflag.	days	all	unflag.
1	27	2220	1270	26	2220	1231	4	138	113
2	27	3772	2997	27	3900	3124	6	627	550
3	30	4338	2873	30	4647	3166	4	190	144
4	29	4277	1893	30	4533	2020	6	690	314
5	24	3272	1185	31	4017	1498	8	1327	678
6	29	5434	3453	30	6241	4367	8	1148	742
7	31	5344	2461	31	5512	3050	16	2947	1695
8	30	4866	2799	31	4908	3208	12	1829	1296
9	30	4186	2612	30	4376	2984	5	809	702
10	31	2830	1056	27	2986	1608	11	1131	638
11	29	2333	922	30	2537	1173	10	846	359
12	31	1983	1260	31	2352	1189	1	38	36
2019	348	44,855	24,781	354	48,229	28,618	91	11,720	7,267
2018	347	44,818	23,518	330	40,882	21,502	189	25,193	11,399

Brewer direct sun measurements at Arosa and Davos in 2019

	B040 (Arosa)			B072 (Davos)			B156 (Davos)		
month	days	all	unflag.	days	all	unflag.	days	all	unflag.
1	24	1192	948	24	1210	976	24	1332	885
2	26	2001	1745	27	1883	1603	27	2144	1690
3	31	2656	1843	31	2666	1836	31	2945	1566
4	29	2791	1324	30	2905	1369	26	2795	1110
5	31	3364	1047	30	3222	962	30	3526	871
6	30	3742	2382	27	3442	1880	30	4057	2147
7	31	3587	1810	31	3486	1692	31	3770	1669
8	31	3063	1820	31	3141	1798	31	3489	1679
9	30	2442	1608	29	2554	1646	30	2721	1331
10	30	1763	1101	31	1823	1212	31	1960	984
11	29	1279	818	28	1309	949	28	1585	932
12	24	899	752	21	682	550	29	1065	715
2019	346	28,779	17,198	340	28,323	16,473	348	31,389	15,579
2018	341	28,015	15,971	326	29,093	15,527	344	31,266	14,819

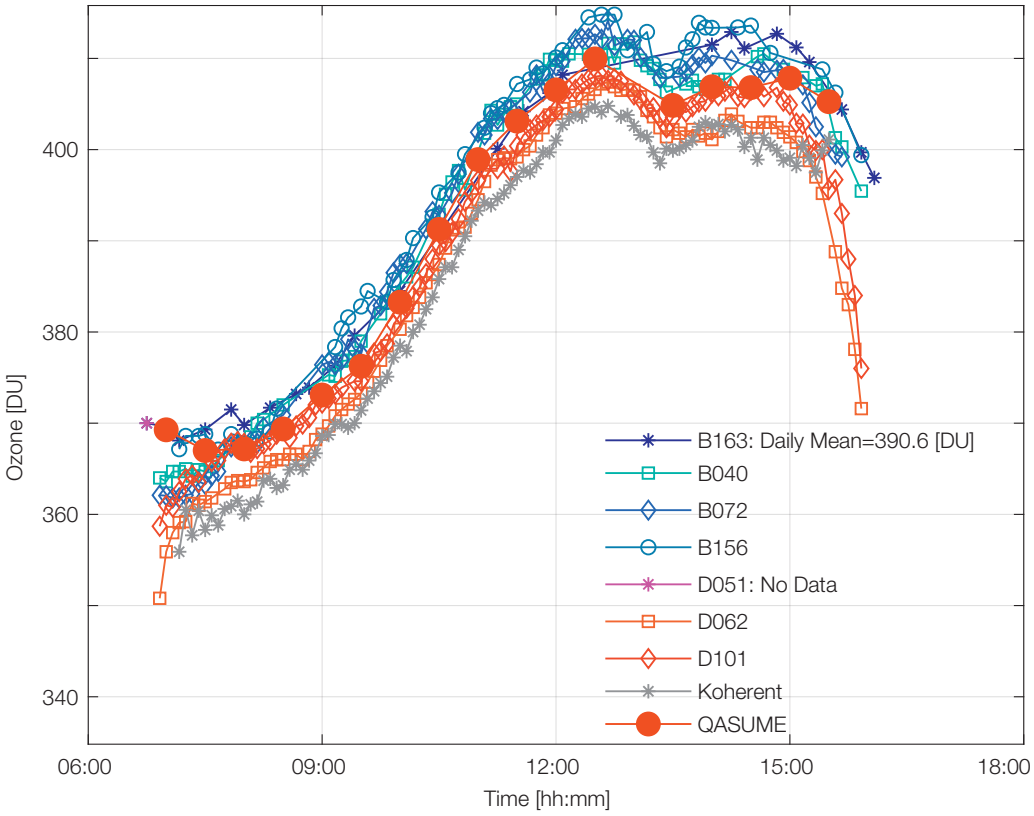

Figure 2. Comparison of the daytime variation in total column ozone on 23 March 2020 at Davos from Dobson, Brewer, QASUME and Koherent instruments.

Figure 3. From left to right: René Stübi (MeteoSwiss), Werner Siegrist (MeteoSwiss) and Marek Šmid (Czech Metrology Institute) during the characterisation of Dobson D101 at PMOD/WRC, Davos.

Instrument Development

Space Experiments

Manfred Gyo, Lloyd Beeler, Valeria Büchel, Wolfgang Finsterle, Christian Fringer, Matthias Gander, Patrik Langer, Margit Haberreiter, Louise Harra, Silvio Koller, Philipp Kuhn, Dany Pfiffner, Pascal Schlatter, Werner Schmutz, Yanick Schoch, Marcel Specha

EUI and SPICE

The Extreme UV Imager (EUI) experiment and the SPICE EUV spectrograph are payload instruments onboard the ESA/NASA Solar Orbiter Mission.

Within the EUI consortium, PMOD/WRC is responsible for the optical bench structure (OBS) of the EUI instrument. For the SPICE instrument, PMOD/WRC built the low voltage power supply and coordinated the contribution of the slit change mechanism and the SPICE door mechanism.

Figure 1. Solar Orbiter at the IABG test centre, Germany, before it was transported to the launch site at Cape Canaveral, USA. Image credit: Airbus.

In 2019, Solar Orbiter continued to undergo testing at the IABG test centre in Ottobrunn near Munich (Fig. 1). These tests included electromagnetic compatibility, vibration and thermal vacuum, as well as deployment of solar arrays and booms from the spacecraft. All tests were successfully completed. Subsequently, the spacecraft was transported to the launch site, assembled and rolled to the launch pad (Fig. 2) at Cape Canaveral, Florida, USA.

Figure 2. The ATLAS V rocket, with Solar Orbiter onboard, being rolled to the launch pad after assembly. Image credit: ULA.

DARA

The Digital Absolute Radiometer (DARA), is a payload onboard the ESA PROBA-3 formation flying mission. DARA is a 3-channel radiometer designed for the long-term stable and highly accurate measurement of TSI which is fully traceable to SI.

A large part of the performed tasks concerned assembly and testing of the two DARA flight models, the Engineering Qualification Model/Flight Spare (EQM/FS) and the Flight Model (FM). In the first few months, most of the mechanics and electronics hardware were manufactured for both flight models. The different printed circuit boards were tested at board level and the mechanical parts were prepared for instrument assembly.

The DARA On-board and EGSE software testing period finished in parallel. The abbreviation, EGSE, stands for “Electronics Ground Support Equipment” and designates, in this case, the software to be applied for on-ground instrument operation. The On-board software is the operational software, installed on the instrument internal processor. The development and test tasks

Figure 3. DARA EQM/FS mounted on the WRC main solar tracker.

for both software packages were formally completed, and were based on the FM of JTSIM-DARA, a parallel development for the Chinese FY-3E mission.

In the second half of the year, the structural and thermal analyses were updated and completed. Several discussions were still necessary to find agreement about which vibration input and notching levels were to be used for the vibration test.

The EQM/FS model was fully assembled in autumn, and electrical calibration was performed in a vacuum tank with an instrument temperature range from -50°C to + 50°C. The FM electronics was assembled and operated in order to test it in a so-called flat-sat configuration.

An agreement with the Centre Spatiale de Liège, Belgium, was signed for delivery and analysis of witness plates for contamination monitoring during the assembly, testing and integration period. Detecting contamination, on a molecular and particle level, began with the first action after the cleaning and assembly of the EQM/FS parts, which occurred during the electrical calibration. As planned, the EQM/FS was mounted in its handling box (incl. purging), and first solar measurements were performed using the PMOD/WRC radiometer calibration infrastructure (Figure 3).

Instrument qualification: The vibration test was performed on the EQM/FS with qualification levels (Figure 4). Apart from some differences to calculated eigenmodes, no major difficulties were observed. The conducted EMC test showed some susceptibility issues, which might require further investigation.

The adapted DARA multilayer insulation design began in parallel but a final design was not completed by the end of the year.

Due to various reasons, the PROBA-3 launch has been re-scheduled several times during the last few years. Currently, the launch is expected in mid-2022. Launch delays can introduce difficulties, but also allow longer instrument calibration and on-ground operational times at PMOD/WRC.

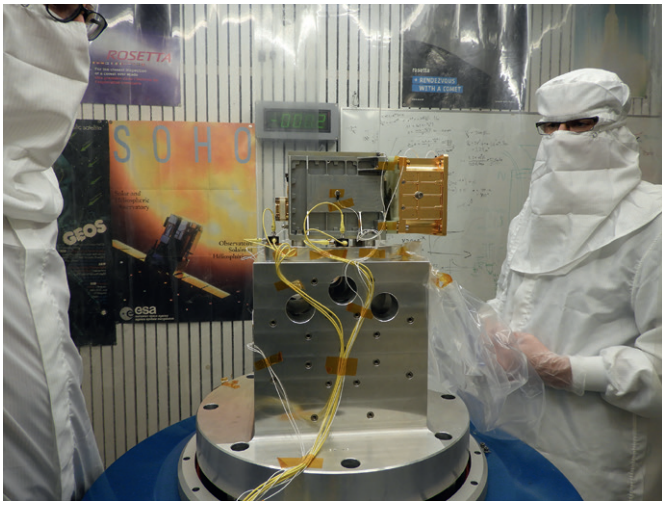

Figure 4. DARA EQM/FS mounted on a vibration adapter (University of Bern).

JTSIM-DARA

The Joint Total Solar Irradiance Monitor-DARA (JTSIM-DARA), is a radiometer onboard the Chinese FY-3E mission. JTSIM-DARA will measure TSI along with a Solar Irradiance Absolute Radiometer (SIAR), designed by CIOMP (China).

The JTSIM-DARA Proto Flight Model (PFM) was assembled in the first months of 2019 into its final configuration, and was prepared for final internal testing and calibration at PMOD/WRC.

Most of the environmental tests were planned to be conducted in China by our Chinese partner institute, the Changchun Institute of Optics, Fine Mechanics and Physics (CIOMP). The reason is, environmental tests will not occur at a single instrument level,

Figure 5. Hand-over ceremony of JTSIM-DARA at PMOD/WRC with representatives from the Chinese Embassy in Bern.

but on Solar Tracker level, including the mounted instruments: JTSIM-DARA, SIAR (CIOMP absolute radiometer) and the common sun sensor of the tracker mechanism.

For internal qualification/verification reasons, PMOD/WRC performed the following tests with the JTSIM-DARA Proto-Flight Model (PFM) in Switzerland, prior to delivery:

- An EMC test based on CIOMP requirements.
- A vibration test, but only resonance searches (to determine JTSIM-DARA eigenmode frequencies).
- A high-level sine test at acceptance levels.
- Thermal cycling at acceptance range levels.

In parallel, PMOD/WRC developed data level transformation software, and our contractor dlab GmbH finished the testing phase of the On-board and EGSE software. Before the official acceptance review meeting with CIOMP in Switzerland, solar measurements were performed at PMOD/WRC to verify instrument scientific performance.

On 12 April 2019, PMOD/WRC was visited by representatives of the Chinese Embassy in Bern to plan the official instrument

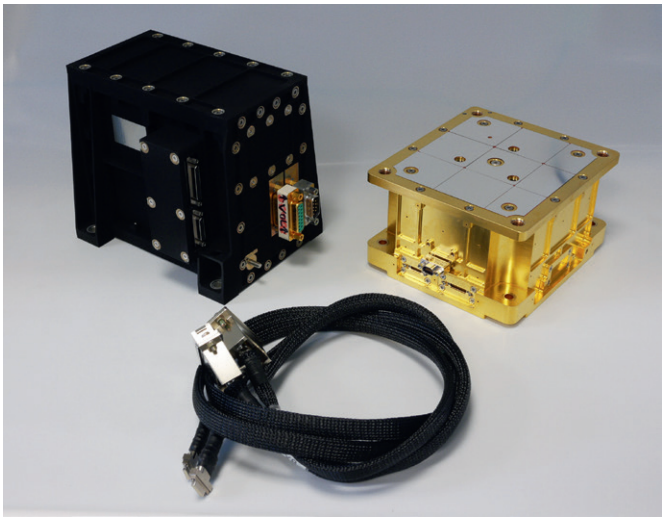

Figure 6. The JTSIM-DARA Electronics Box / Sensor Box.

acceptance review meeting in Davos. This meeting included the hand-over ceremony on 21 June 2019 at PMOD/WRC (Figure 5) which was also held with the Chinese Embassy. In addition, CIOMP provided an acceptance review plan during the meeting. All requirements were tested, and the conformity of the JTSIM-DARA PFM was verified. In September 2019, JTSIM-DARA was shipped to CIOMP, China, where the instrument arrived safely.

A month later, PMODW/WRC was present at CIOMP to mount the JTSIM-DARA PFM Sensor Box (Figure 6) onto the JTSIM solar tracker and conduct first integration tests (Figure 7). In December 2019, a two-week radiometer cross-calibration campaign was held in Lijiang, China. Both absolute radiometers (SIAR from CIOMP and JTSIM-DARA from PMOD/WRC) were compared to two PMO6-cc absolute radiometers, which were used as transfer standards of the World Standard Group at PMOD/WRC. Two PMOD/WRC collaborators were present in Lijiang to run our instruments and provide support for data treatment and analysis. The integration of JTSIM-DARA on the FY-3E satellite is planned for early next year. The launch date is now foreseen for the end of 2021.

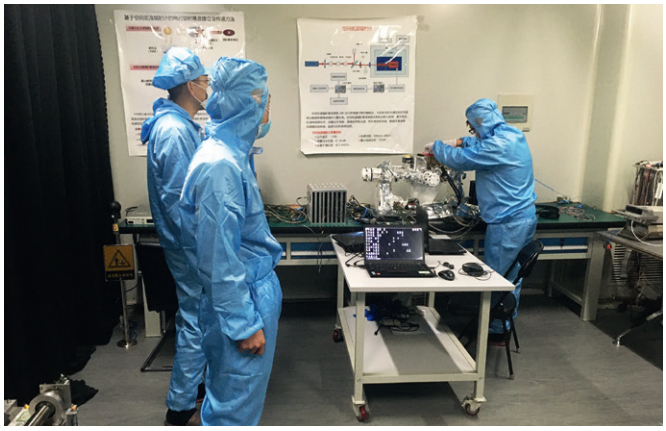

Figure 7. Instrument integration at CIOMP, China.

LUCI

The Lagrange EUV Coronal Imager (LUCI) is an extreme UV imager onboard the ESA Lagrange mission within the Space Safety Programme to the L5 Lagrange point.

LUCI is one of the remote sensing instruments on the spacecraft and is dedicated to imaging the full solar disk and the region of the outer corona up to 2.5 solar radii in a direction towards the Earth (Figure 8). It builds on the heritage of the SWAP) Sun Watcher using Active Pixel System Detector and Image Processing) telescope on PROBA-2 as well as the EUI telescope on Solar Orbiter. LUCI will obtain images of the extreme ultra-violet (EUV) wavelength range at 195 Å. Measurements will provide input to enable reliable space weather forecasting, and to provide new insights into solar activity and its impact on Earth.

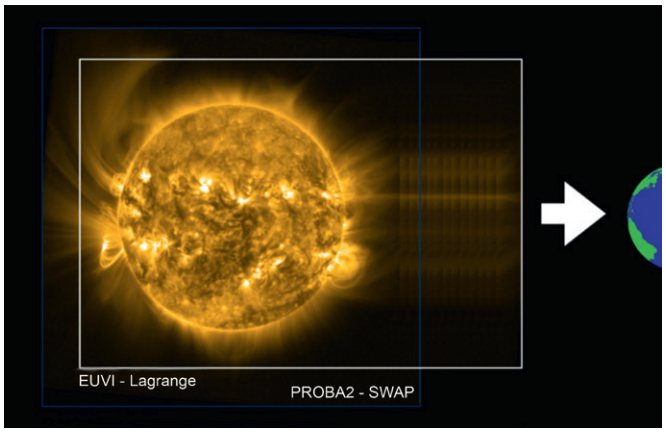

Figure 8. Field-of-view of the LUCI instrument onboard ESA's Space Safety Mission, Lagrange. Image credit: Matthew West.

In particular, the design of LUCI, together with the side view of the Sun-Earth line, will allow us, for the first time, to observe the onset and the early acceleration phase of a Coronal Mass Ejection (CME) travelling towards the Earth. This is important in order to determine the arrival time of CMEs at Earth with higher accuracy than currently possible. In addition, the EUV images of the Sun obtained with LUCI will allow us to improve our understanding and models of the variability of EUV radiation. Variability in EUV drives the temperature, density and total electron content of Earth's upper atmosphere. As such, LUCI will provide key observations to advance our knowledge of the Earth's response to solar activity.

The LUCI consortium (Centre Spatiale de Liège, CSL, Belgium; The Royal Observatory of Belgium, ROB, Belgium; PMOD/WRC),

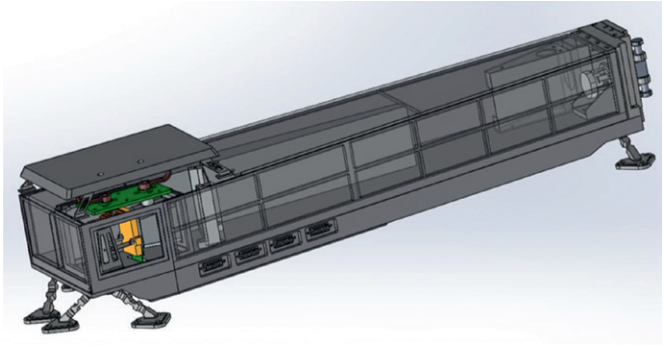

Figure 9. Mechanical design of the LUCI instrument.

has successfully completed Phases A and B1. The Instrument Science Requirements Review (ISRR) collocation meeting took place on 3 September 2019 and the subsequent ISRR close-out meeting on 20 September 2019.

Figure 9 shows the mechanical design of the instrument, which is the basis of the finite element model (FEM), developed and validated in Phase B1. Figure 10 shows an example result of the structural analysis carried out with the FEM at a frequency of 276 Hz. The series of structural analyses at different frequencies allows us to determine any critical mechanical parts in the LUCI structure that might not sustain strong vibrations, such as the loads during the rocket launch.

On the Front-End Electronics (FEE) side (Figure 11), analogue and digital electronic outlines and technical requirements were advanced. In addition, a FEE User Guide was prepared and all engineering budgets were determined.

Subsequent design activities are currently ongoing as part of the Pre-Development (PD) for the FEE and Thermal-Mechanics (TM) design of the instrument. The PD kick-off meeting was held at PMOD/WRC on 11 September, 2019 (see Figure 12).

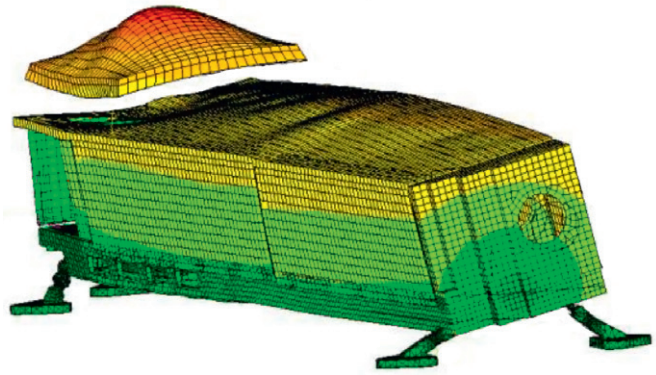

Figure 10. Example of the structural vibration analysis of the LUCI instrument at 276 Hz.

The Bridging Phase (BP), running in parallel to the PD since the ISRR close-out until July 2020, covers activities such as: i) radiation assessment of the instrument, ii) reliability assessment of the instrument, iii) electromagnetic cleanliness, and iv) other quality assurance tasks. The first BP milestone meeting (BPM1) took place on 9-10 December 2019 at the European Space Operations Centre (ESOC) in Darmstadt, Germany.

The instrument performance model of LUCI is also being continuously developed in order to: i) better model the detector signal and, ii) ensure in particular, a good signal-to-noise ratio of the faint signal expected in the far field-of-view. This is specifically relevant for the detection of solar eruptions along the Sun-Earth line. As only sparse observations of solar eruptions in the EUV are available this far from the Sun, we rely on realistic models to infer the performance of the instrument. These have been carefully implemented in the instrument performance model.

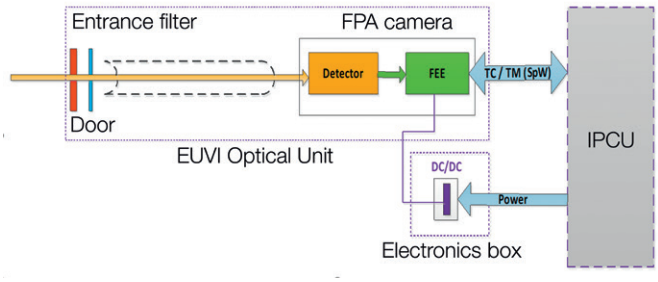

Figure 11. Functional architecture of LUCI.

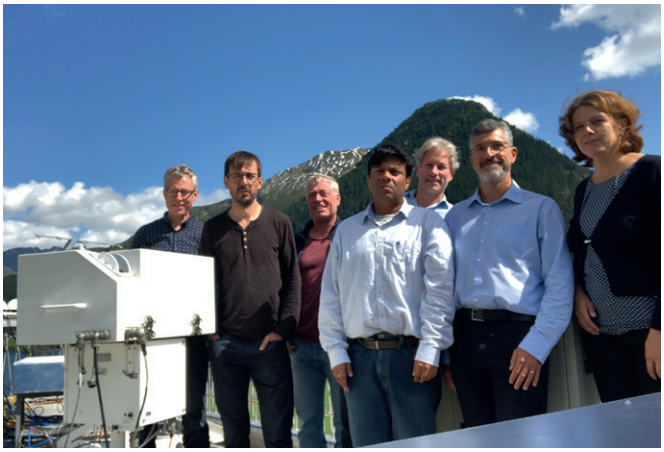

Figure 12. Participants at the kick-off meeting of the LUCI FEE and TM pre-development study. From left to right: Silvio Koller (PMOD/WRC), Dany Pfiffner (PMOD/WRC), Manfred Gyo (PMOD/WRC), Indraneil Biswas (ESA/ESOC), Philippe Bouchez (CSL), Fancesco Ratti (ESA/ESTEC), Margit Haberreiter (PMOD/WRC).

Scientific Research Activities

Overview

Louise Harra

Projects at PMOD/WRC are related to solar radiation in which we address questions regarding the radiation energy budget in the terrestrial atmosphere, as well as problems in solar physics in order to understand the mechanisms concerning the variability of solar irradiance. Hardware projects at our institute are part of investigations into Sun-Earth interactions which involve measurements of solar irradiance.

The choice of projects to be conducted at the institute is governed by the synergy between the know-how obtained from the Operational Services of the World Radiation Center (WRC) and other research activities. The same instruments are built for space-based experiments as are utilised for ground-based measurements. In addition, with the involvement in Solar Orbiter and Lagrange, the instrumentation extends to imaging and spectroscopy. The research activities can be grouped into four themes:

- Climate modelling
- Atmospheric physics
- Development of meteorological radiation instruments
- Solar physics

The majority of research activities are financed through third party funding. During 2019, there were a range of funding sources which included projects supported by the Swiss National Science Foundation, Karbacher Fonds, Innosuisse, European COST action, Meteoswiss, European H2020, ESA, EURAMET. These funding sources supported three PhD thesis projects and four post-doctoral positions and two instrument scientists.

Swiss participation in ESA's PRODEX programme (PROgramme de Développement d'EXpériences scientifiques) funds the hardware development of space experiments. The institute's four PRODEX projects paid for the equivalent of five technical department positions.

In the area of climate modelling, the research studies both long and short-term changes in the Earth's atmosphere. The ozone layer evolution is being modelled and predicted. The impact of solar protons on the ionosphere has been assessed and particularly strong historical events are analysed. A new area of study is understanding outgoing radiation at the top of the Earth's atmosphere with the NorSat-1 CLARA mission.

The solar physics focus turns to Solar Orbiter following its launch in February 2020. These topics cover the creation of the slow and fast solar wind.

The institute's infrastructure and most of its overheads are paid for by the operational service of the WRC. We are proud of the fact that at the PMOD/WRC, the Center's services are based on research that is state-of-the-art in their respective fields. The data from new instruments are being analysed such as the cloud measurements from a far infrared camera. The accuracy of measurements are constantly being improved, such as the correction of stray-light in our Precision Spectroradiometers. The exact ozone absorption coefficients of three Dobson spectrometers have also been measured while a new TSI radiometer detector has been developed. The research carried out at PMOD/WRC is intertwined with the instrumentation, both ground and space-based. In addition, a transfer of knowledge on solar radiation is being applied to the goals of the EC renewable energy directive.

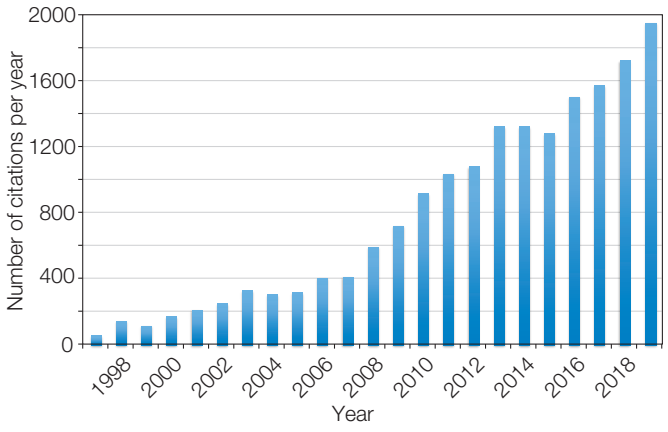

Figure 1. Number of annual citations to articles including an author with a PMOD/WRC affiliation. Up to May 2020, there were 19,060 citations (h-index 67) to 708 articles included in Thomson Reuter's Web of Science. The articles were selected using the search criteria address = (World Rad C*) OR (PMOD* NOT PMOD Technol* OR pmodak) OR (Phys* Met* Obs*).*

Leading Towards the Science of Solar Orbiter

Louise Harra, Margit Haberreiter, Conrad Schwanitz, and Werner Schmutz

The Solar Orbiter mission has been planned for two decades. The mission's main aims are to understand how the heliosphere is created and maintained. The research areas around this embrace the sources of both fast and slow solar wind. The mission was successfully launched in February 2020.

PMOD/WRC has been involved in the development of two instruments on Solar Orbiter. The EUV Imager (EUI) and the Spectral Imaging of the Coronal Environment (SPICE) instrument. EUI has three telescopes onboard: a Full Sun Imager (FSI) along with a filter wheel which allows coverage of 17.4 nm and 30.4 nm, and two High Resolution Imagers (HRI), one of which observes at the Lyman α wavelength and the other at 17.4 nm. EUI has a wide field-of-view that will explore the dynamics of the outer corona, and high-resolution telescopes that will explore the fundamental processes that create the solar wind. The details of the instrument are described in Rochus et al. (2019). The SPICE instrument is a high-resolution imaging spectrometer with the wavelength ranges 70.4 - 79.0 nm and 97.3 - 104.9 nm. SPICE data will allow the determination of plasma parameters such as the Doppler velocity, density, non-thermal velocity and abundances. These are key to providing a linkage to in-situ measurements of the solar wind. The SPICE paper is summarised in Anderson et al. (2019). The instruments papers are published in *Astronomy and Astrophysics* and will appear as a special edition book in 2020. These instrument papers have been the culmination of more than ten years of work, and will be highly cited. They feature various PMOD/WRC staff: Harra, Haberreiter, Schmutz, Gyo, Pfiffner, Koller, Spescha, Schlatter.

There are ten instruments onboard the mission consisting of a mix of remote sensing and in-situ instruments. The remote sensing instruments, in particular, have serious constraints on telemetry, which means clever forward planning must be carried out, including choosing targets, and ensuring that instruments are coordinated. An example is that several of the instruments have 'triggers'. Both EUI and STIX have solar flare triggers that react when there is a flare. They will communicate with each other to coordinate which flare data to store. The telemetry constraints are very tight so careful data selection will take place both onboard the spacecraft and selected by the observers, taking advantage of the low-cadence synoptic observations. The interaction between the remote sensing instruments is summarised by Auchère et al. (2019). Each orbit has to be carefully planned, to ensure the science goals will be achieved. This has also been worked on over many years.

The solar wind is a key science target for the Solar Orbiter mission. There are many components that can form the solar wind, and jets are one element. These have been observed for many years, and many are a single spire structure usually with a jet bright point on one side of its base. Magnetic reconnection is a key component to jets. Two-sided jets have also been observed – these have two 'spires' with a middle bright point. As spatial resolutions have improved, it has been found that some of the single jet examples are caused by cold filaments erupting. This is essentially similar to

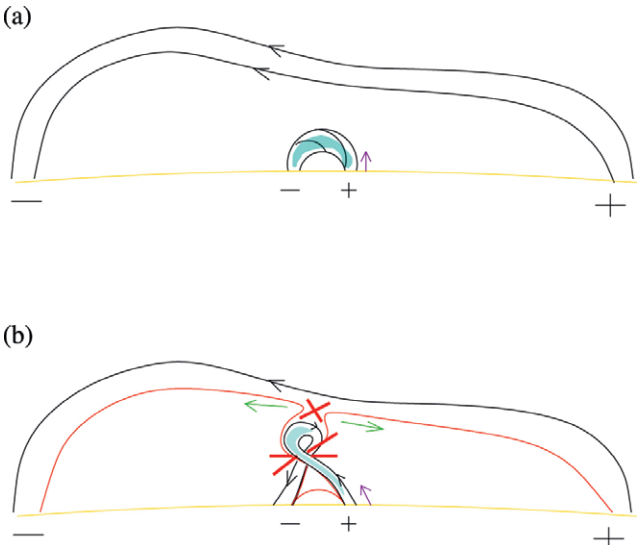

Figure 1. Schematic showing the production of a two-sided jet. Panel (a) shows the set-up before the jet. The blue feature is a cool mini-filament inside a twisted loop. Panel (b) shows the configuration after the filament erupted and reconnection occurred at the locations marked with a red cross. From Sterling et al. (2019).

a solar flare model but on a smaller scale. In the work by Sterling et al. (2019), a filament was the trigger of a two-sided jet. This is illustrated in Figure 1, where a twisted filament erupts, interacting with the over-lying large low-lying magnetic fields. Reconnection results in jets flowing in two directions. Research in jets is important for Solar Orbiter science and will be a focus in the next years.

Linking the solar wind sources on the Sun to those measured in the solar wind is a key challenge of the Solar Orbiter mission. In the work by Macneil et al. (2019), the challenge of the linkage was carried out, and the impact of an emerging active region near a coronal hole was quantified. Significant changes in the structure and composition of the solar wind were measured due to the active region emergence. The observations were consistent with an increased occurrence of interchange reconnection during solar wind production compared with the quiet Sun case.

References:

Auchère F., et al.: 2019, Coordination within the remote sensing payload on the Solar Orbiter mission, doi.org/10.1051/0004-6361/201937032

Macneil A.R., Owen C.J., Baker D., Brooks D., Harra L.K., Long D.M., Wicks R.T.: 2019, Active region modulation of coronal hole solar wind, doi.org/10.3847/1538-4357/ab5586

Rochus P., et al.: 2019, The Solar Orbiter EUI instrument: The Extreme Ultraviolet Imager, doi.org/10.1051/0004-6361/201936663

SPICE consortium: 2019, The Solar Orbiter SPICE instrument: An extreme UV imaging spectrometer, doi.org/10.1051/0004-6361/201935574

Sterling A.C., Harra L.K., et al.: 2019, A two-sided loop X-ray solar coronal jet driven by a mini-filament jet eruption, doi.org/10.3847/1538-4357/aaf1d3

Total Solar Irradiance Measured with CLARA Onboard NorSat-1

Margit Haberreiter, Wolfgang Finsterle, Werner Schmutz, Manfred Gyo, Silvio Koller, and Dany Pfiffner in collaboration with UTIAS-SLF (Canada) and the Norwegian Space Agency (Norway)

Total Solar Irradiance (TSI) is the main energy source at Earth. For a correct evaluation of the Earth's energy budget, it is important to measure TSI with high accuracy and precision from space. The CLARA instrument onboard the Norwegian micro-satellite NorSat-1, is PMOD/WRC's latest operational absolute radiometer to measure TSI.

Continuous and accurate measurements of the essential climate variable (ECV), TSI, is crucial in order to determine the role of solar irradiance on the terrestrial climate. TSI is one important parameter that drives the Earth's energy budget. The Compact Lightweight Absolute Radiometer (CLARA) onboard NorSat-1 is one of PMOD/WRC's contributions to the almost gapless series of space-borne TSI measurements since 1978.

CLARA, onboard NorSat-1, was launched on 14 July 2017, and after a successful commissioning phase, measurements started on 21 Aug. 2017. Unfortunately, the platform experienced problems with one of the spinning wheels in early 2018, which unfortunately failed in May 2018. Subsequently, the platform and operation teams had to develop a new pointing scheme so that CLARA could still be pointed to the Sun to obtain solar measurements. During this developing phase, the satellite could not be stabilised, and CLARA could not be pointed to the Sun to take solar measurements. Thanks to the effort of the NorSat-1 teams, reasonable pointing was restored with two reaction wheels during the course of 2019, and CLARA saw its second "First Light" on 8 Nov. 2019.

However, as the new pointing performance is not optimal, the newly received TSI data need to be carefully filtered using the available pre-flight cavity alignment measurements as well as the onboard pointing information of the Precision Sun Sensor (PSS). To illustrate this, Figure 1 shows the PSS pointing vector in the x and y-directions (light blue and orange diamonds, respectively) during the sun-pointing phases of the orbit on 28 November 2019. The horizontal lines indicate the required pointing precision determined from the pre-flight alignment measurements in the x-direction (blue dotted) and y-direction (red dashed).

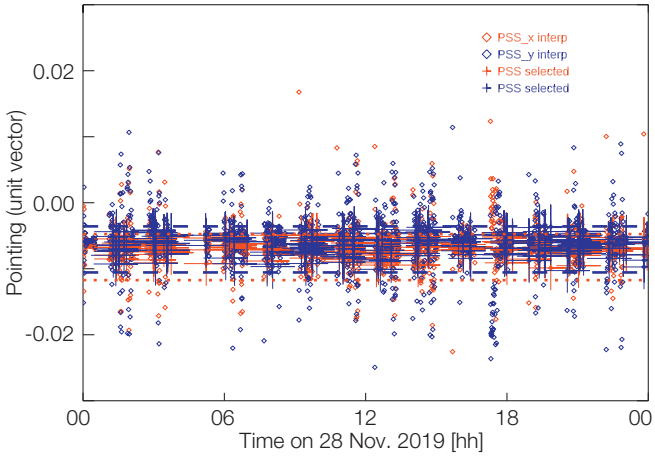

Figure 1. Fine-pointing performance of NorSat-1 during solar measurements from the onboard PSS sensor. The required pointing accuracy is indicated by the horizontal, dotted and dashed lines. The red and blue crosses between the horizontal lines show the data points that meet this requirement, and which are ultimately used in the CLARA TSI time-series.

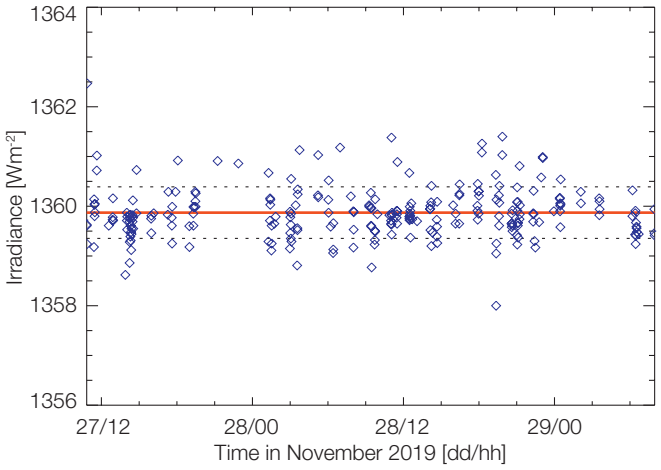

Figure 2. Pointing-filtered CLARA TSI data for 27 - 29 November 2019.

Figure 2 shows the pointing-corrected CLARA TSI data for 27 - 29 November 2019, when good solar pointing was established. The CLARA data give a mean TSI value of 1359.87 Wm^{-2}, with a standard deviation of 0.52 Wm^{-2} (k=1). This data-set is not yet degradation-corrected and thus should be considered as a lower limit. We note that some outliers still need to be further investigated.

Since the end of 2019, CLARA is being operated continuously during the full orbit in order to also measure the Top of the Atmosphere Outgoing Radiation (TOR) on the night-side of the Earth (see separate report).

References:

Finsterle W., Haberreiter M., Remesal Oliva, A.: 2019, CubeSats for measuring the Earth's energy imbalance, EGU2019, Proc. 7-12 April, 2019, Vienna, Austria, id.19143

Haberreiter M., Finsterle W., Schmutz W. et al.: 2020, Latest TSI Measurements from NorSat-1 / CLARA, Sun Climate Symposium, Tucson, USA.

Walter B., Andersen B., Beattie A., et al.: 2018, First TSI results and status report of the CLARA/NorSat-1 solar absolute radiometer, Astronomy in Focus, Proc. IAU, Vienna, Austria, pp. 358-360, doi: 10.1017/S1743921319004617

In-Flight Demonstration of Top-of-the-Atmosphere Outgoing Radiation Measurement with CLARA Onboard NorSat-1

Margit Haberreiter and Wolfgang Finsterle

A positive Earth Energy Imbalance (EEI) is the energy, which is continuously stored by the Earth and will ultimately be released to the atmosphere, causing global warming. The EEI has been identified to be around 0.5 to 1.0 Wm^{-2}. In order to determine its exact value, both the Total Solar Irradiance (TSI) and the Top-of-the-Atmosphere (ToA) Outgoing Radiation (TOR) need to be measured with unprecedented accuracy and precision. First TOR measurements obtained with CLARA onboard NorSat-1 are presented here.

The radiation budget at the top of the atmosphere (TOA) regulates the overall energy content of the Earth system, i.e. atmosphere and ocean. Human activities have led to rising levels of heat-trapping greenhouse gases (GHGs) in the atmosphere with less terrestrial radiation being able to escape, creating the so-called positive Earth Energy Imbalance (EEI). As a result, the Earth system is warming up. The most obvious sign of it is the long-term increase in global surface temperatures, which in turn enhances the flux of outgoing energy.

The Compact Lightweight Absolute Radiometer (CLARA) onboard NorSat-1 was launched on 14 July 2017, and after a successful commissioning phase, measurements started on 21 August 2017. Besides measuring TSI, which is the main science goal, CLARA also has the ability to measure TOR when the satellite is on the night-side of Earth.

Since the end of 2019, CLARA is being operated continuously during each full orbit to demonstrate the measurement of the Earth's outgoing radiation with an SI-traceable radiometer. As such CLARA is paving the way for future continuous TOR measurements with state-of-the-art radiometers (see Finsterle et al., 2019).

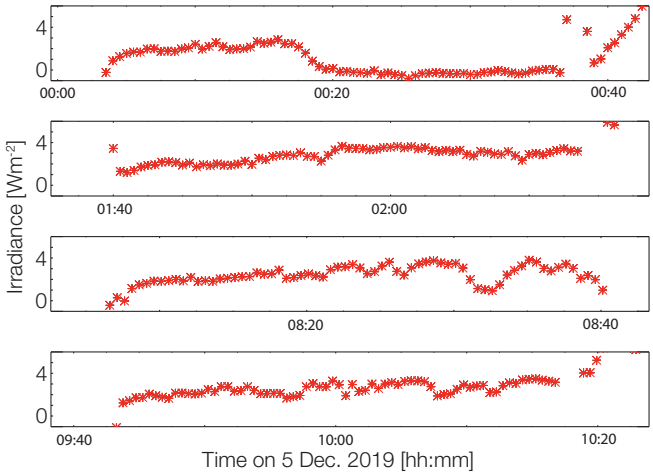

Figure 1. The CLARA irradiance measurements during four consecutive eclipse phases when the radiometer was looking at the night-side of Earth on 5 December 2019.

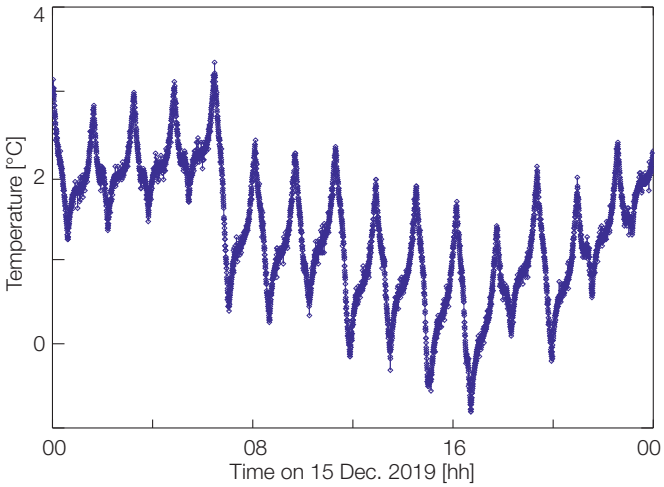

Figure 2. Heat sink temperature for the entire day on 15 December 2019.

The TOR measurements with CLARA started at the end of 2019, soon after solar measurements were able to be resumed with CLARA. As an example, Figure 1 shows the first four orbits of unfiltered Earth observations obtained with CLARA on 5 December 2019. The observations clearly exhibit some variability which might be due to the unstable platform.

One parameter that plays an important role is the temperature of the heat sink. Figure 2 shows this parameter on 3 March 2020. The plot indicates that the temperature drops during the time when CLARA is in eclipse and then rises as soon as the platform sees the Sun again.

While NorSat-1 is fine-pointed to the Sun when the solar measurements are obtained, the platform is only inertia-stabilised for the remaining part of the orbit. Therefore, a careful filtering of the pointing will be needed to make sure only measurements are used in the final data product that qualitatively correspond to nadir pointing.

References: Finsterle W., Haberreiter M., Remesal Oliva A.: 2019, CubeSats for measuring the Earth's energy imbalance, EGU2019, 7-12 April 2019, Vienna, Austria, id.19143.

Comparison of Solar Spectral Irradiance Modelling

Margit Haberreiter in collaboration with NSO and NCAR (Boulder, USA)

As part of an ISSI International Team, we compared in detail the uncertainty coming from using standard radiative transfer codes for modelling the variability of the solar irradiance over the solar cycles. The work has been threefold: first we have validated the codes against observations, then compared the spectra for different solar activity features and finally compare the model results-based 3D MHD simulations.

In the first step we compare the syntheses performed using a recently updated version of the COSI code, developed at PMOD/WRC, and the RH code (Uitenbroek, 2001) with the ATLAS3 observations. The results are shown in Figure 1 from which we conclude that the COSI and RH codes agree within the observational uncertainties. Figure 2 then shows the comparison of the COSI and RH codes for the calculation of the absolute contrast of various surface features on the solar disk with respect to the quiet Sun. Shown are the contrast of the network (top panel, Model E), plage (middle panel, Model P) and sunspots (bottom panel, Model S).

While there are some discrepancies, both codes give very good agreement, specifically for the contrast of sunspots. Finally, we have also calculated the contrast from three sets of 3D MHD simulations. A simulation without any magnetic field strength, and simulations with 100 G and 200 G. Figure 3 shows the contrast obtained from these simulations. For the UV spectral range, we obtain a contrast of 1.01 for the 100 G case, and 0.99 for the 200 G case. Further statistical analysis is currently being conducted.

Acknowledgement: We thank the International Space Science Institute, Bern, Switzerland for hosting the International Team on Modeling Solar Irradiance with 3D MHD simulations, led by Serena Criscuoli. This work was kindly supported by Daniel Karbacher.

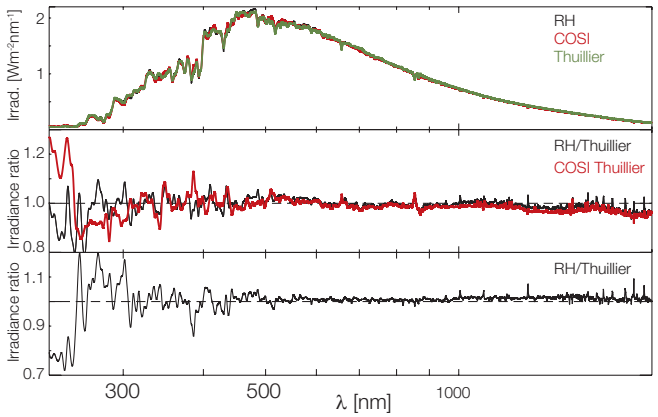

Figure 1. Top and middle panels: comparison of synthetic spectra obtained using the quiet Sun model FAL99-C with the COSI and RH codes, respectively, and the reference solar spectrum by Thuillier et al. (2004). Bottom panel: ratio of spectra obtained using the COSI and RH codes. All spectra have been smoothed with a 3 nm-wide Gaussian function and then interpolated to a common spectral grid, adopted from Criscuoli et al. (2020).

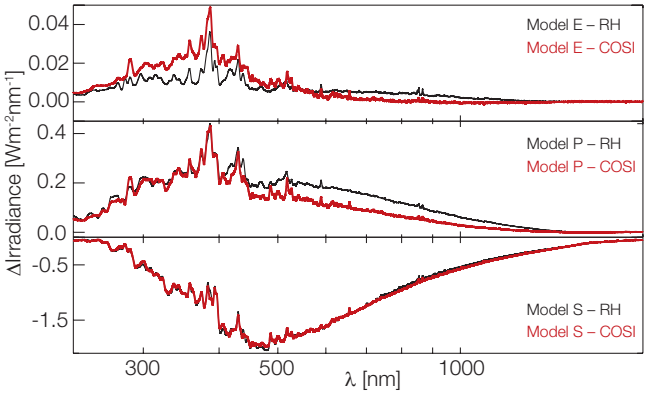

Figure 2. Absolute difference contrast of irradiance computed using atmosphere models representing magnetic features and the quiet Sun model.

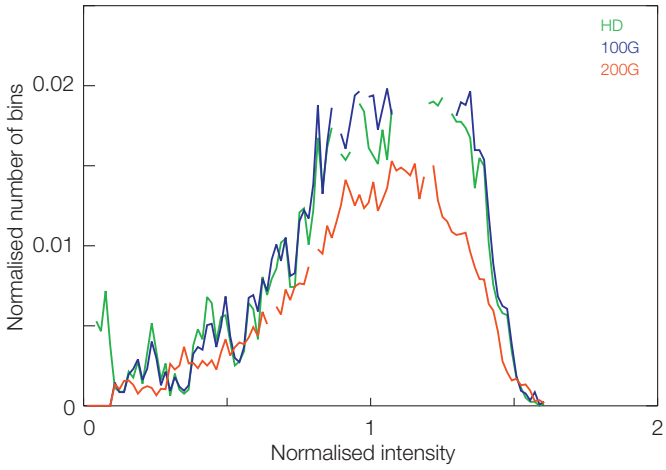

Figure 3. Contrast of the emergent intensity calculated with the updated COSI code based on a HD (green), 100G (blue), and 200G (red) 3D MHD simulation snapshot for the 380 - 390 nm spectral range (adapted from Haberreiter et al., 2020).

References:

Criscuoli S., Rempel M., Haberreiter M. et al.: 2020, Comparing radiative transfer codes and opacity Samplings for solar irradiance reconstructions, Solar Physics, 295, id.50, doi: 10.1007/s11207-020-01614-2

Haberreiter M., Criscuoli S., Rempel et al: 2020, to be submitted.

Thuillier G., Floyd L., Woods T.N., Cebula R., Hilsenrath E., Hersé M., Labs, D.: 2004, Solar irradiance reference spectra for two solar active levels, Advances in Space Research, 34, 256.

Uitenbroek, H.: 2001, Multilevel Radiative Transfer with Partial Frequency Redistribution, Ap.J., 557, pp. 389-398.

Characterisation of a new TSI Radiometer

Alberto Remesal Oliva and Wolfgang Finsterle

A new TSI radiometer detector has been developed in a joint project by PMOD/WRC and Davos Instruments. New coating technology has been applied and a new geometry has been evaluated for a future generation of radiometers.

Instead of the previously used polyurethane or silicon-based absorbers, we are applying a new coating technique of carbon nanotubes (CNTs) by Surrey Nanosystems. This sprayable paint will improve potential future research from long-term measurements of space radiometers as it is expected to degrade less when it is exposed continuously to the sun. As a result, the uncertainty budget will be smaller.

The geometry of the instrument has been changed. The cavity shape, optimised for the previous silicon-based glossy paint, has been modified to a flat receiver with a reflective dome, simplifying the manufacture process without losing, but improving, the optical and electrical properties of the sensor. This new TSI sensor has been characterised at three different wavelengths (375 nm, 532 nm, 633 nm) and the reproducibility of the sensor was tested for the instrument calibration, as shown in Table 1. The values in CNTs refer to the reflectance of the sensor coating without a dome, i.e. the paint itself. The column CNTs + Dome refers to the detector fully implemented with the dome installed over the coating. The transmittance of the receiver is also tested to quantify the losses that may occur through the labyrinth due to imperfect specularity of the dome, as seen in Table 2.

Table 1. Reflectance (with and without dome) of the receiver at three wavelengths.

Wavelength (nm)	CNTs (ppm)	CNTs + Dome (ppm)
375	1927	285
532	1716	289
633	1620	256

Table 2. Transmittance of the receiver at three wavelengths.

Wavelength (nm)	Transmission (ppm)
375	13
532	36
633	7

Figure 1. Left panel: Old cavity installed in previous radiometers. Right panel: the new flat receiver.

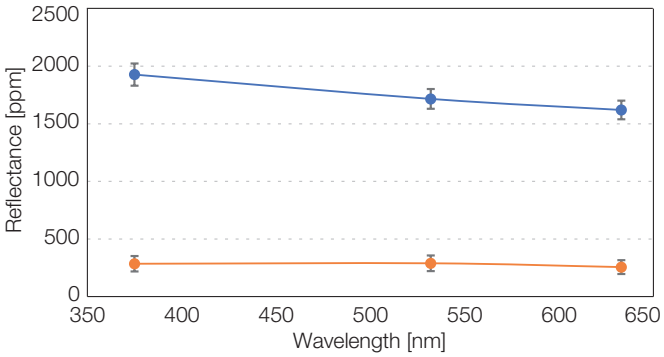

Figure 2. Reflectance of the flat receiver with dome (CNTs + Dome, red line) and without it (CNTs, blue line).

The incident beam shines onto the carbon nanotubes coating. As we have seen in the optical properties, less than 0.2% is reflected. To minimise these losses, we have designed a dome in an ellipsoidal shape (oblate spheroid, an ellipse rotating by its semi-minor axis). The shape was selected because of the optical properties of the ellipses.

Every beam from the focal point reflects on the ellipse and goes to the other focal point. Then, every beam coming from any point between the focal points, will be reflected back into the focal points. When we rotate the ellipse to create the ellipsoid, we generate a “focal circle”. Every beam from inside this circle will be reflected back by the ellipsoid (our dome) into the circle. The circle is the area that we coat, our absorber.

The dome improves the absorptance of the detector by a factor of 6. It is made of polished aluminium with a protective layer to avoid oxidation/degradation. It has been characterised to determine its optical properties and to confirm that the dome will reflect the beam. It has been measured at three different wavelengths (375 nm, 532 nm, and 633 nm) and the reflectivity of the dome is 99.8% (0.2 - 2%). This high value added to the ellipsoidal shape, ensures that the only source of loss from this sensor is the beam that is reflected back through the aperture of the dome that will not be absorbed. However, this can be measured and taken into account for the calibration of the whole instrument.

In summary, a new TSI sensor has been successfully developed and characterised. The new geometry and coating will provide more accurate and stable measurements, even in the long-term. We want to thank and acknowledge Davos Instruments for the collaboration in this work and Innosuisse for the funding.

Impact of Natural Ionisation Sources on Atmospheric Electricity

Eugene Rozanov and Arseniy Karagodin-Doyennel in collaboration with University of Oulu (Oulu, Finland) and Saint Petersburg State University (St. Petersburg, Russia)

We performed and analysed several numerical experiments with the chemistry-climate model (CCM) SOCOL. The atmospheric ionisation rates produced by Radon-222 (Rn-222) and galactic cosmic rays (GCR) were used to calculate the global distribution of the vertical current density (J_z). We also evaluated the impact of the extreme solar proton event (SPE), corresponding to the 774 AD event. We found that the SPE could lead to a large (up to 10 times) enhancement of J_z on a global scale.

The objectives of the work are: i) development of the new model version allowing numerical simulations of ionisation from Rn-222, ii) calculation of the global distribution of the atmospheric conductivity and fair-weather current density (J_z) using the ionisation produced by GCR, SPE, and Rn-222. To reach these objectives, we added emission, decay, and advective transport of Rn-222 to CCM SOCOL v2. For the convective transport, we apply a dry convection scheme for regions with instability layers and wet convection for regions with convective cloudiness (Jacob et al., 1990). When a column of air is unstable with respect to a dry lapse rate, the air gets mixed uniformly within the column. When a column of air is unstable with respect to a wet lapse rate, 50 % of the air in the lowest layer of the column moves directly to the highest layer at which it is stable, with no entrainment of air from intermediate layers. This air mass then descends and mixes homogeneously with the air from intermediate layers.

We performed several 2-year long model experiments for the 2004 - 2005 period for two different cases. For the first case, we used CCM SOCOL to simulate the variability of ionisation rates and conductivity in the clean air (ignoring aerosols and clouds), thus considering only GCR flux and radon, the latter affecting only the lower troposphere. We showed that the radon contribution leads to an enhanced variation in ionisation rates near the surface. In the free troposphere between 300 and 700 hPa, ionisation rates are defined mostly by GCR. For the second case, we estimate the effects of an extreme SPE, corresponding to the 774 AD event (Mekhaldi et al., 2015), on the atmospheric electricity.

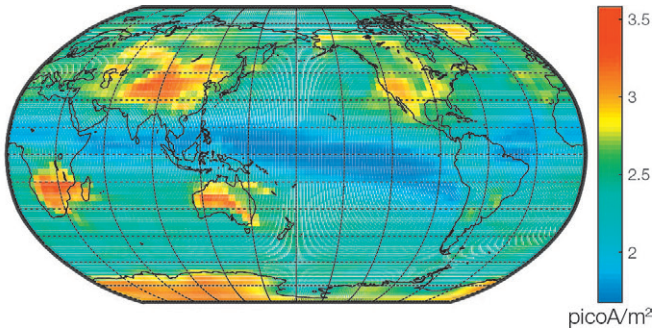

Figure 1. Global map of the vertical current density distribution (pA/m²) for the quiet scenario (GCR+Rn-222).

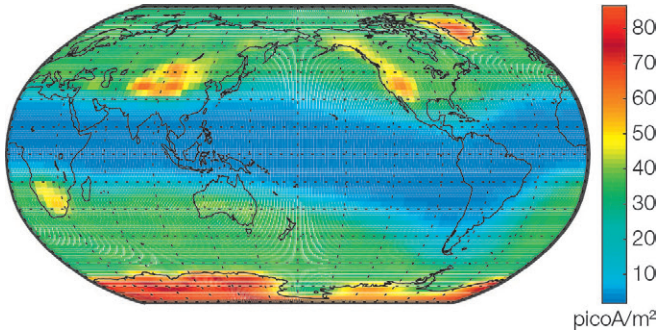

Figure 2. Global map of the vertical current density distribution (pA/m²) for the extreme scenario (GCR+Rn-222+SPE).

Strong SPE are events that occur very rarely, while the quiet scenario, with the ionisation induced only by GCR and Rn-222, is observed during most of the time. In this case (see Figure 1), the atmospheric vertical current density reaches a maximimum (reaching ~ 3.8 pA/m²) in radon source regions, and in the polar regions where the GCR induced ionisation is the highest. The contribution of Rn-222 is essential in middle and low latitude/altitude regions where the GCR-induced air conductivity is significantly lower than that at greater heights/latitudes.

The maps of the fair-weather vertical current are shown in Figure 2 for the scenario with extreme SPE. In this case, J_z is dramatically enhanced, particularly in high-elevated polar regions (Greenland and Antarctica) for the vertical atmospheric current density, which reaches ~90 pA/m² in high-elevated polar regions with only a small enhancement in equatorial regions.

We note that only the effects of the increased ionisation rate due to solar energetic particles were considered here, while other effects, such as the influence of a geomagnetic storm on the ionospheric potential, were not, making this estimate conservative. It is concluded that an extreme solar particle event may lead to a dramatic (a factor of up to 30) increase of the vertical atmospheric current density, reaching ~90 pA/m² in high-elevated polar regions, with much weaker enhancement in equatorial regions.

The work is based on the results obtained during the IU and KG short-term science missions by Ilya Usoskin and Kseniia Golubenko to PMOD/WRC supported by European COST Action CA15211 (ELECTRONET).

References: Jacob D., Prather M.: 1990, Radon-222 as a test of convective transport in a general circulation model, Tellus B: Chemical and Physical Meteorology, 42, 1, 118-134, doi:/10.3402/tellusb.v42i1.15196

Mekhaldi F., et al.: 2015, Multiradionuclide evidence for the solar origin of the cosmic-ray events of AD 774/5 and 993/4, Nat. Commun., 6, 8611, doi:/10.1038/ncomms9611

Past and Future of the Ozone Layer Evolution (POLE): Development of the AOACCM SOCOL v.4.0

Tatiana Egorova, Timofei Sukhodolov, Eugene Rozanov and Arseni Doyenel in collaboration with IAC ETH Zurich

It is now recognised and confirmed that the ozone layer is not only shielding the biosphere from dangerous solar UV radiation, but is also important for the global atmosphere and climate. To understand the past and to predict the future behaviour of the ozone layer, the PMOD/WRC Climate Group is working on the SNF project, Past and Future of the Ozone Layer Evolution (POLE), for 4 years. Here we describe the progress during the first year of the project.

During the first year of the POLE project we completed the development and testing of a model tool to study the ozone evolution. Our new Atmosphere-Ocean-Aerosol-Chemistry-Climate Model (AOACCM) SOCOLv4.0, consists of the Max Planck Institute Earth System model (MPI-ESM) coupled with our chemical and sulphate aerosol microphysics modules. The MPI-ESM contains the middle atmosphere general circulation model ECHAM6, the dynamic ocean model MPIOM, the JSBACH model for terrestrial biosphere and HAMOCC for the ocean´s biogeochemistry.

The chemical and microphysical processes are treated using the latest versions of MEZON and AER modules inherited from CCM SOCOL - AERv2 (Feinberg et al., 2019). The model treats the majority of the processes responsible for the behavior of the ozone layer from the ground up to the mesopause. In addition to the interactive gas-phase/heterogeneous chemistry and bin-resolved stratospheric sulphate aerosol microphysics, the model now can simulate all major components of the climate system. During the first year of the project, several recently discovered halogen-containing ozone depleting substances (hODSs) and very short-lived species (VSLSs), were added to the chemical module.

We have carried out the reference run driven by all available forcing for the 1950 - 2015 period. The comparison of the results

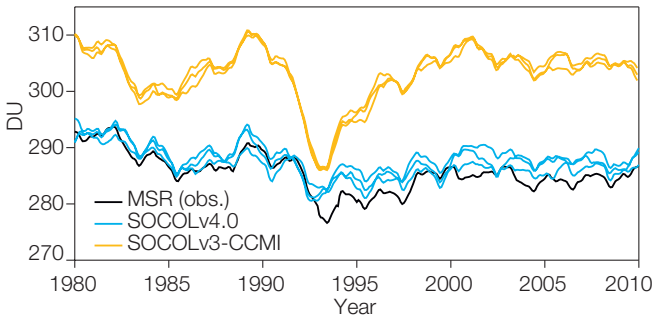

Figure 1. Time evolution of the annual and near global mean total ozone column (DU) from 1980 to 2010 simulated with AOACCM SOCOLv4.0 (blue lines) and SOCOLv3.0 (yellow lines) in comparison with the observational composite MSR. (black line). Multiple lines of the same colour stand for different ensemble members.

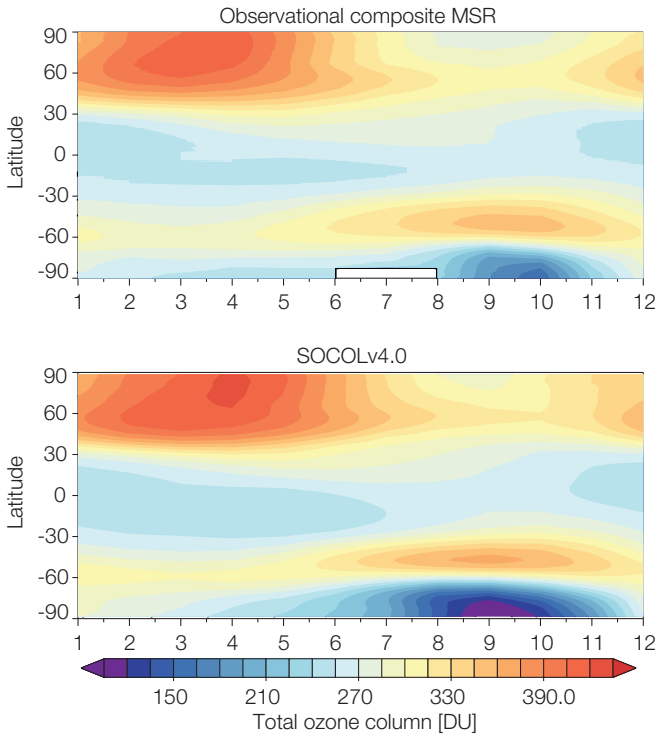

Figure 2. Mean over 1980-2010 seasonal cycle of the total ozone column simulated with ESM SOCOLv4.0 in comparison with observations.

with satellite observations and additional sensitivity experiments revealed some problems in the treatment of the photolysis rates and HNO_3 deposition. After the applied corrections, we carried out a new reference run covering the historical satellite period. Figure 1 shows the evolution of the annual near global mean total column ozone. The results show that AOACCM SOCOLv4.0 reproduces total ozone very close to the observations for those latitudes and outperforms the previous model version.

Figure 2 illustrates the zonal mean seasonal cycle of total column ozone and demonstrates that the model agrees well with the observations for most seasons and locations. There is some overestimation and time shift of the ozone hole that will be addressed in the future. A detailed analysis of other quantities simulated by the model and their validation is in progress and will be discussed in the upcoming paper.

References: Feinberg A., Sukhodolov T., Luo B.-P., et al.: 2019, Improved tropospheric and stratospheric sulfur cycle in the aerosol–chemistry–climate model SOCOL - AERv2, Geosci. Model Dev., 12, 3863-3887, doi: 10.5194/gmd-12-3863-2019.

Response of the Ionosphere to Solar Protons Simulated with the EAGLE Model

Timofei Sukhodolov and Eugene Rozanov in collaboration with IZMIRAN (Kaliningrad, Russia)

The Entire Atmosphere Global Model (EAGLE) and Total Electron Content (TEC) observations were used to evaluate the ionospheric response to Solar Proton Events (SPE). We showed that even though the protons do not deposit a lot of energy directly in the thermosphere, the ionosphere is still significantly affected due to indirect effects coming from below.

It is known that the main part of the solar proton energy is deposited in and below the ionosphere D region, therefore the direct effects of Solar Proton Events (SPE) on the ionosphere E and F layers are not expected to be strong. However, it is also known that chemical and thermodynamic perturbations in the mesosphere and stratosphere can drive the changes in the ionosphere and around 20% of ionospheric variability is caused by the forcing coming from the lower and middle atmosphere, namely through the vertically propagating planetary waves, atmospheric tides, and gravity waves (Forbes et al., 2000).

The study of this complex vertical coupling requires models that allow an uninterrupted calculation of the wave propagation from the formation region to their breaking in the thermosphere and the corresponding atmosphere–ionosphere feedbacks. Our recently developed Entire Atmosphere Global Model (EAGLE) perfectly fits these requirements. EAGLE consists of the chemistry-climate Hamburg Model of the Neutral and Ionised Atmosphere (HAMMONIA) and Global Self-consistent Model Thermosphere, Ionosphere, Protonosphere (GSM TIP) model, and has been recently tested for the sudden stratospheric warming conditions (Klimenko et al., 2019).

For this study, we carried out a set of numerical simulations for SPE in January 2005, which was one of the strongest directly observed events. As shown in Figure 1, it consisted of a sequence of sub-events with a different proton energy spectrum and fluxes. The two strongest cases took place on 17 and 20 of January. The first one was characterised by a large flux of solar protons with energies peaking at 10 MeV, while the second had a lower flux but a harder spectrum with a peak at 100 MeV. The ionisation rates of these two events maximised at about 60 km and 40 km, respectively.

The model results revealed a notable increase in the critical frequency of the equatorial and northern high-latitude F2 layer (foF2) after the SPE on 17 January, while the 20 January proton event did not lead to any additional significant changes. FoF2 is a measure of the highest frequency of radio signal that may be reflected back by the F2 layer, and it is associated with the ionospheric peak electron density in the F2 layer. An increase of foF2 at high latitudes is attributed to the effect of direct ionisation of a neutral gas by softer protons, which are present in small amounts during SPE. However, the tropical signal cannot be caused by protons directly and might be the result of dynamical processes initiated by high latitude direct proton effects in lower layers of the atmosphere. In particular, the mesospheric and upper stratospheric high-latitude chemistry modulation by protons would cause a local disturbance of the temperature. This local temperature anomaly would further modulate the dynamics of this region and therefore the propagation conditions for atmospheric waves.

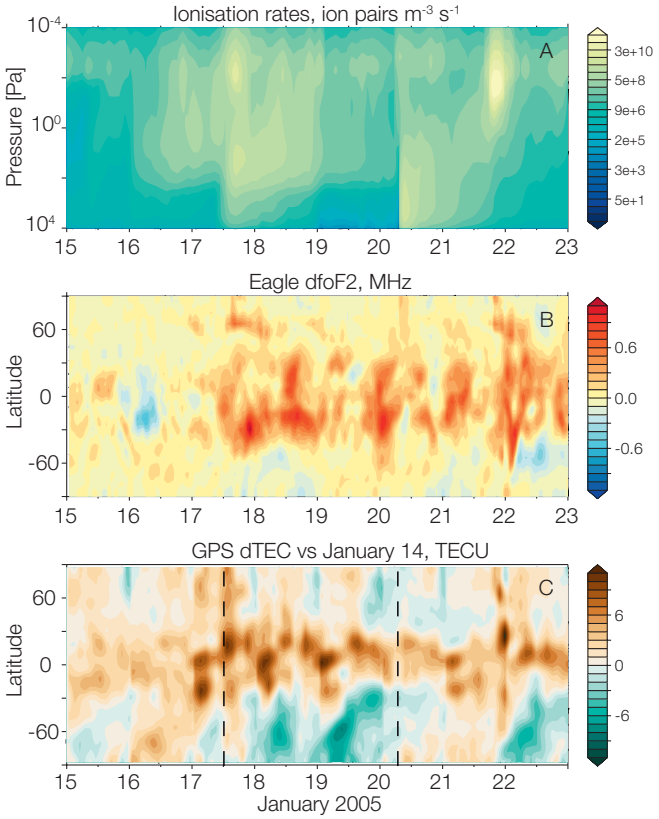

Figure 1. Upper panel: Northern polar cap mean proton ionisation rates provided by the AIMOS model. Middle panel: modelled changes of the ionospheric F2 layer critical frequency with respect to quiet conditions. Lower panel: GPS measurements of changes in the Total Electron Content (TEC) with respect to quiet conditions.

Ionospheric disturbance at low latitudes is also well pronounced in the GPS TEC data showing a good qualitative agreement with the modelled foF2 response. Detailed analysis of the involved feedback chains is still ongoing along with a paper in preparation.

References: Forbes J.M., Palo S.E., Zhang X.: 2000, Variability of the ionosphere, J. Atmos. Sol. Terr. Phys., 62, 685-693.

Klimenko M.V., et al.: 2019, Identification of the mechanisms responsible for anomalies in the tropical lower thermosphere/ionosphere caused by the January 2009 sudden stratospheric warming, J. Space Weather Space Clim, doi: 10.1051/swsc/2019037

The Role of Iodine Chemistry in Stratospheric Ozone Depletion

Arseniy Karagodin-Doyennel, Eugene Rozanov, Tatiana Egorova, and Timofei Sukhodolov in collaboration with IQFR-CSIC (Spain), NCAR (USA), NCAS (UK), IAC ETH Zurich (Switzerland)

We have added gas-phase iodine chemistry to our chemistry-climate model (CCM) SOCOL. The results reveal a strong iodine induced ozone depletion in the tropical troposphere. However, the analysis of the total column ozone shows that the added iodine cycle reduces the ozone by only about 3%. Stratospheric injection of iodine from a volcanic eruption leads to a severe (up to 50%) ozone loss over the polar lower stratosphere.

The main objective of this study is to simulate the total amount of iodine in the atmosphere as well as to clarify the role of iodine chemistry in stratospheric ozone depletion, which is still rather uncertain. We addressed the effects of reactive iodine on global ozone climatology, and the long-term forecast of this effect assuming an increase of the iodine emissions rate in the future as well as the sensitivity of the ozone to volcanic iodine.

The new CCM SOCOL AERv2-iodine model is CCM SOCOL AERv2 with an extended iodine gas-phase chemistry scheme, organic and inorganic iodine emissions, transport, wet/dry deposition and photolysis rates of iodine species. The iodine chemistry scheme consists of four iodine source gases (ISG), nine product gases (PG) and two mixed species (HOI/I_2) which are both being emitted and produced in the atmosphere. Overall, 13 iodine species are included in the chemistry module of CCM SOCOL. The organic emissions of CH_3I and CH_2I_2 are originally taken from the GEOS-Chem study presented by Ordonez et al. (2012). Inorganic HOI/I_2 emission fluxes are calculated via an incorporated numerical parameterisation from MacDonald et al. (2014) which depends on the surface ozone concentration, wind speed, and sea-surface temperature.

We conducted a series of experiments to estimate the potential of iodine as an ozone-depleting substance, and the stratospheric ozone response to volcanic iodine. In the simulation of the ozone layer response to the volcanic iodine, injected HI is assumed to be equal to 0.3% of SO_2 emissions from the Mt. Pinatubo eruption. Experiments with volcanic iodine consisted of six ensemble members covering the 1990 - 1995 period. The results of this experiment are presented in Figure 1. The annual-averaged maximum of ozone loss is up to 40%, with a higher loss over the southern polar region with maxima located in the lower polar stratosphere. In the bottom panel, the transport of volcanic iodine after the Pinatubo eruption is presented as a latitudinal distribution at the 100 hPa pressure level. The largest amount of total iodine is seen over the southern polar region during austral winter. Thus, the analysis shows that the effect of volcanic iodine is rather strong even if a small amount is being injected into the stratosphere.

A more accurate assessment will require using a more advanced deposition scheme and heterogeneous chemistry of iodine on cloud ice particles that could lead to a total iodine increase in the lower stratosphere, resulting in a noticeable ozone depletion

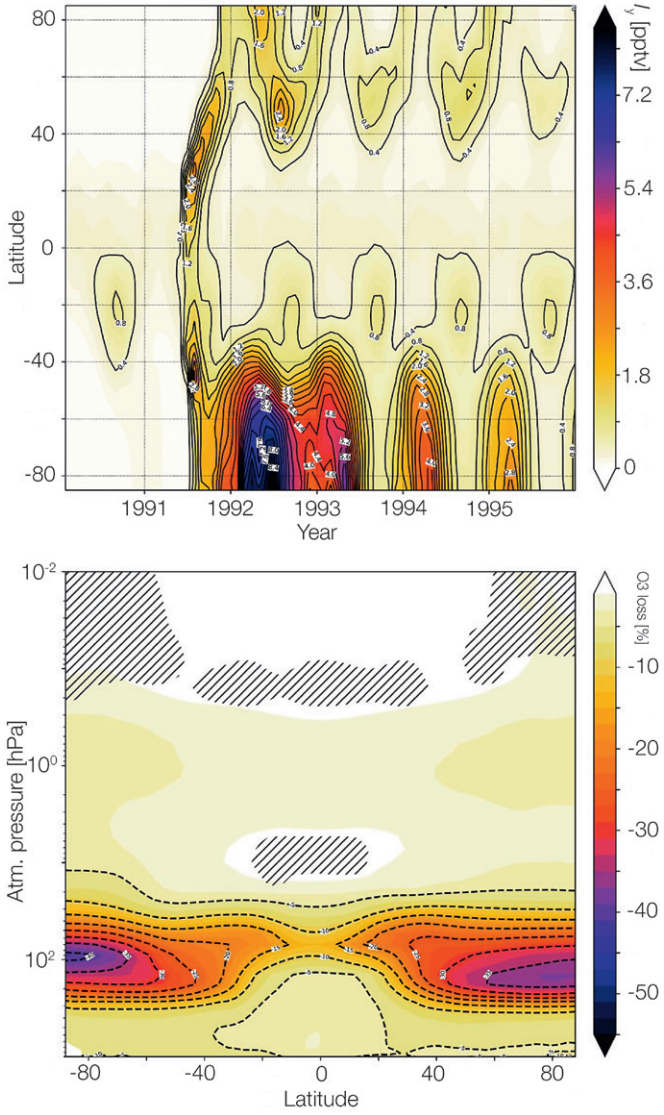

Figure 1. Upper panel: The latitudinal distribution of total iodine from an experiment with volcanic iodine during 1991 - 1995 at the 100 hPa pressure level. Lower panel: The response in ozone mixing ratio to volcanic iodine for 1992 - 1995.

there. We intend to continue this work by including heterogeneous reactions involved in the iodine ice-recycling mechanism since this mechanism could enhance the iodine content in the lower stratosphere (Saiz-Lopez et al., 2015).

References:

MacDonald S., Gómez Martín J., Chance R., et al.: 2014, Atmos. Chem. Phys., 14, 5841-5852, doi:10.5194/acp-14-5841-2014

Ordóñez C., Lamarque J.-F., Tilmes S., et al.: 2012, Atmos. Chem. Phys., 12, 1423-1447, doi:10.5194/acp-12-1423-2012

Saiz-Lopez A., Baidar S., Cuevas C., et al.: 2015, Geophys. Res.Lett.,42,6852-6859, doi:10.1002/2015GL064796

The ^{10}Be Deposition after the Solar Proton Event on 23 February 1956

Eugene Rozanov and Timofei Sukhodolov in collaboration with University of Oulu (Finland), St. Petersburg State Univ. (Russia)

We simulated the ^{10}Be deposition in ice for several sites after the solar proton event on 23 Feb. 1956. We used the chemistry-climate model (CCM) SOCOL and ^{10}Be production rates calculated with a revised integral energy spectrum. The results showed that the ^{10}Be response is hardly distinguishable from the background deposition defined by galactic cosmic rays and local meteorological conditions even for such strong events.

We simulated production, transport and deposition of ^{10}Be during 1950 - 1960. This period covers almost one solar cycle, and includes the solar activity maximum of the 19th cycle as well as the solar proton event in February 1956. The effects of galactic cosmic rays (GCR) were treated using the solar modulation potential (Usoskin et al., 2017) which had previously been used for the solar forcing calculation of the 6th phase of the IPCC Coupled Model Intercomparison Project (CMIP6). The necessary parameters of the SPE 1956 were obtained using the most recent flux and energy spectrum reconstructions. We assumed that all SPE-related ^{10}Be production occurred during one day on 23 Feb. 1956. Vertical profiles of ^{10}Be production by GCR and SPE for all considered geographical locations and days were calculated using the ^{10}Be yield function (Poluianov et al., 2016).

Advective transport, and wet and dry deposition of the ^{10}Be produced by GCR and SPE were calculated with CCM SOCOL v3. The applied model set-up was identical to the study of the ^{10}Be response to SPE in 774 CE (Sukhodolov et al., 2017). However, the applied boundary conditions (e.g., sea surface temperature, sea ice concentration, greenhouse gas concentration, land use, geomagnetic field strength etc.) were taken for the current period of interest, 1940 - 1960. The model run was initiated in 1940 to reach a proper ^{10}Be distribution in 1950. In the model, we treated GCR and SPE-produced ^{10}Be as different species to better understand their production, transport and deposition.

The simulated daily deposition flux of ^{10}Be (atoms/cm^2/sec) was stored for several drilling sites separately for the GCR and SPE-produced components. Figure 1 (left panel) demonstrates that the simulated deposition flux of the GCR-related component is very noisy due to peculiarities of the local weather patterns. However, several interesting features, such as the seasonal cycle driven by seasonally dependent intrusions of stratospheric air and the inverted solar cycle, are clearly visible. Almost all blue curves reach their maximum values around 1955 which is close to the minimum of the 19th solar cycle. It should be noted that the magnitude of the simulated ^{10}Be deposition seasonal variability exceeds the 11-year cycle related variability in most of the sites, while short-term spikes have a similar range.

The simulated ^{10}Be deposition related to the SPE is shown by red curves in Figure 1, and is not distinguishable from the short-term seasonal and regional scale variability of the GCR-related field. This fact does not make high-resolution ^{10}Be data very useful in the search for SPE signals.

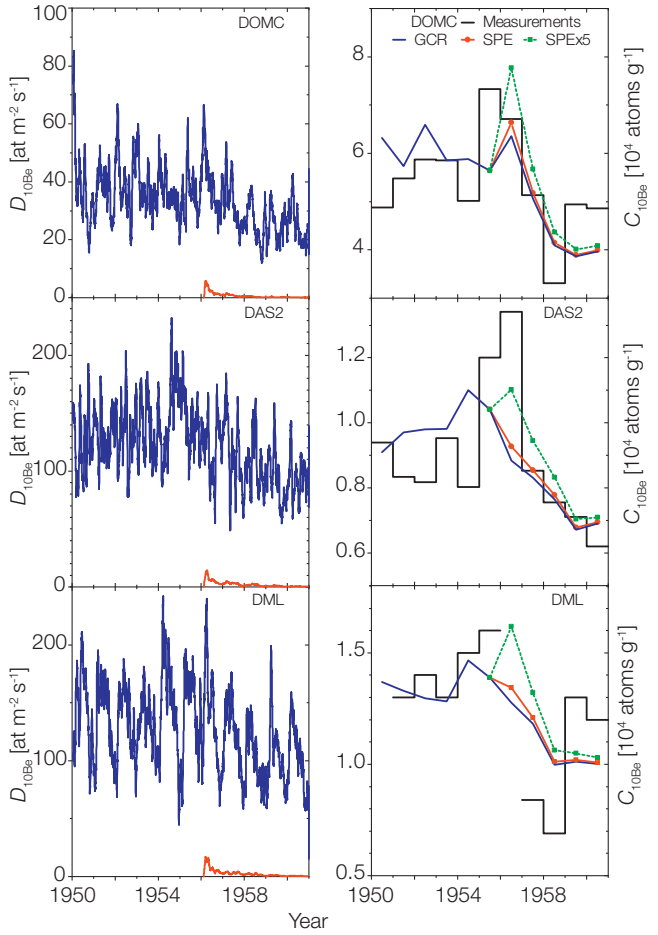

Figure 1. Left panel: Deposition flux of ^{10}Be for the three ice core locations simulated here using CCM SOCOL for the 1950 - 1960 period. Blue lines illustrate the deposition flux of GCR-produced ^{10}Be, while the red lines show the SPE contribution. All curves are smoothed 31-day running mean values. Right panel: Annual mean concentration of ^{10}Be in ice cores from different sites. The measured values are shown in black. Simulated values are shown in blue (GCR only), red (GCR+SPE) and green (GCR + SPE scaled up 5 times).

This conclusion is supported by the comparison of the simulated and observed ^{10}Be concentrations in ice shown in Figure 1 (right panel). It is clearly seen that the SPE signal illustrated by the difference between the red and blue curves is extremely close to the background concentration produced by GCR. Figure 1 also shows that a SPE signal can only be detected for much stronger events.

References:

Poluianov S., et al.: 2016, Production of cosmogenic isotopes ^{7}Be, ^{10}Be, ^{14}C, ^{22}Na, and ^{36}Cl in the atmosphere: Altitudinal profiles of yield functions, J. Geophys. Res., 121, 8125-8136. doi: 10.1002/2016JD025034

Sukhodolov T. et al.: 2017, Atmospheric impacts of the strongest known solar particle storm of 775 AD, Sci. Rep., 7, 45257. doi: 10.1038/srep45257

Usoskin I.: 2017, A history of solar activity over millennia, Living Rev. Solar Phys., 14, 3, doi: 10.1007/s41116-017-0006-9

Evolution of the Ozone Layer in the Early 20th Century

Tatiana Egorova, Eugene Rozanov, and Timofei Sukhodolov in collaboration with EMPA

The evolution of ozone in the past is important to know but is largely undetermined for most of the time. Here we address the ozone layer evolution during the early 20th century. For the study, we used the chemistry-climate model SOCOL-MPIOM, and obtained a significant global-scale increase in the total column ozone. We concluded that the total column ozone changes during this period were driven mostly by the enhanced solar UV radiation, while the near-surface ozone followed the evolution of anthropogenic ozone precursors. This finding can be used to constrain the solar forcing magnitude.

To understand the pattern of the ozone layer evolution in the past and define which factors are the most important for the assessment of ozone layer evolution in the future, we used the chemistry-climate model (CCM) SOCOL-MPIOM which is driven by all known anthropogenic and natural forcing agents as well as their combinations (Muthers et al., 2014). We carried out seven 10-member ensemble model simulations covering the 1851 - 1940 period which are listed in Table 1 of Egorova et al. (2020). Here we present only the results of the experiment, "ALL", driven by all available observed and reconstructed forcing agents.

The geographical distribution of the changes in annual mean total ozone from 1910 to 1940, driven by all considered forcing agents, is illustrated in Figure 1. The simulated total ozone changes are positive and statistically significant all over the globe except in the western Pacific. In the tropical and high latitude belts, the changes are about 6 DU. A more pronounced total column ozone trend is found over the middle latitudes in both hemispheres. There, the ozone change from 1910 to 1940 reaches 12 DU (about 4%) over North America, as well as over the northern and southern parts of the Pacific Ocean. Over Europe, the total ozone increase is slightly smaller but still exceeds 10 DU. These areas are the typical locations of the spring maxima of the total column ozone distribution caused by spring-time acceleration of the meridional circulation, transporting ozone down from its production area. Therefore, these changes in the total column ozone can be largely attributed to the increase in the stratospheric production by the enhanced solar UV irradiance.

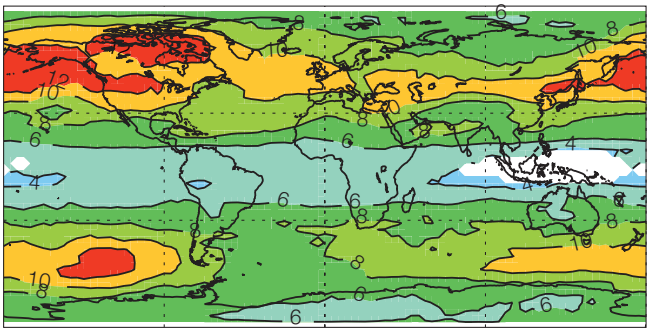

Figure 1. Geographical distribution of the annual mean total column ozone trend (DU/30 years) during the 1910 - 1940 time period from the results of the run, "ALL".

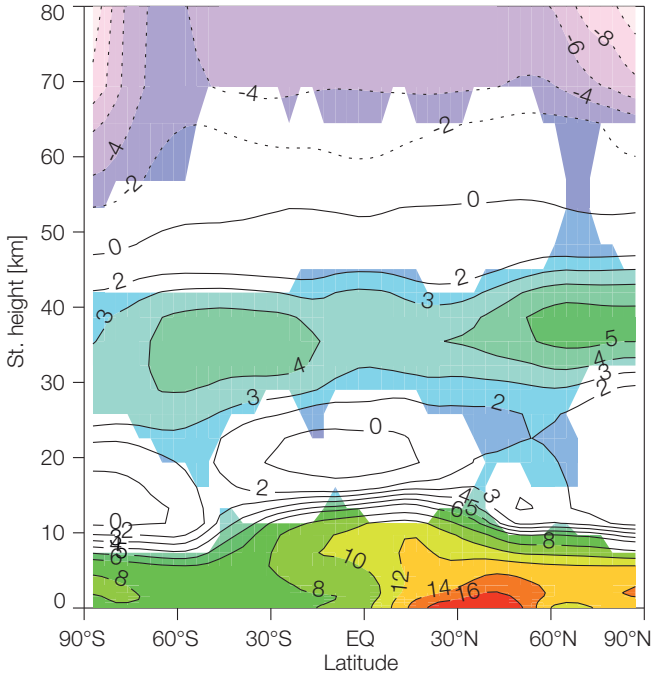

Figure 2. The annual and zonal mean ozone linear trend (%/30 years) during the 1910 - 1940 period for the "ALL" experiment. The area where the trend is significant at a level of 90% or better is shown by the coloured areas.

The ozone trends caused by all considered forcings are presented in Figure 2. Ozone depletion is visible in the entire mesosphere, with maxima in the polar regions of up to 10%. The opposite effect occurs in the middle stratosphere and troposphere, where the ozone concentration increases up to 5% and 20%, respectively. In the lower and upper stratosphere, ozone trends are small and statistically insignificant. More detailed analysis can be found in Egorova et al. (2020).

References: Egorova T., et al.: 2020, Ozone layer evolution in the early 20th century, Atmosphere, 11, 169, doi:10.3390/atmos11020169

Muthers S., et al.: 2014, The coupled atmosphere–chemistry–ocean model SOCOL-MPIOM, Geosci. Model Dev., 7, 2157-2179, doi:10.5194/gmd-7-2157-2014

The HEPPA-III Model-Measurement Intercomparison Initiative: Ionisation and NO Production in the Mesosphere During a Geomagnetic Storm in April 2010

Timofei Sukhodolov and Eugene Rozanov in collaboration with KIT (Germany) and the HEPPA-III community

The international HEPPA-III activity is devoted to the comparison of the observed chemical responses to energetic electrons with available model simulations. We participated in this project with the HAMMONIA chemistry-climate model.

Chemistry-climate model studies suggest that the impact of energetic particle precipitation on stratospheric dynamics might be comparable to the impact of solar spectral irradiance variation. While the proton energy input associated with rare solar proton events and its impact on atmospheric chemistry is well quantified, the energy input of the more frequent energetic electron precipitations events is not well-established yet.

Energetic electrons accelerated in the radiation belts and the magnetotail precipitate into the atmosphere at high geomagnetic latitudes. Primary collisions with the abundant atmosphere lead to dissociation, excitation and ionisation of the most abundant species, N_2, and O_2 or O depending on altitude. This leads to a chain of reactions, changing the neutral atmosphere, e.g., by forming nitric oxide (or nitrogen oxides) followed by catalytic ozone loss. Ozone changes the radiative balance of the atmosphere, initiating a chain of radiative-dynamical coupling mechanisms which affects atmospheric dynamics over large areas, from high to mid-latitudes, and down to tropospheric weather systems. This type of geomagnetic forcing has therefore been recognised as part of the natural forcing of the climate system, and recommendations for implementation of this forcing into chemistry-climate models, were given for the first time for CMIP6 model experiments (Matthes et al., 2017).

However, recent studies suggest that the ionisation rates recommended for CMIP6 may be underestimated, particularly during periods of strong geomagnetic activity. In this study, we compared nine ionisation rate datasets (including AIMOS, APEEP, and OULU), all based on the POES MEPED electron flux observations before, during and after an isolated geomagnetic storm accompanied by strongly enhanced substorm activity in April 2010. Model runs with four chemistry-climate models (WACCM, HAMMONIA, EMAC, KASIMA) were carried out with a subset of these ionisation rate datasets for the period 16 March to 30 April 2010, covering the storm onset, main phase, and recovery. Model results are compared to observations of nitric oxide (NO) in the mesosphere and lower thermosphere (60 - 120 km) from three satellite instruments (SOFIE/AIMS, SCIAMACHY/ENVISAT, MIPAS/ENVISAT). In Figure 1, we show the comparison of the SOFIE NO observations with the multi-model mean using three ionisation rate forcings. All models and forcings tend to agree around the mesopause but deviate in other regions due to different specific reasons. Two papers, discussing in detail the processes, the datasets, the models, and the results are now in preparation.

References: Matthes K., et al.: 2017, Solar forcing for CMIP-6. Geosci. Model. Dev., 10, 2247-1047 2302. doi: 10.5194/gmd-10-2247-2017.

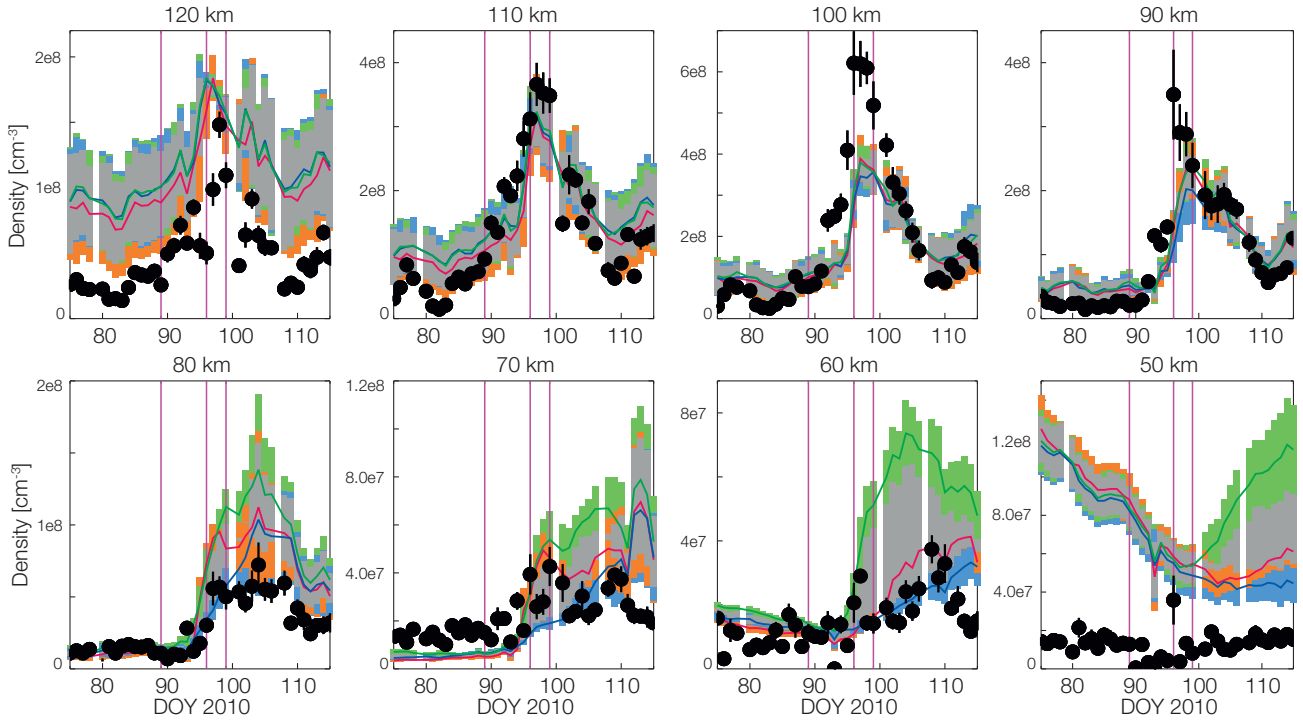

Figure 1. Comparison of SOFIE (black dots) daily mean NO densities (cm^{-3}) from 16 March 2010 (day 75) to 25 April 2010 (day 115) in 10-km steps from the lower thermosphere (120 km) to the mid-mesosphere (60 km) in the Southern hemisphere to multi-model mean (MMM) results of the three core model exptss using ionisation rates from AIMOS (green), APEEP (blue), and OULU (green). SOFIE error bars: one standard deviation. Shaded areas mark the standard error of the mean, grey: all model expts, orange: AIMOS, light blue: APEEP, light green: OULU. The purple lines mark 30 March, 6 and 9 April.

The Response of Mesospheric H_2O and CO to Solar Irradiance Variability in Models and Observations

Arseniy Karagodin-Doyennel, Eugene Rozanov, and William Ball in collaboration with LIM (Germany), EMPA (CH), NASA LRC Hampton (USA), Inst. Atmos. Phys. (Germany), Inst. Meteor. Atmos. Dyn. (Germany), ECCC (Canada), IAC ETH Zurich (CH), NCAR (USA), Priestley IAC (UK)

We retrieve the mesospheric H_2O and CO response to solar irradiance variability from the Chemistry-Climate Model Initiative (CCMI-1) models and satellite data using multiple linear regression (MLR) analysis. Our results show a well-pronounced and statistically robust solar signal in mesospheric H_2O and CO. Results from CCMI-1 models generally agree with observations and reproduce an expected negative and positive correlation for H_2O and CO, respectively, with solar irradiance.

We present an MLR analysis of the simulations with several CCMI models performed in a specified dynamics mode for the period 1984 - 2011 and available observations from UARS/HALOE (1991 - 2004) and Aura/MLS (2005 - 2018). The MLR method is used here to retrieve a solar signal in H_2O and CO in the mesosphere as well as to quantify the agreement of the solar signal in chemistry-climate models (CCMs) with the observations. It allows potential model limitations to be revealed, including transport in the middle atmosphere (dynamic), absence (or poor parameterisation) of thermospheric source, photochemistry and chemical production or loss of considered species.

H_2O and CO were chosen for this study since they are highly sensitive to solar irradiance variations in the mesosphere (Remsberg et al., 2018; Lee et al., 2018). To perform a model inter-comparison and evaluate responses in mesospheric H_2O and CO, output data from the following were chosen for the period 1984 - 2011: i) CMAM, ii) EMAC (with two different vertical resolution settings: EMAC-L47MA and EMAC-L90MA), iii) CCM SOCOLv3, and iv) CESM1-WACCM from reference REF-C1SD experiments with specified dynamic.

Figure 1 shows the time-series of H_2O and CO averaged over the tropics (20°N - 20°S) at 0.01 hPa from CCMI-1 models and observations with the UARS/HALOE and Aura/MLS instruments. As seen in Figure 1, there is a clear response of H_2O and CO to F10.7 index variation (right y-axis). In the case of H_2O, there is a pronounced decrease in the concentration during the solar maximum, but it is opposite for CO, which increases during the solar maximum.

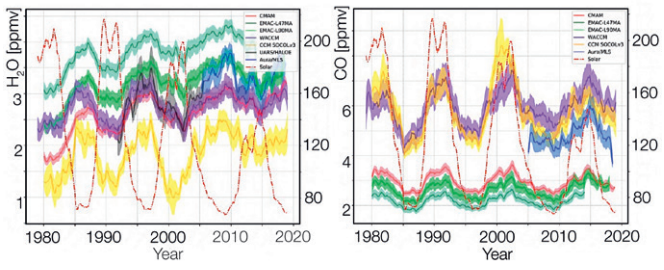

Figure 1. Time-series of H_2O and CO mixing ratios averaged over 20°N - 20°S from CCMI-1 models, and measured with HALOE and MLS instruments at 0.01 hPa. Shaded areas show one standard deviation of the zonal means.

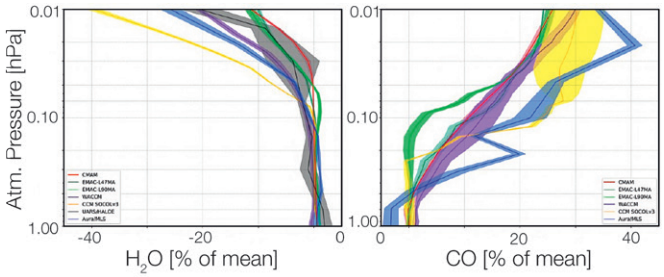

Figure 2. Vertical profiles of the tropical mean response of H_2O and CO (presented as % of mean) to solar irradiance variability from CCMI-1 models (1984 - 2011) as well as from HALOE (1992 - 2004) and MLS (2005 - 2018) observations. The uncertainty is shown with shaded areas.

The MLR model used in this study is based on the x-regression tool consisting of the Python statistical models library coupled with the "xarray" package for multi-dimensional arrays. As predictors, we use the solar F10.7 index (solar flux units), El Nino–Southern Oscillation (ENSO) ERSSTv5 Nino4 index (Kelvin degrees), two wind speed proxies for QBO at 30 and 50 hPa (m/s) and stratospheric aerosol optical depth (SAOD) (dimensionless). The de-seasonalised time-series of response variables are reconstructed as a function of time (t) by the MLR model as follows:

$$Y(t) = \alpha + \beta SOLAR(t) + \gamma ENSO(t) + \delta 1QBO30(t) + \delta 2QBO50(t) + \varepsilon SAOD(t) + \zeta TREND(t) + e(t)$$

Figure 2 shows the tropical response of H_2O and CO (in % of mean) to solar irradiance variability. The inter-comparison showed problems in current simulations, which require a process-oriented validation involving model teams.

Our study has demonstrated how state-of-the-art models represent solar signal responses in comparison with observations and showed some discrepancies of the model simulation results. Thus, it is important to continue the model inter-comparison studies to improve the representation of the solar signal in global chemistry-climate models.

References: Lee J., Wu D., Ruzmaikin A., Fontenla J.: 2018, Solar cycle variations in mesospheric carbon monoxide, JASTP, 170, 21-34, doi: 10.1016/j.jastp.2018.02.001

Remsberg E., Damadeo R., Natarajan M., Bhatt P.: 2018, Observed responses of mesospheric water vapor to solar cycle and dynamical forcings, JGR Atmos., 123, 3830-3843, doi:10.1002/ 2017JD028029

Diurnal Cycle of the Stratospheric Ozone Long-Term Trends

Eugene Rozanov and Will Ball in collaboration with Meteoswiss

We compare the long-term stratospheric ozone trend obtained with high temporal resolution measurements from the Payerne microwave radiometer (MWR) and the chemistry-climate model (CCM) SOCOLv3.0. Analysis of the local solar time (LST) dependent trends for the observed and simulated O_3 allowed to conclude, that the constant shift of sampling time does not have a significant influence on stratospheric ozone trends for the 2000 - 2018 period.

The recovery of the ozone layer is widely discussed in the literature. After 1998, stratospheric ozone trends calculated from ground-based instruments, satellite datasets and chemistry-climate models do not agree, which makes it difficult to clearly confirm stratospheric ozone recovery. Addressing this problem requires careful analyses of the potential problems of the satellite and ground based instruments involved in the trend analysis. In particular, the change of sampling time could have an influence on the estimation of ozone trends (Damadeo et al., 2018).

The variation of the trends with LST should be characterised to establish the representativity of the trends extracted from different satellite and ground-based instruments. This problem can be tackled using high cadence stratospheric ozone measurements with the SOMORA microwave radiometer (MWR) in Payerne and hourly output of CCM SOCOL, which allows the dependence of the long term ozone trend on the local solar time (LST) to be estimated, and to understand the mechanisms regulating this process.

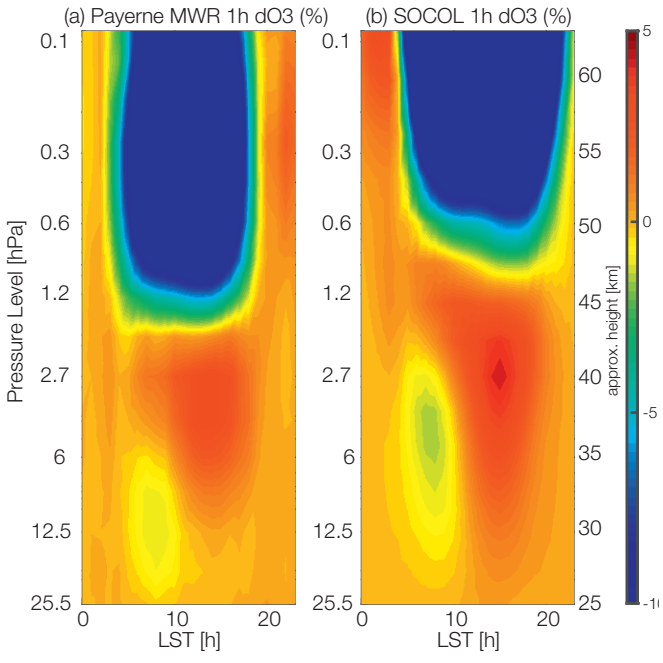

Figure 1. Annual mean O_3 daily cycle in % of midnight value measured by: (a) Payerne MWR and (b) simulated by SOCOL v3.0 with a time step of 1hr.

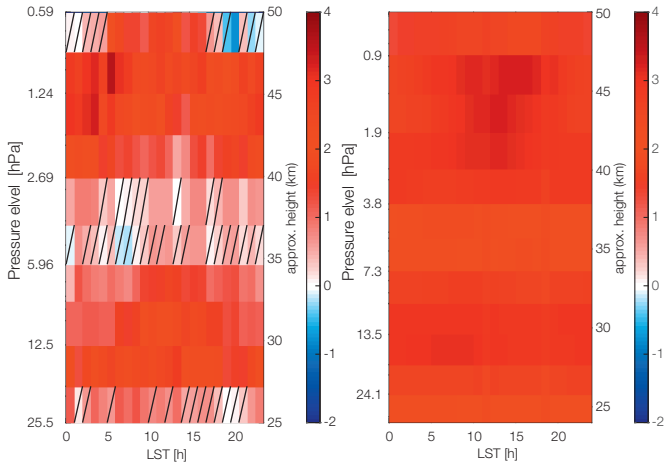

Figure 2. The long-term ozone trends as a function of LST from the MWR (left panel) and CCM SOCOL (right panel). Trend estimates not significantly different from zero at 95% are hatched.

The observed and simulated climatological means agree within 15% in the upper stratosphere in about the 1 hPa layer. In the mesosphere, the disagreement is larger during the nighttime, reaching up to 40% at 0.2 hPa. The annual mean diurnal cycle (in % relative to the daily mean) of ozone over Payerne from the MWR and CCM SOCOL data is illustrated in Figure 1. The model reproduces the shift of the diurnal cycle phase, but the transition height is not perfectly reproduced due to the decrease of the model vertical resolution with height. The agreement between the Payerne MWR and SOCOL v3.0 ozone concentrations between 30 to 50 km (not shown) and their diurnal variations (see Figure 1) allows the dependence of long-term ozone trends on LST from both datasets to be compared.

Figure 2 illustrates the long-term ozone trends as a function of LST from the MWR and CCM SOCOL. The results demonstrate that stratospheric ozone trends do not depend on LST at the 95% confidence level. Significant long-term changes of the diurnal cycle are not observed even if we look at the altitude difference of the ozone diurnal cycle minimum (morning) and maximum (afternoon). Our estimates of the dependence of ozone long-term trends on LST allow to conclude that systematic sampling differences between instruments cannot explain significant differences in trend estimates for the 2000 - 2018 period in the stratosphere. A more detailed description of the results can be found in Maillard Barras et al. (2020).

References:

Damadeo R., Zawodny J., Remsberg E., et al.: 2018, The impact of non-uniform sampling on stratospheric ozone trends derived from occultation instruments, Atmos. Chem. Phys., 18, 535-554, doi: 10.5194/acp-18-535-2018

Maillard Barras E., Haefele A., Nguyen L., et al.: 2020, Study of the dependence of stratospheric ozone long-term trends on local solar time, Atmos. Chem. Phys. Discuss., doi:10.5194/acp-2020-101, in review.

Preparations for the Interactive Stratospheric Aerosol Model Intercomparison Project (ISA-MIP)

Timofei Sukhodolov and Eugene Rozanov in collaboration with the ISA-MIP community

An interactive stratospheric aerosol model intercomparison "ISA-MIP" has been established as part of the SPARC SSIRC project (Timmreck et al., 2018) to compare interactive stratospheric aerosol models against a range of satellite and in-situ observations. The project aims to improve the model and to provide a sound scientific basis for future studies of stratospheric aerosol. We are participating in this activity with our SOCOL-AERv2 model (Feinberg et al., 2019).

The stratospheric aerosol layer is a key component of the climate system. It affects the radiative balance of the atmosphere directly through interactions with solar and terrestrial radiation, and indirectly through its effect on stratospheric ozone. Therefore, it is important to understand how the stratospheric aerosol layer could drive future climate change and vice-versa. The SPARC core project, SSiRC (Stratospheric Sulfur and its Role in Climate), coordinates international research activities on modelling and observation of stratospheric sulphate aerosols (and precursor gases) to assess its climate forcing and feedback.

Chemistry-Climate models with interactive aerosol microphysics help to understand how stratospheric aerosol perturbations impact the climate system, as they interactively account for all the main components involved. At present more than 15 global 3-D stratospheric aerosol models exist. The model development benefits from an increasing number of observations of stratospheric aerosols and precursor gases as well as an improved understanding of processes which govern the variability of the stratospheric aerosol layer. However, a comprehensive model intercomparison has not been carried out to identify the differences among global 3-D models that interactively simulate the stratospheric aerosol size distribution. Studies show important uncertainties related to differences in the sulphur emission (amount and altitude), in transport, chemistry, and removal processes, as well as in the formulation of microphysical processes. Disagreement between various data sets and global aerosol models further indicates that significant questions remain regarding the ability to characterise stratospheric aerosols during volcanically perturbed and unperturbed periods. The ISA-MIP activity was initiated to fill this gap in our knowledge. Four model experiments were designed to answer the following key science questions:

• (Background exp., BG) How large is the quiescent stratospheric sulphate loading and how sensitive are the simulation results to microphysical parameterisations and transport processes?

• (Transient aerosol record, MITAR) Can the models represent the observed increase in the stratospheric aerosol since 2000?

• (Historical Eruptions SO_2 Emissions Assessment, HErSEA) Can stratospheric aerosol observations constrain uncertainties in the initial amount of sulphur injection and the altitude distribution of the three largest volcanic eruptions of the last 100 years?

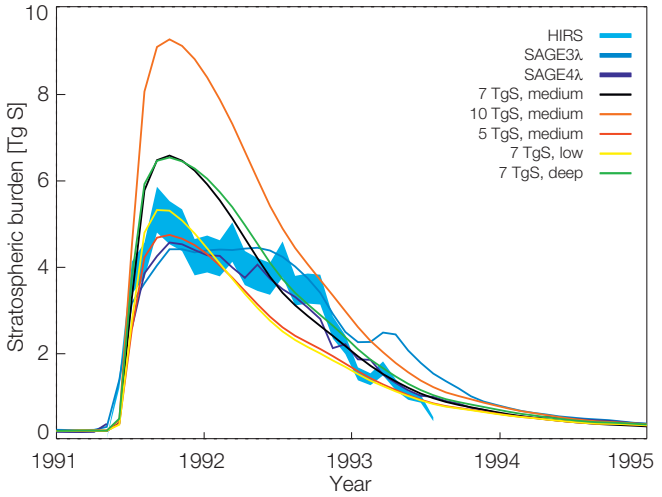

Figure 1. Evolution of model-calculated global stratospheric aerosol burden (Tg of S) compared with the HIRS- and SAGE-II-derived data (SAGE-3,4λ). Light blue shaded area: uncertainties of HIRS. All model experiments are shown as ensemble means.

• (Pinatubo Emulation in Multiple Models, PoEMS) What is the confidence interval for the Pinatubo volcanic forcing simulated by interactive stratospheric aerosol models and which parameter uncertainties are the predictions most sensitive to?

We are participating in all four experiments. Figure 1 illustrates HErSEA Pinatubo simulations with SOCOL-AERv2 performed to investigate the uncertainty in estimates of the injected SO_2 amount and altitude. The Mt. Pinatubo eruption was simulated using three injection amounts (5, 7, and 10 Tg of S) and three injection altitudes (medium at 21 - 23 km, low at 18 - 20 km, and over a deep altitude range of 18 - 25 km). The modelling results are compared to three observational time-series, all of which, however, had technical problems in capturing the first year after the eruption due to a too thick aerosol cloud. The analysis suggests that our model is more realistic with lower emissions and that the altitude of eruption is a critical parameter for the overall volcanic aerosol evolution. A mistake of just 1 - 2 km in altitude can lead to a much faster removal of aerosols from the system. At the moment, we are finalising the experiments, homogenising the output and collecting the post-processed data on the project servers. First model intercomparison papers are expected to be prepared this year.

References: Feinber A., Sukhodolov T., et al.: 2019, Improved tropospheric and stratospheric sulfur cycle in the aerosol–chemistry–climate model SOCOL-AERv2, Geosci. Model Dev., 12, 3863-3887, doi: 10.5194/gmd-12-3863-2019

Timmreck C., et al.: 2018, The Interactive Stratospheric Aerosol Model Intercomparison Project (ISA-MIP): Motivation and experimental design, Geosci. Model Dev., doi: 10.5194/gmd-2017-308

JTSIM-DARA Pointing Measurements

Gregor Hülsen, Daniel Pfiffner, Manfred Gyo, and Julian Gröbner

The pointing of the JTSIM-DARA radiometer was measured four times during its construction in the PMOD/WRC optics laboratory. The final offset of the pointing before shipping relative to the optical axis, defined by a removable alignment cube, is 1.07°/0.67° (β/γ-axis) for the four-quadrant sensor and 0.095°/-0.017° for the radiometer cavity A.

Continuous and precise TSI measurements are indispensable to evaluate the influence of short and long-term solar radiative emission variations on the Earth's climate. PMOD/WRC has constructed JTSIM-DARA (Joint Total Solar Irradiance Monitor - Digital Absolute Radiometer) for the Chinese FY-3E mission. JTSIM-DARA is one of PMOD/WRC's contributions to the almost seamless series of spaceborne TSI measurements since 1978. It will be mounted on the FY-3E satellite, which is the 5th flight unit of the Feng-Yun-3 (FY-3) series. Key aspects of the FY-3 satellite series include collecting atmospheric data for intermediate and long-term weather forecasting and global climate research.

The JTSIM-DARA instrument is a cooperation with CIOMP (Changchun Institute of Optics, Fine Mechanics and Physics of the Chinese Academy of Sciences), and the China Meteorological Administration (CMA). Next to JTSIM-DARA, a solar irradiance absolute radiometer (SIAR) was designed by CIOMP. The JTSIM-DARA design is based on DARA for the PROBA-3 mission as well as the Compact Lightweight Absolute Radiometer (CLARA) onboard NorSat-1. The two JTSIM radiometers are mounted on the sun-tracker of the satellite enabling independent pointing toward the sun whereas the other instruments point toward the earth. As two devices are mounted on the sun-tracker, the pointing of JTSIM-DARA is a critical parameter of the mission. The instrument is currently integrated into the Chinese FY-3E weather satellite and is being made ready for launch in 2020 (http://www.nsmc.org.cn/en/NSMC/ Channels/ FY_3E.html).

Measurements of the pointing of the three JTSIM-DARA cavities relative to each other were performed on the WSG sun-tracker. The pointing relative to a cube alignment mirror was measured at the angular response facility in the WRC optic laboratory. This setup (Figure 1) consists of a 1 kW Xe-Lamp emitting a collimated light beam towards the test device which is mounted on a goniometer about 3 m away from the light source (Hülsen et al., 2007). The variability of the light intensity of a 50 mm^3 cube around the optical axis was characterised prior to the measurements. The homogeneity within this entire cube is 3% and inside a 10 mm^3, below 0.5%. Figure 2 shows the alignment relative to the optical axis using a laser. First, JTSIM-DARA was orientated using the removable alignment cube. Thereafter, one selected cavity and the four-quadrant sensor (4Q) was moved into the center. The measurements where performed by rotation around the β-axis of JTSIM-DARA and after a 90° rotation of the device around the γ axis. The experiment was repeated four times: before the end assembly (1), before (2) and after (3) the vibration tests and before shipping (4).

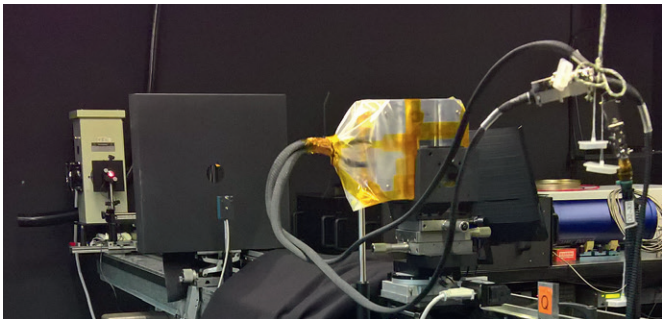

Figure 1. The angular response setup showing the Xe Lamp in the back, a WG305 filter and a baffle in the middle and JTSIM-DARA mounted on the goniometer.

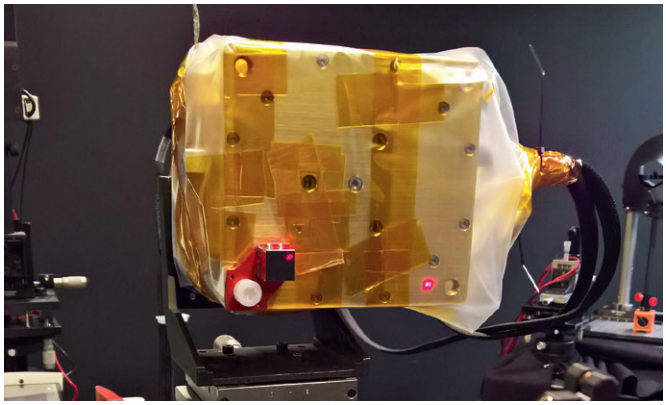

Figure 2. Pointing measurements of JTSIM-DARA, showing the alignment cube in the lower left corner, the three holes of the radiometer cavities in the centre, and the four-quadrant sensor next to the cube.

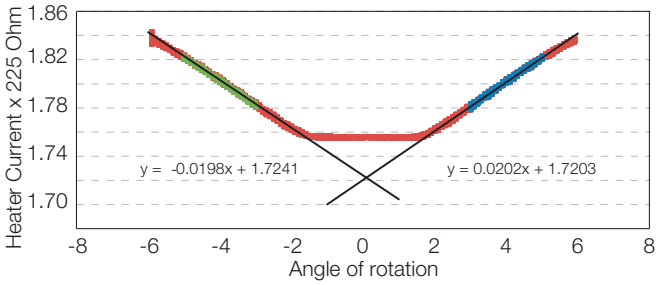

Figure 3. Pointing of the cavity A around the β-axis. The heater current is plotted versus the angle of rotation.

Figure 3 shows results of the pointing measurements of the cavity A. The assembling has a major influence on the optical axis of the sun sensor and the cavity. The β-angle measurements changed after the vibration test. All other measurements are consistent within the estimated uncertainty of ±0.1°. The vibration test did not show any shift of the optical axis defined by the alignment cube. The setup used for the pointing measurements is limited to a ~20 Nm load on the goniometer. A new mechanical setup was constructed to enable loads up to 200 Nm.

References: Hülsen G., et al.: 2007, Characterization and calibration of ultraviolet broadband radiometers measuring erythemally weighted irradiance, Appl. Optics, 46, 5877 - 5886.

Sky Temperature Brightness and Cloud Measurements using a far Infrared Hemispherical Sky Imager

Julian Gröbner and Christine Aebi in collaboration with Meteoswiss

The Infrared Cloud Camera (IRCCAM) measures the effective sky brightness temperatures in the thermal infrared range. From the measurements, the fractional cloud cover and cloud height can be retrieved due to their higher thermal emission compared to the cold sky.

The Infrared Cloud Camera (IRCCAM) consists of an infrared camera sensitive in the 8 - 14 µm wavelength range with a microbolometer detector array of 640 x 480 pixels. A convex gold-plated mirror images the upper sky hemisphere onto the camera to obtain images of the sky radiance and sky brightness temperature with a 1 K uncertainty (Aebi et al., 2018). Furthermore, the sky brightness temperatures can be used to determine the fractional cloud cover by comparison to a clear sky radiance map obtained from a look-up-table (LOT) using surface temperature and humidity measurements. The vertical cloud distribution can also be retrieved from the sky brightness temperatures by assuming a vertical temperature profile (for example from a microwave radiometer or a radiosonde) and a cloud emissivity. Figure 1 shows an image and cloud retrieval on 24 Sep. 2019 from a campaign at Geneva airport.

Since the camera relies on the cloud emissivity itself, cloud properties can also be retrieved during the night-time, allowing the continuous determination (24/7) of the cloud fraction and cloud height at a rate of 1 image/minute or even faster. The cloud height retrieval uses the temperature profile from a co-located microwave radiometer to retrieve cloud height from the relationship between cloud brightness temperature and the temperature-height profile. The cloud height retrieved from the ceilometer and the IRCCAM for a whole day is shown in Figure 2 (cloud emissivity = 1 was assumed). The right panel in Figure 1 shows that clou edges become thinner and therefore their emissivity and corresponding brightness temperature decreases, resulting in an overestimation of the cloud height. While the ceilometer only determines the cloud base in a small patch of the sky, typically close to the zenith, IRCCAM can retrieve the cloud height for the whole upper hemisphere.

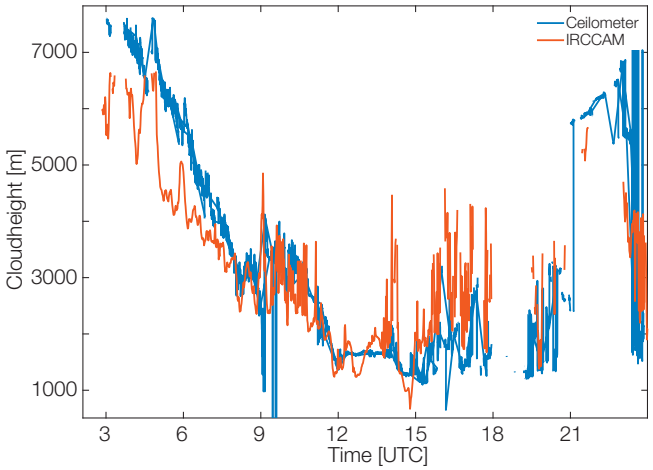

Figure 2. Cloud height from a ceilometer (blue) and IRCCAM (red) on 24 September 2019.

The uncertainty of the cloud height retrieved with IRCCAM depends mainly on the uncertainty of the measured sky radiance (about 1 K) and the gradient in the vertical temperature profile. For example, assuming a standard temperature profile with a decrease in temperature of 6.3 K per 1000 m, the cloud height retrieved from IRCCAM would result in an uncertainty of 159 m when neglecting the impact of the emissivity and the atmosphere lying between the cloud base and the surface. When temperature inversions or very small temperature gradients close to the surface occur, the low lying cloud height cannot be retrieved. Thus, cloud height is best retrieved for mid-level to high clouds, where temperature gradients are pronounced, and the uncertainty of the retrieved cloud height is less significant.

Acknowledgement: We thank the meteorological staff at Geneva airport for the logistical support and availability of the ancillary meteorological data.

References: Aebi C., Gröbner J., Kämpfer N.: 2018, Cloud fraction determined by thermal infrared and visible all-sky cameras, Atmos. Meas. Tech., 11, 5549-5563.

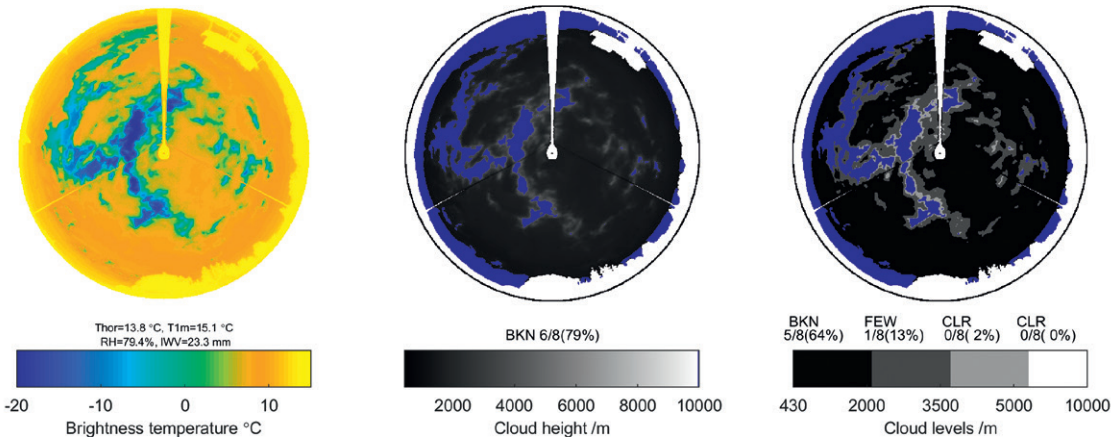

Figure 1. Sky brightness temperature (left panel) and cloud height information (middle and right panels) from measurements of the sky radiance at 16:34 UTC on 24 September 2019, Geneva airport.

Stray-Light Correction Methodology for the Precision Solar Spectroradiometer

Natalia Kouremeti and Julian Gröbner in collaboration with PTB (Germany)

A stray-light correction methodology for the Precision Solar Spectroradiometer (PSR) based on laboratory-measured line spread functions is presented. The radiation from the 2nd and 3rd grating orders is accounted for and the efficiency of the correction is validated using solar and lamp measurement data. The results are compared to those obtained with a PSR equipped with an order-sorting filter and with a Precision Filter Radiometer.

The Precision Solar Spectroradiometer (PSR) is a grating-type array spectroradiometer, developed at PMOD/WRC for spectral solar irradiance measurements in the spectral range from 330 nm to 1030 nm and for the determination of aerosol optical depth. While previous PSR units were built using an order-sorting filter (OSF) in front of the detector, later instruments were constructed without a physical filter, relying instead on post-processing of the measured spectra using a correction method based on line-spread functions (LSF) and extending the method by Zong et al. (2006).

The LSFs were measured at PMOD/WRC throughout the full spectral range of the spectroradiometers using a ns-pulsed OPO system. The LSF measurements were performed over 5 to 6 orders of magnitude by varying the laser beam output power and integration time of the PSR. The measured LSFs of PSR 008 were validated by analogous measurements performed at a similar ns-OPO facility at PTB. The measured LSFs were used to derive a stray-light correction matrix. One problem to be solved was that the wide spectral range of the instrument (about 700 nm) is covered by a detector array with 1024 pixels. As the bandpass is ~2 nm, only few pixels are within LSF peaks. To reduce the related uncertainties, when inverting the LSF matrix, it was first necessary to interpolate the LSFs to a denser pixel grid before building the matrix.

The uncertainty of the stray-light correction has been evaluated by considering: i) the variability of the measured signal and dark counts, ii) the uncertainty resulting from different integration times,

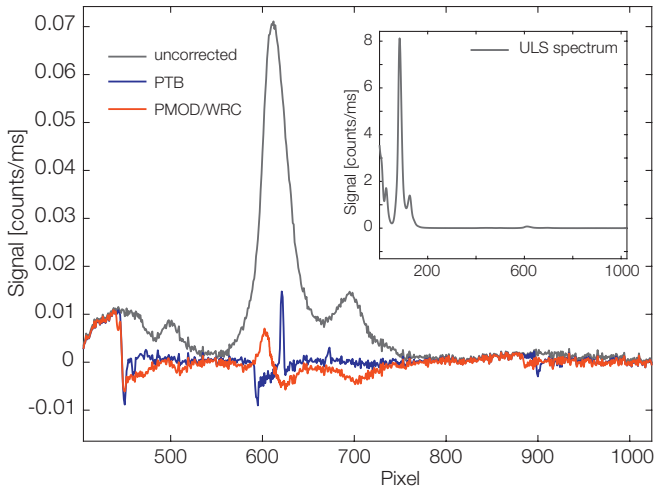

Figure 1. UV-LED source spectrum corrected for the straylight contribution (red: PTB data, blue: PMOD data) and uncorrected spectrum (black).

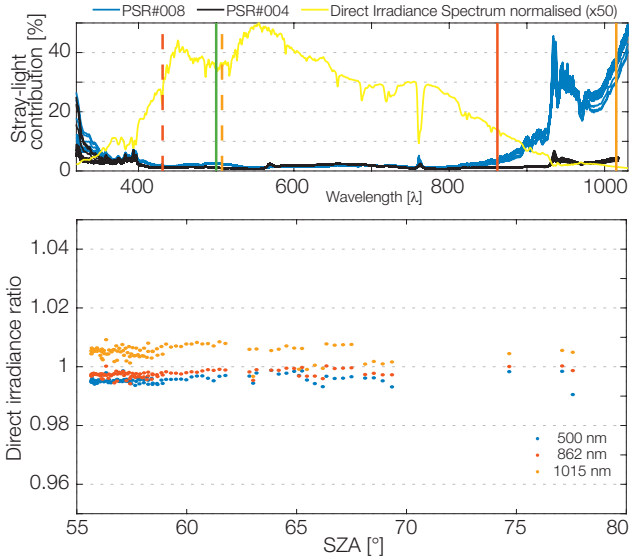

Figure 2. Upper panel: stray-light contribution in the direct solar irradiance spectra measured by PSR#004 (black) and PSR#009 (blue). Lower panel: direct solar irradiance ratio PSR #009/#004 at selected wavelengths.

and iii) merging of saturated and unsaturated measurements. Moreover, wavelength shifts introduce an uncertainty component, especially when correcting for the 2nd and 3rd dispersion orders. The combined uncertainty for measurements on a transfer standard lamp ranges between 0.05% and 1.47% with a median 0.32% (PMOD/WRC Annual Report 2018, pp. 35).

The efficiency of the PSR stray-light correction with respect to the suppression of the radiation from higher dispersion orders (620 nm - 1030 nm) was evaluated using laboratory-based and sun measurement data. More specifically, a UV LED-based source (Sildoja et al., 2018) with an emission spectrum in the range 300 nm - 420 nm was used. The stray-light contribution of 0.8% due to the higher grating orders was able to be corrected by nearly a factor of 10 as shown in Figure 1. Moreover, a comparison of direct solar irradiance spectra measured with both types of PSRs showed agreement to within ±1% when correcting for up to 40% of the stray-light contribution (Figure 2). Similar results were obtained when comparing the solar irradiance at 862 nm and 500 nm from PSR#009 to those measured by a Precision Filter Radiometer, PFR-N24, which is part of the AOD WMO reference PFR-Triad. The comparison of 9724 common measurements covering solar zenith angles from 40° to 75° showed a normalised agreement of within 1% for both wavelengths.

The results lead to the conclusion that a mathematical suppression of the stray-light due to higher grating orders can be realised with an uncertainty of less than 1%, producing results equivalent to those using an order-sorting filter.

References: Gröbner J., Kouremeti N.: 2019, Solar Energy 185, 199-210.
Sildoja M., et al.: 2018, Metrologia 55, S97.
Zong Y., et al.: 2006, Appl. Opt. 45, 1111-1119.

E-Shape: EuroGEO Showcases: Applications Powered by Europe

Stelios Kazadzis, in collaboration with NOA (Greece), MINES ParisTech (France), Transvalor (France), Centre Env. & Dev. Arab Region (Egypt)

E-Shape (https://e-shape.eu/) has received funding from the European Union's Horizon 2020 Research and Innovation Programme (April 2019 - March 2023).

E-Shape aims to bring together Earth Observation and in-cloud capabilities into services for decision-makers, citizens, industry and researchers. EuroGEO, as Europe's contribution to the Global Earth Observation System of Systems (GEOSS), aims to bring together Earth Observation resources in Europe. In E-Shape, 27 pilot applications under seven thematic areas address societal challenges, foster entrepreneurship and support sustainable development, in alignment to the three main priorities of GEO (SDGs, Paris Agreement and Sendaï Framework).

One of the seven thematic areas in E-Shape is Solar Energy. Three pilot studies have started which deal with: solar radiation and energy forecasting, high photovoltaic penetration at the urban scale, and wind energy. PMOD/WRC is leading the "Solar radiation and energy forecasting" pilot that is based on the results of a previous EU funded project: GeoCradle.

The pilot will contribute towards the goals of the EC Renewable Energy Directive that establishes an overall policy for the production and promotion of energy from renewable sources in the EU. Renewables currently account for more than 22% of total global electricity generation, of which more than 400 GW is produced from solar systems (2017). This brings to the fore the simultaneous vital need for improved Earth Observation (EO) solutions for the continuous monitoring of solar energy potential and to fulfil the increasing integration of solar farms into the electricity grids, the load exchanges, as well as efficient electricity transmission and distribution. Therefore, through joint solar energy implementation funded projects, the EC's renewable energy policy aims to set up a low carbon environment with relevant services and support by existing and new EO techniques, dealing with accurate, nowcast, short-term (STF) and long-term forecast estimates of solar energy. The pilot is based in a solar energy nowcasting and solar forecasting system called nextSENSE. Major objectives of the pilot are:

• To use, improve and incubate EU-funded (Geo-Cradle) and other (CAMS) available innovation instruments, relative to next-SENSE products.
• To upscale existing techniques in larger domains and serve a large variety of users (decision makers, citizens, national bodies).
• To demonstrate and further deploy the nowcasting and STF solar energy products.
• To use existing CAMS-related products (HelioClim-3v5, McClear) for short-term forecasting in specific regions.
• To engage relative stakeholders: end-users but also to uptake commercialisation and internationalisation-related service industry.
• To showcase through GEOSS-related and developed tools and the renewable energy related benefits, towards a sustainable energy development.

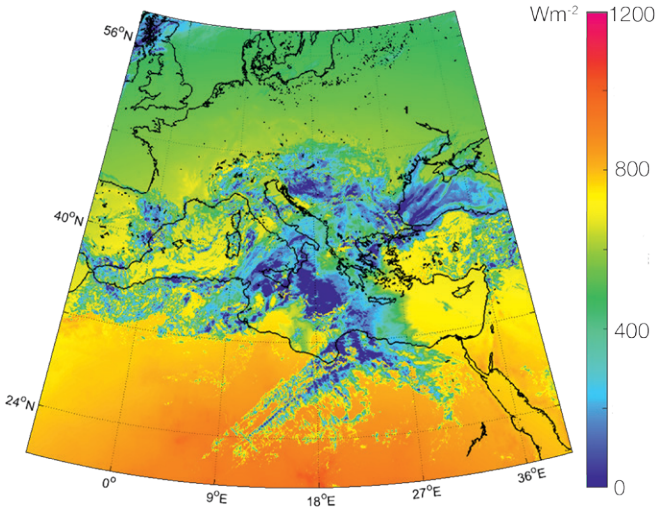

Figure 1. Surface total solar irradiance forecast at 11 UTC on 25 March 2020. Based on the nextSense system.

• To contribute towards GEO vision for co-ordinated EO information to citizens, businesses and science.

NextSense is a system that is going to be developed with the aim of forecasting short-term solar energy at a high spatial and temporal resolution. This real-time service uses and produces large data-sets for 1.5 million pixels (5 x 5 km grids at a pan-European and N. African level)) every 15 minutes based on the Solar Energy Nowcasting SystEm (SENSE) which was designed, developed and applied as a pilot in the framework of the EU-funded project, GEO-CRADLE. NextSENSE will exploit advanced technical capacities of Earth Observation data sources in combination with scientific measurement, radiative transfer and machine learning modelling results. The development of this system includes:

• The development of a cloud forecasting system based on a hybrid method of cloud motion vector and probabilistic methods.

• The validation and use of an aerosol forecasting system based on the Copernicus Atmospheric Monitoring Service data.

• The use of a radiative transfer model in order to calculate solar radiation and energy for horizontal, inclined and direct solar receivers.

• The validation of the system using surface based solar radiation measurements from the existing Baseline Surface Radiation Network.

The main goal of the pilot study is to contribute to the improvement of solar energy forecasting based on the PMOD/WRC expertise in measurements and modelling of solar radiation and aerosols.

The Effect of the Dobson Spectrophotometer Slit Characterisations at the PMOD/WRC on the Ozone Absorption Coefficients

Luca Egli, Herbert Schill, Franz Zeilinger, and Julian Gröbner in collaboration with the Czech Metrology Institute and Meteoswiss

In the framework of the INFO3RS-project, one of the main goals concerning the Dobson measurements for 2019 was to measure the slit functions of each Dobson.

In the framework of the INFO3RS project, one of the main goals concerning the Dobson measurements for 2019 was to measure the slit functions of each Dobson, which allow detailed information about the effective wavelengths that pass the slits to be obtained, and therefore to calculate the exact ozone absorption coefficients for each instrument. This task was conducted with a tuneable radiation source (TuPS) of the Czech Metrology Institute in October 2019 on all three Dobsons at both sites in Davos and Arosa. While the characterisation process of D051 and D101 was successful, it failed on D062: due to the very dark coating of the optical wedge in the region of the A_{long} wavelength (325 nm), it was not possible to get a reliable signal that allowed the slit function of slit 3 to be measured.

Dobson 101 underwent a similar procedure in spring 2016 at the Physikalisch-Technische Bundesanstalt (PTB) in Braunschweig, Germany, and it was of special interest to compare the two characterisations (Figure 1) and its effects on the absorption coefficients for this instrument. The 2016 absorption coefficient for the AD wavelengths pair is clearly higher and even of reversed sign to those of 2019 with respect to the WMO Bass-Paur coefficients which are in worldwide use since 1992. The reason for this difference could be in the mechanical interventions on the optical system of D101 during the Regional Dobson Calibration Campaign (RDCC), held in summer 2018 in Arosa with regional standard D064 from DWD Hohenpeissenberg, Germany, even though the slits themselves were not adjusted during these operations.

Table 1. Relative differences of total ozone values of D101 for the different absorption coefficients vs. the Bass-Paur WMO 1992 values.

D101	Bass-Paur Cross-Section			Bremen Cross-Section		
λ	Bass-Paur nominal	Bass-Paur 2016	Bass-Paur 2019	Bremen nominal	Bremen 2016	Bremen 2019
A	-0.43	2.83	-0.76	-0.72	2.65	-1.01
C	-0.11	1.50	-4.37	-0.88	0.85	-4.95
D	1.50	3.28	-1.22	0.45	-0.94	-4.32
AD	-0.95	2.71	-0.64	-1.03	3.55	-0.17
CD	-1.46	0.00	-7.09	-2.00	2.26	-5.48

In the next step, ozone measurements of the characterised Dobsons were recalculated for the different absorption coefficient sets and compared with the values based on the WMO Bass-Paur absorption coefficients. The D101 figures for the 2019 total ozone measurements are given in Table 1. The detailed analysis of these comparisons and those between the two Dobsons at the PMOD/WRC is still ongoing.

References: Egli L.: 2019, Dobson slit function characterisation. Update from INFO3RS, internal PMOD-WRC presentation, 27 Nov. 2019.

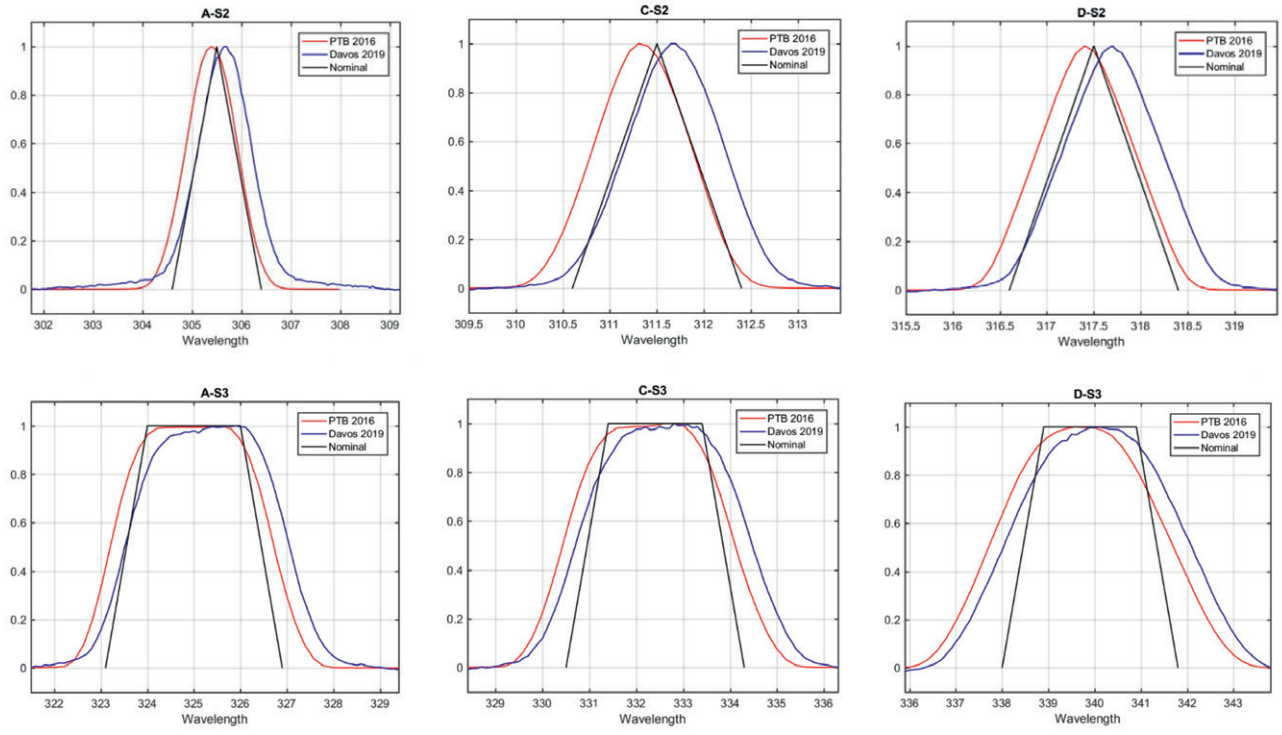

Figure 1. D101 slit geometry for the three wavelength pairs A, C and D: PTB 2016 (red), Davos 2019 (blue), nominal (black).

Publications and Media

Refereed Publications

Arsenovic P., Damiani A., Rozanov E., Funke B., Stenke A., Peter T.: 2019, Reactive nitrogen (NOy) and ozone responses to energetic electron precipitation during Southern Hemisphere winter, Atmospheric Chemistry and Physics, 19, 9485-9494, doi: 10.5194/acp-19-9485-2019

Ball W., Alsing J., Staehelin J., Davis S., Froidevaux L., Peter T.: 2019, Stratospheric ozone trends for 1985-2018: sensitivity to recent large variability, Atmospheric Chemistry and Physics, 19, 12731-12748, doi: 10.5194/acp-19-12731-2019

Ball W., Rozanov E., Alsing J., Marsh D., Tummon F., Mortlock D., Kinnison D., Haigh J.: 2019, The upper stratospheric solar cycle ozone response, Geophysical Research Letters, 46, doi: 10.1029/2018GL081501

Barreto A., Román R., Cuevas E., Pérez-Ramírez D., Berjón A. J., Kouremeti N., Kazadzis S., Gröbner J., Mazzola M., Toledano C., Benavent-Oltrad J. A., Doppler L., Juryšek J., Almansa A. F., Victori S., Maupin F., Guirado-Fuentes C., González R., Vitale V., Goloub P., Blarel L., Alados-Arboledas L., Woolliams E., Taylor S., Antuña J. C., Yela M.: 2019, Evaluation of night-time aerosol measurements and lunar irradiance models in the frame of the first multi-instrument nocturnal intercomparison campaign, Atmospheric Environment, 202, 190-211.

Chrysanthou A., Maycock A., Chipperfield M., Dhomse S., Garny H., Kinnison D., Pitari G., Akiyoshi H., Deushi M., Garcia R., Jöckel P., Kirner O., Visioni D., Plummer D., Revell L., Rozanov E., Stenke A., Tanaka T., Yamashita Y.: 2019, The effect of atmospheric nudging on the stratospheric residual circulation in chemistry–climate models, Atmospheric Chemistry and Physics., 19, 11559-11586, doi:10.5194/acp-19-11559-2019

Coddington O., Lean J., Pilewskie P., Snow M., Richard E., Kopp G., Lindholm C., DeLand M., Marchenko S., Haberreiter M., Baranyi T.: 2019, Solar irradiance variability: Comparisons of models and measurements, Earth and Space Science, 6, 12, 2525-2555, doi.org/10.1029/2019EA000693

Cuevas E., Romero-Campos P. M., Kouremeti N., Kazadzis S., Räisänen P., García R. D., Barreto A., Guirado-Fuentes C., Ramos R., Toledano C., Almansa F., Gröbner J.: 2019, Aerosol optical depth comparison between GAW-PFR and AERONET-Cimel radiometers from long-term (2005-2015) 1 min synchronous measurements, Atmospheric Measurement Technology, 12, 4309-4337, doi.org/10.5194/amt-12-4309-2019

Eichinger R., Pitari G., Dietmüller S., Garny H., Šácha P., Birner T., Bönisch H., Jöckel P., Visioni D., Stenke A., Rozanov E., Revell L., Plummer D., Zeng V., Oman L., Deushi M., Kinnison D., Garcia R., Morgenstern O., Stone K., Schofield R.: 2019, The influence of mixing on the stratospheric age of air changes in the 21st century, Atmospheric Chemistry and Physics, 19, 921-940, doi: 10.5194/acp-19-921-2019

Feinberg A., Sukhodolov T., Luo B.-P., Rozanov E., Winkel L., Peter T., Stenke A.: 2019, Improved tropospheric and stratospheric sulfur cycle in the aerosol–chemistry–climate model SOCOL - AERv2, Geosci. Model Dev., 12, 3863-3887, doi: 10.5194/gmd-12-3863-2019

Gillett Z., Arblaster J., Dittus A., Deushi M., Jöckel P., Kinnison D., Morgenstern O., Plummer D., Revell L., Rozanov E., Schofield R., Stenke A., Stone K., Tilmes S.: 2019, Evaluating the relationship between interannual variations in the Antarctic Ozone Hole and Southern Hemisphere surface climate in chemistry-climate models. J. Climate, 32, 3131-3151, doi:10.1175/JCLI-D-18-0273.1

Golubenko K., Mironova I., Rozanov E.: 2019, Impact of middle range energy electron precipitations on polar winter ozone losses, E3S Web of Conferences, 127, 01005, doi:10.1051/e3sconf/201912701005

Gröbner J., Kouremeti N.: 2019, The Precision solar Spectroradiometer (PSR) for direct solar irradiance measurements, Solar Energy 185, 199-210.

Hinode Review Team, Al-Janabi K., Antolin P., ... Harra L. … et al.: 2019, Achievements of Hinode in the first eleven years, Publications of the Astronomical Society of Japan PASJ, 71, R1.

Karagodin A., Rozanov E., Mareev E., Mironova I., Volodin E., Golubenko K.: 2019, The representation of ionospheric potential in the global chemistry-climate model SOCOL, Science of the Total Environment, 697, 134172, doi: 10.1016/j.scitotenv.2019.134172

Klimenko M., Klimenko V., Bessarab F., Sukhodolov T., Vasiliev P., Karpov I., Korenkov Y., Zakharenkova I., Funke B., Rozanov E.: 2019, Identification of the mechanisms responsible for anomalies in the tropical lower thermosphere/ionosphere caused by the January 2009 sudden stratospheric warming. J. Space Weather Space Clim. 9, A39, 2019, doi:10.1051/swsc/2019037

Klimenko V., Klimenko M., Bessarab F., Sukhodolov T., Koren'kov Yu., Funke B., Rozanov E.: 2019, Global EAGLE Model as a Tool for Studying the Influence of the Atmosphere on the Electric Field in the Equatorial Ionosphere, Russ. J. Phys. Chem. B, 2019, 13, 720. doi:10.1134/S1990793119040079

Klimenko V., Klimenko M., Bessarab F., Sukhodolov T., Rozanov E.: 2019, The dependence of four-peak longitudinal structure of the tropical electric field on the processes in the lower atmosphere and geomagnetic field configuration, Advances in Space Research, doi: 10.1016/j.asr.2019.06.029

Lamy K., Portafaix T., Josse B., Brogniez C., Godin-Beekmann S., Bencherif H., Liley B., Akiyoshi H., Bekki S., Hegglin M., Jöckel P., Kirner O., Archibald A., Marecal V., Morgenstern O., Stenke A., Zeng G., Abraham N., Dhomse S., Butchart N., Chipperfield M., Di Genova G., Deushi M., Michou M., Hu R.-M., Kinnison D., Kotkamp M., McKenzie R., Rozanov E., O'Connor F., Oman L., Pitari G., Plummer D., Pyle J., Saint-Martin D., Sudo K., Tanaka T., Visioni D., Yoshida K.: 2019, Clear-sky ultraviolet radiation modelling using output from the Chemistry Climate Model Initiative, Atmospheric Chemistry and Physics, 19, 10087-10110, doi: 10.5194/acp-19-10087-2019

Macneil A.R., Owen C.J., Baker D., Brooks D., Harra L. K.: 2019, Active region modulation of coronal hole solar wind, Astrophysical Journal, 887, 146.

Marchenko S.V., Woods T., DeLand M.T., Mauceri S., Pilewskie P., Haberreiter M.: 2019, Improved Aura/OMI solar spectral irradiances: Comparisons with independent datasets and model predictions, Earth and Space Science, 6, 12, 2379-2396, doi.org/10.1029/2019EA000624

Mironova I., Artamonov A., Bazilevskaya G., Rozanov E., Kovaltsov G., Makhmutov V., Mishev L., Karagodin A.: 2019, Ionization of the polar atmosphere by energetic electron precipitation retrieved from balloon measurements, Geophysical Research Letters, 46, 990-996, doi:10.1029/2018GL079421

Mironova I., Bazilevskaya G., Kovaltsov G., Artamonov A., Rozanov E., Mishev A., Makhmutov V., Karagodin A., Golubenko K.: 2019, Spectra of high energy electron precipitation and atmospheric ionization rates retrieval from balloon measurements, Science of the Total Environment, 693, 133242, doi:10.1016/j.scitotenv.2019.07.048

Nyeki S., Wacker S., Aebi C., Gröbner J., Martucci G., Vuilleumier L: 2019, Trends in surface radiation and cloud radiative effect at four Swiss sites for the 1996-2015 period, Atmospheric Chemistry and Physics, 19, 13227-13241, doi.org/10.5194/acp-19-13227-2919

Pelouze G., Auchère F., Bocchialini K., Harra L., et al.: 2019, Comprehensive determination of the Hinode/EIS roll angle, Solar Physics, 294, 59.

Schmidtke G., Finsterle W., van Ruymbeke M., Haberreiter M., Schäfer R., Zhu P., Brunner R., 2019, Solar autocalibrating XUV-IR spectrometer system (SOLACER) for the measurement of solar spectral irradiance, Applied Optics, 58, 22, p. 6182, doi: 10.1364/AO.58.006182

Schmutz W., Koenigsberger G.: 2019, Long uninterrupted photometric observations of the Wolf-Rayet star EZ CMa by the Toronto BRITE satellite reveal a very fast apsidal motion, Astronomy & Astrophysics Letters, 624, L3 (5 pp), doi: 10.1051/0004-6361/201935094

Skinner S. L., Schmutz W., Güdel M., Zhekov S.: 2019, High energy processes in Wolf-Rayet stars, Astronomische Nachrichten, 340, 50-53, doi: 10.1002/asna.201913558

Sterling A.C., Harra L.K., Moore R.L., et al.: 2019, A Two-sided loop X-ray solar Coronal jet driven by a minifilament eruption, Astrophysical Journal, 871, 220.

Vasiliev P., Bessarab F., Karpov I., Klimenko V., Klimenko M., Sukhodolov T., Rozanov E.,: 2019, Tidal and planetary waves in the lower thermosphere and ionosphere simulated with the EAGLE model for the January 2009 sudden stratospheric warming conditions, Izvestiya, Atmospheric and Oceanic Physics, 55, 2, 178-187,doi: 10.1134/S0001433819020130

Zhao Y., Saunois M., Bousquet P., Lin Xin, Hegglin M., Canadell J., Jackson R., Hauglustaine D., Szopa S., Stavert A., Abraham N., Archibald A., Bekki S., Deushi M., Jöckel P., Josse B., Kinnison D., Kirner O., Marécal V., O'Connor F., Plummer D., Revell L., Rozanov E., Stenke A., Strode S., Tilmes S., Dlugokencky E., Zheng Bo: 2019, Inter-model comparison of global hydroxyl radical (OH) distributions and their impact on atmospheric methane over the 2000-2016 period, Atmospheric Chemistry and Physics, 19, 13701-13723, 2019, doi:10.5194/cp-19-13701-2019

Non-Refereed Publications

Bessarab F., Sukhodolov T., Klimenko M., Klimenko V, Korenkov Yu., Rozanov E.: 2019, Effects of solar proton events in the thermosphere-ionosphere system in the full-atmosphere model EAGLE, ISARD-2019, St. Petersburg, Russia, June 2019.

Criscuoli S., Rempel M.D., Haberreiter M., Pereira T., Uitenbroek H., Fabbian D.: 2019, On the challenges of synthetizing solar and stellar spectra for irradiance reconstructions, American Astronomical Society Meeting Abstracts, Volume 234, 217.02, https://ui.adsabs.harvard.edu/abs/2019AAS...23421702C/abstract

El-Askary H., Li W., Kazadzis S., Kosmopoulos P.G., Struppa D., Piechota T., Amiridis V., Qurban M., Garay M.J., Kalashnikova O.V., Kontoes C., 2019: Case studies on using Earth observations addressing key environmental challenges along the sustainable development goals, AGU Conference, San Francisco, USA, 9-13 December, 2019.

Feinberg A., Sukhodolov T., Luo B.-P., Peter T., Rozanov E., Winkel L., Stenke A.: 2019, Modelling the role of volcanoes in the stratospheric aerosol layer from Pinatubo to the early 21st century, Geophysical Research Abstracts Vol. 21, EGU2019-16328, 2019 EGU General Assembly.

Finsterle W., Haberreiter M., Remesal A.: 2019, CubeSats for measuring the Earth's energy imbalance, EGU General Assembly Conference Abstracts, 19143, https://ui.adsabs.harvard.edu/abs/2019EGUGA..2119143F/abstract

Gröbner J., Hülsen G., Egli L., 2019: Solar UV radiation metrology: Supporting health and climate research, 17th International Congress on Photobiologoy, European Society for photobiology, Barcelona, 25-30 August 2019.

Haberreiter M.: 2019, Improved EUV dataset for ionospheric response studies, EGU General Assembly Conference Abstracts, 17300, https://ui.adsabs.harvard.edu/abs/2019EGUGA..2117300H/abstract

Karagodin A., Arsenovic P., Rozanov E., Ball W., Remsberg E., Kuchar A.: 2019, H_2O and CO responses to solar irradiance variability in the observations and CCMI models, HEPPA/SOLARIS workshop, Granada, Spain, September 2019.

Karagodin A., Rozanov E., Egorova T., Sukhodolov T., Ball W.: 2019, Elucidating the contribution of the reactive iodine to ozone depletion in the lower stratosphere using chemistry-climate model SOCOLv3, ISARD-2019, St. Petersburg, Russia, June 2019.

Kazadzis S., Kouremeti N., 2019: Aerosol Optical Depth Measurements at the WMO Global Atmospheric Watch - PFR Network Stations, AGU Conference, San Francisco, USA, 9-13 December, 2019.

Klimenko M.V., Klimenko V.V., Bessarab F.S., Vasiliev P.A., Korenkov Y.N., Rozanov E., Sukhodolov T., Funke B.: 2019, Neutral atmosphere influence on ionospheric electric field and electron density variations: results of the EAGLE model, ISARD-2019, St. Petersburg, Russia, June 2019.

Kosmopoulos P.G., Kazadzis S., Kontoes C., Blanc P., El-Askary H., El-Khayat M., Zografos D., 2019: Addressing SDG7 Through the NextSENSE Showcase, AGU Conference, San Francisco, USA, 9-13 December, 2019.

Macneil A., Owen C., Baker D., Harra L., Long D., Wicks R.: 2019, Origins and Properties of Active Region Solar Wind, EGU General Assembly Conference Abstract #9712.

Raptis I.P., Kazadzis S., Pinardi G., 2019: Validation of TROPOMI NO2 Retrievals Using PANDORA Measurements in Athens, Greece, AGU Conference, San Francisco, USA, 9-13 December, 2019.

Rochus P.L., Auchere F., Berghmans D., Harra L., Schmutz W.K., Schühle U.: 2019, The Solar Orbiter EUI instrument: The Extreme Ultraviolet Imager, AGU Fall Meeting Abstract #SH21D-3291.

Rozanov E., Egorova T., Arsenovic P.: 2019, Contribution of natural and anthropogenic factors to ozone layer evolution during early 20th century, ISARD-2019, St. Petersburg, Russia, June 2019.

Rozanov E., Egorova T., Arsenovic P.: 2019, Ozone layer evolution during early 20th century, International Workshop on Chemistry-Climate Interactions, Lanzhou, China, October 2019.

Rozanov E., Egorova T., Arsenovic P.: 2019, Which climate drivers are responsible for the climate warming during early 20th century? EMS Annual Meeting, Copenhagen, Denmark, September 2019.

Rozanov E., Matthes K., Funke B., CMIP6 solar forcing team: 2019, CMIP6 solar forcing recommendations for CCMI-2, The Chemistry Climate Model Initiative (CCMI) Science Workshop, Hong Kong, China, July 2019.

Rozanov E., Sukhodolov T., Egorova T., Karagodin A., Ball W., Chiodo G., Revell L., Stenke A., Zilker F., Peter T.: 2019, Study of the Ozone Layer Evolution in the past and future with ESM SOCOLv4, The Chemistry Climate Model Initiative (CCMI) Science Workshop, Hong Kong, China, July 2019.

Sterling A.C., Harra L.K., Moore R.L., Falconer D.A.: 2019, A two-sided-loop X-ray solar coronal jet and a sudden photospheric magnetic-field change, both driven by a minifilament eruption, AGU Fall Meeting Abstract #SH11D-3382.

Sukhodolov T., Bessarab F., Funke B., Klimenko M., Klimenko V, Korenkov Yu., Kulyamin D., Meraner K., Rozanov E.: 2019, Coupled modelling of the atmosphere/ionosphere system with the whole atmosphere model EAGLE, Geophysical Research Abstracts Vol. 21, EGU2019-16983, 2019 EGU General Assembly.

Sukhodolov T., Feinberg A., Luo B.-P., Peter T., Rozanov E., Winkel L., Stenke A.: 2019, Modelling of the atmospheric sulfur cycle from Pinatubo to the early 21st century, The Chemistry Climate Model Initiative (CCMI) Science Workshop, Hong Kong, China, July 2019.

Veronig A., Podladchikova T., Dissauer K., Temmer M., Seaton D., Long D., Guo J., Vrsnak B., Harra L., Kliem B.: 2019, Genesis, magnetic morphology and impulsive evolution of the coronal mass ejection associated with the X8.2 flare on 2017 September 10, EGU General Assembly Conference Abstract #9243.

Veronig A., Podladchikova T., Dissauer K., Temmer M., Seaton D.B., Long D., Guo J., Vrsnak B., Harra L.K., Kliem B.: 2019, Genesis and impulsive evolution of the fast CME associated with the X8.2 flare on 2017 September 10, AGU Fall Meeting Abstract #SH13A-02.

West M.J., Seaton D.B., Davies J.A., Kintziger C., Rodriguez L. Mierla M., Scolini C., Haberreiter M., D'Huys E.: 2019, EUV observations of the middle corona from the L5 perspective, AGU Fall Meeting Abstracts, SH11C-3396, https://ui.adsabs.harvard.edu/abs/2019AGUFMSH11C3396W

Zilker F., Revell L., Peter T., Rozanov E., Sukhodolov T., Stenke A.: 2019, Towards an improved representation of tropospheric ozone in CCM SOCOLv3.1, The Chemistry Climate Model Initiative (CCMI) Science Workshop, Hong Kong, China, July 2019.

Zubov V., Rozanov E., Egorova T.: 2019, Response of the Earth's atmosphere to a powerful gamma ray burst: modeling study with the chemistry-climate model, ISARD-2019, St. Petersburg, Russia, June 2019.

Publications in Discussion Phase

Ball W., Chiodo G., Abalos M., Alsing J.: 2019, Inconsistencies between chemistry climate model and observed lower stratospheric trends since 1998, Atmos. Chem. Phys. Diss., doi: 10.5194/acp-2019-734

Kuai L., Conley A., Bowman K., Worden H., Miyazaki K., Kulawik S., Conley A., Lamarque J.-F., Paulot F., Paynter D., Oman L., Strode S., Rozanov E., Stenke A., Revell L., Plummer D., Deushi M., Jockel P., Kunze M.: 2019, Attribution of Chemistry-Climate Model Initiative (CCMI) ozone radiative flux bias from satellites, Atmos. Chem. Phys. Diss., doi: 10.5194/acp-2019-231

Nicely J., Duncan B., Hanisco T., Wolfe G., Salawitch R., Deushi M., Haslerud A., Jöckel P., Josse B., Kinnison D., Klekociuk A., Manyin M., Marécal V., Morgenstern O., Murray L., Myhre G., Oman L., Pitari G., Pozzer A., Quaglia I., Revell L., Rozanov E., Stenke A., Stone K., Strahan S., Tilmes S., Tost H., Westervelt D., Zeng G.: 2019, A machine learning examination of hydroxyl radical differences among model simulations for CCMI-1, Atmos. Chem. Phys. Diss., doi: 10.5194/acp-2019-772

Book Chapters

Jull T., Baroni M., Feinberg A., Kovaltsov G., Mekhaldi F., Muscheler R., Poluianov S., Rozanov E., Sukhodolov T., Usoskin I.: 2019, Cosmogenic isotopes as proxies for solar energetic particles. In: "Extreme Solar Particle Storms", Fusa Miyake, Ilya Usoskin and Stepan Poluianov (eds.), 12/2019; ISBN: 978-0-7503-2232-4, doi:10.1088/2514-3433/ab404ach4

Rozanov E., Dyer C., Sukhodolov T., Feinberg A.: 2019, Possible impacts. In: "Extreme Solar Particle Storms", Fusa Miyake, Ilya Usoskin and Stepan Poluianov (eds.), 12/2019; ISBN: 978-0-7503-2232-4, doi:10.1088/2514-3433/ab404ach8

Media in 2019

22 Feb. 2019
Obituary: Claus Fröhlich, 22 Feb. 2019, "Until almost his last day, Claus Fröhlich put his heart and soul into being a researcher",
PMOD/WRC Press Release,
www.pmodwrc.ch/wp-content/uploads/2019/06/PressRelease_20190222_Claus_Froehlich_Obituary.pdf

8 Mar. 2019
Neue Direktorin für das PMOD/WRC in Davos und affiliierte Professorin an der ETH Zürich,
SFI Medienmitteilung,
www.pmodwrc.ch/wp-content/uploads/2019/03/PressRelease_20190308_SFI_Neue-Direktorin_PMODWRC.pdf

26 Mar. 2019
Louise Harra, die neue Direktorin am PMOD/WRC im Gespräch mit der DZ,
Davoser Zeitung,
www.pmodwrc.ch/wp-content/uploads/2019/04/PressArticle_20190326_DZ_Harra.pdf

7 Jun. 2019
Schlüsselübergabe am PMOD/WRC,
Davoser Zeitung,
www.pmodwrc.ch/wp-content/uploads/2019/06/PressArticle_20190607_DZ_Schluesseluebergabe.pdf

6 Jun. 2019
Neue Direktorin am PMOD/WRC,
Südostschweiz Zeitung,
www.pmodwrc.ch/wp-content/uploads/2019/06/PressArticle_20190606_SO_Neue_Direktorin.pdf

21 Jun. 2019
JTSIM-DARA Handover Ceremony,
PMOD/WRC website news,
www.pmodwrc.ch/en/events-media/events-media/jtsim-dara-handover-ceremony/

23 Jun. 2019
"Made in China" schiesst 3,23 kg "Made in Davos" ins Weltall,
Südostschweiz Zeitung,
www.pmodwrc.ch/wp-content/uploads/2019/06/PressArticle_20190623_SO_Made_in_Davos.pdf

10 Oct. 2019
Letter of Intent Signed,
PMOD/WRC website news,
https://www.pmodwrc.ch/en/events-media/events-media/letter-of-intent-signed/

18 Oct. 2019
Der Solar Orbiter verlässt Europa,
Davoser Zeitung,
www.pmodwrc.ch/wp-content/uploads/2020/02/PressArticle_20191018_DZ.pdf

24 Oct. 2019
A step closer to the sun in Davos,
Südostschweiz Zeitung,
www.pmodwrc.ch/wp-content/uploads/2019/10/PressArticle_20191024_SO.pdf

31 Oct. 2019
Let the games begin: 1st Davos Science Olympics
Davoser Zeitung,
www.pmodwrc.ch/wp-content/uploads/2019/11/PressArticle_20191031_DZ.pdf

4 Dec. 2019
Symposium in honour of the retirement of Prof. Werner Schmutz as the PMOD/WRC director,
PMOD/WRC website news,
www.pmodwrc.ch/events-media/events-media/symposium/

Personnel Department

Barbara Bücheler

Inspired and full of enthusiasm, we welcomed the new year 2019. A new era in solar physics began for our institute with Prof. Dr. Louise Harra, our new director, who took over the PMOD/WRC from Prof. Dr. Werner Schmutz on 1 June 2019. Several workshops and successful project completions were held.

As hosts of the INFO3RS meeting on 13 February 2019, our scientists gave lectures on their projects, POLE (start: 1 January 2019), ATMOZ, and OZON, in the ETH workshop. These were supplemented by the ETH with analyses and research results, which generated keen interest on both sides. The ETH guests got a good overview of the current situation and we were able to rate the ideas that had arisen for the mutual use of synergies and the planned cooperation of students and technology, as particularly insightful.

In the course of research and development together with the ETHZ, the joint SOCOL activities were planned and discussed with the 10+ participants on 28 August 2019 during the “SOCOL day” workshop.

The third SCOSTEP workshop took place from 6-7 March 2019 at the PMOD/WRC. The participants came from Swiss universities and research institutes such as the ETHZ, FHNW, FHGR, EMPA, MeteoSwiss, PSI, IRSOL, University of Oxford (UK), the University of Oulu (Finland) and the MPS (Germany), and ensured a lively scientific exchange.

The short visit by three representatives from the Chinese Embassy in Bern on 12 April 2019 to clarify and to process the handover of our JTSIM-DARA instrument was followed by the CIOMP Acceptance Review Meeting from 17 to 21 June 2019, during which all technical requirements were verified. The official handover of instruments to CIOMP took place on 21 June 2019 in the presence of Chinese embassy representatives from Bern. In September, the time had finally come: the space instrument JTSIM-DARA was shipped to China by freight (see article in section on “Instrument Development”.

While the spring meeting of the Supervisory Board was held in Arosa on 13 June 2019, the decision was made to hold the autumn meeting on 1 November 2019 at the PMOD/WRC. After the introduction by our SFI President Dr. Walter Ammann and the Vice Director of MeteoSwiss, Dr. Bertrand Calpini, Prof. Dr. Louise Harra presented the research and strategy focus for the next few years. This gave the workforce the opportunity to ask the Supervisory Board questions about the future.

With a lot of energy and enthusiasm, our employees guided groups of visitors through our Institute and tackled topics such as outer space, climate research, space research, the construction of instruments for satellites, and finally the current state of research and development. In particular, many school classes from Davos visited the PMOD/WRC in 2019.

On 23 August 2019, METAS combined pleasure with work in an ingenious way. Without further ado, they relocated their internal meeting with 20 participants to our premises in Davos and also benefited from a guided tour of our Institute.

During the annual “holiday pass”, organised by the Pro Juventute, we presented the world of technology in a playful way to the youngest school children from several schools in Davos.

In the field of space instruments, we reached another milestone with the LUCI instrument onboard the ESA LAGRANGE mission. At the kick-off meeting on 11 September 2019, all project goals were discussed and planned in detail with participants from ESA, RAL, CSL together with the project management on-site at the PMOD/WRC. The meeting was hailed to have been a success by all.

The foundation stone for the "Science Rally Davos" was laid last year, and the first Davos Science Olympics was held with the PMOD/WRC, SIAF, SLF, WSL, AO and the GRF on 25 October 2019. With the international flair of Davos, the event made for an unforgettable experience. Our thanks go to the organisers, Dr. Wolfgang Finsterle with the support of the NGD board members. We are particularly proud of the winner from our ranks and warmly congratulate, Conrad Schwanitz.

At the symposium in honour of our former director, Prof. Dr. Werner Schmutz, the PMOD/WRC was once again the centre of national interest. The event consisted of lectures, memories and scientific anecdotes about Werner.

Only an extraordinary meeting of the SFI Foundation Council on 5 December 2019 did justice to such a memorable day.

At the end of the year, we and our research partner Davos Instruments successfully completed the Innosuisse project 28550 1 IP-EE, which identifies the cavity for the reference radiometer for measuring solar radiation. In order to give the project the “right” weight, we proudly called it our “InnoPMOD”. We were also able to successfully complete the two projects, GCOS-GAWPFR and 3D-SOLSPEC, in November and December.

The technical interest of our workforce knows no boundaries and so we were again able to contribute to personnel development this year through numerous public seminars.

Ongoing developments with the PMOD/WRC staff enabled us to implement our visions: Ms. Verena Danuser, who oversees the ozone measuring station in Arosa, Mr. Herbert Schill as a scientist and the technical know-how of Mr. Franz Zeilinger as of October 2019, all led to further intensive research in the field of ozone.

We congratulate Dr. William Ball on becoming an Assistant Professor at the University of Delft, The Netherlands. He joined the Faculty of Civil Engineering and Geosciences in March 2020. We wish him all the best and look forward to future collaborations. In addition, after many years as a physicist in the Solar Physics Group, Dr. Nuno Guerreiro was able to expand and strengthen his position at the renowned IRSOL institute as of May 2019 in sunny Ticino.

In April 2019, our former SAMD EFZ graduate, Stefan Hartmann, went abroad for a study leave. After returning to Switzerland, he started his studies in Information & Cyber Security in Lucerne. We wish him every success.

Our two new doctoral students from ETH Zurich, Mr. Arseni Doyennel and Mr. Conrad Schwanitz, both in their first year, continued to contribute to the scientific success of the PMOD/WRC. While Arseni is involved in the POLE project, Conrad is concerned with coronal jets, i.e. the small emissions of plasma in the solar corona. In August, we welcomed three new apprentices to the PMOD/WRC. Dario Tannô started a 4-year sports apprenticeship (hockey), Sotirios Filios a 3-year EFZ-Businessman training and Nic Matthes a 4-year EFZ-Polymechanic training. We are also proud of our commercial high school intern, Andri Schneider, from the SAMD (Swiss Alpine Middle School Davos), who will complete the vocational baccalaureate in 2020 in addition to the EFZ-Businessman training. Dr. Krysztof Barczynski joined us on 1 January 2020 and will strengthen the PMOD/WRC in the field of satellite observations of the sun, the origin of the solar wind, and the analysis of measurement data from the Solar Orbiter mission.

We are grateful for the valuable addition to the Administration department of Ms. Alexandra Sretovic as of 1 January 2019, our former commercial apprentice, who was actively involved in the PMOD/WRC during her studies as an IT specialist. In October 2018, Ricco Soder left for a working pause and rejoined us in April 2019 to take on more responsibility in the science section for calibrations and as head of the quality management system.

After almost 5 years of activity, our project manager, Philipp Kuhn, left us at the end of September. Fortunately, from November 2019, we were able to count on the support of the experienced technology project manager Ms. Valeria Büchel for the L5-LUCI project. At this point, a big thank you to our two temporary employees in the Technology department, Mr. Andri Morandi and Christoph Waupotisch, who helped us for about one and a half months each.

We are particularly pleased about the enrichment of our science team by Dr. Elena Podladchikova as of February 2020 and Dr. Jean-Philippe Montillet as of March 2020. Elena is a solar physicist and works on the Solar Orbiter mission. She will develop software for the advanced solar corona studies of the extreme ultraviolet instruments, EUI and SPICE, onboard the Solar Orbiter, which were developed and built with the participation of the PMOD/WRC. As a TSI instrument scientist, Jean-Philippe is responsible for analysing TSI time-series using machine learning algorithms, which will be used on the VIRGO instrument.

With the inspiration and skill of our dedicated civil servants Lukas Kessler, Julian Koller, Basile Maret, Julian Moosmann, Tishanth Sinnathamby, Sajanth Subramaniam, Pascal Marc Vecsei and Luca Zurmühlen, we managed to implement our mission again this year.

Thanks to the diversity and individuality of our workforce, we continue working together to progress in all our research fields at the PMOD/WRC. Thank you very much.

Scientific Personnel

Prof. Louise Harra	Director (since 01.06.2019), affiliated Prof. at ETH-Zürich; solar physics researcher
Prof. Werner Schmutz	Director (until 31.05.2019); physicist (since 11.07.2019)
Dr. William Ball	Postdoc, Climate Group; physicist (until 31.01.2020)
Dr. Krzysztof Barczynski	Postdoc, Solar Physics Group; physicist (since 01.01.2020)
Dr. Luca Egli	Scientist, WCC-UV and Ozone Sections; physicist
Dr. Tatiana Egorova	Scientist, Climate Group; climate scientist
Dr. Wolfgang Finsterle	Co-Head WRC, Head of WRC-Section Solar Radiometry; physicist
Dr. Julian Gröbner	Co-Head WRC, Head of WRC-Sections IR radiometry, WORCC, WCC-UV and Ozone Section; physicist
Dr. Nuno Guerreiro	Postdoc, Solar Physics Group; physicist (until 30.04.2019)
Dr. Margit Haberreiter	Project manager/scientist Lagrange mission, instrument scientist, CLARA; physicist
Dr. Gregor Hülsen	Scientist, WCC-UV Section; physicist
Dr. Stylianos A. Kazantzis	Scientist, WORCC Section; physicist
Dr. Natalia Kouremeti	Scientist, WORCC Section; physicist
Dr. Jean-Philippe Montillet	Instrument scientist, TSI; geoscientist (since 01.03.2020)
Dr. Stephan Nyeki	Scientist, WRC-IRS Section; physicist
Dr. Elena Podladchikova	Instrument scientist, Solar Orbiter SPICE and EUI (since 01.02.2020)
Herbert Schill	Scientist, Ozone Section; environmental scientist (since 01.01.2019)
Dr. Eugene Rozanov	Scientist, Head of Climate Group; physicist
Dr. Timofei Sukhodolov	Postdoc, Climate Group; climate scientist
Arseni Doyennel	PhD student, 1st year, ETH Zurich (since 01.04.2019)
Alberto Remesal Oliva	PhD student, 4th year, University of Zurich
Conrad Schwanitz	PhD student, 1st year, ETH Zurich (since 01.10.2019)

Technical Personnel

Silvio Koller	Co-Head Technical Department, Project Manager Space, Quality System Deputy
Daniel Pfiffner	Co-Head Technical Department, Project Manager Space
Lloyd Beeler	Electronics Engineer MSc
Valeria Büchel	Project Manager Space (since 01.11.2019)
Christian Fringer	Electronics Apprentice, 2nd year
Matthias Gander	Electronics Engineer BSc
Manfred Gyo	Electronics Engineer MSc
Philipp Kuhn	Project Manager Space (until 30.09.2019)
Patrik Langer	Mechanical Engineer BSc
Nic Matthes	Polymechanical Apprentice, 1st year (since 01.08.2019)
Pascal Schlatter	Mechanical Technician, Head of Workshop, Safety Officer
Yanick Schoch	Electronics Apprentice, 4th year
Marco Senft	IT Systems Administrator
Marcel Spescha	Mechanical Technician
Andri Morandi	Temporary Technician (01.07.2019 - 31.08.2019)
Christoph Waupotitsch	Temporary Technician (28.08.2019 - 31.10.2019)

Technical Personnel within the Science Department

Ricco Soder	Calibration scientist, Quality System manager
Christian Thomann	Technician
Franz Zeilinger	Technician (since 01.10.2019)

Administration

Barbara Bücheler	Head Human Resources / Finances / Administration
Sotirios Filios	Administration, apprentice, 1st year (since 01.08.2019)
Stefan Hartmann	Administration, book-keeping (until 30.04.2019)
Irene Keller	Administration, import/export
Angela Lehner	Administration, book-keeping
Andri Schneider	Administration, intern (Since 01.08.2019)
Alexandra Sretovic	Administration, book-keeping (since 01.01.2019)
Christian Stiffler	Accountant
Dario Tannò	Administration, apprentice, 1st year (since 01.08.2019)

Personnel in Arosa

Verena Danuser	Observer and maintenance ozone measurement station (since 01.01.2019)

Caretaker(s)

Maria Sofia Ferreira Pinto	General caretaker, cleaning
Fatima Da Conceicao Alves D.C.	General caretaker, cleaning (back-up)

Civilian Service Conscripts

Lukas Kessler	01.08.2019 - 31.01.2020
Julian Koller	07.01.2019 - 01.03.2019
Basile Maret	11.11.2019 - 05.02.2020
Julian Moosmann	02.09.2019 - 28.02.2020
Tishanth Sinnathamby	01.07.2019 - 06.09.2019
Sajanth Subramaniam	20.05.2019 - 10.07.2019
Pascal Marc Vecsei	18.03.2019 - 03.07.2019
Luca Zurmühle	03.12.2018 - 25.01.2019

Lecture Courses, Participation in Commissions

Louise Harra	Member of international scientific advisory board of MPS Member of ESA Space Science Advisory Council Co-PI of EUV Imager on Solar Orbiter Co-PI of SPICE instrument on Solar Orbiter Co-I on the NASA IRIS mission Chair of ESA HAUS committee Member of Board of Reviewing Editors for Science Journal Subject editor for Proceedings of the Royal Society A: Mathematical, Physical & Engineering Sciences Chair of ISSI science board Member of ISSI science board Ministerial position on management committee of Armagh Observatory and Planetarium SOC for IRIS 10, China SOC for Hinode 13, Tokyo, Japan
Werner Schmutz	Honorary Member of the International Radiation Commission (IRC, IAMAS) Member of the National Committee on Space Research, SCNAT Member of the Commission for Astronomy, SCNAT
Wolfgang Finsterle	Member of CIMO TT Radiation References Member of EURAMET TC PR Chairman of ISO/TC180 SC1 (Solar Energy, Climate – Measurement and Data) Member of the PROBA-3 Science Working Team
Julian Gröbner	GAW-CH Working group (MeteoSwiss) Member Scientific Advisory Group for UV, WMO GAW Chair of the NEWRAD Scientific committee Chairman of Infrared Working group of Baseline Surface Radiation Network (BSRN) Member IAMAS International Radiation Commission Member of the CIMO Task Group on Radiation References Member International Ozone Commission (IO3C)
Margit Haberreiter	President of the EGU Division on Solar-Terrestrial Sciences (until 04/2019) Member of the EGU Programme Group (until 04/2019) Vice-President of SGAA Member of the Swiss SCOSTEP Committee, Treasurer Swiss Representative of the WMO Inter-programme Team on Space Weather, Information System and Services (IPT-SWeISS) Swiss representative of the UN COPUOS Space Weather Expert Group Member of the IAU Commission E3 "Solar Impact throughout the Heliosphere" Topical Editor Annales Geophysicae

Eugene Rozanov	Co-Leader of SPARC SOLARIS-HEPPA WG3 Member of the Swiss SCOSTEP Committee Co-leader of SCOSTEP PRESTO Pilar 3 project Swiss representative in European COST CA15211, WG3 leader Member of Editorial board of “Atmosphere and Ocean Physics”, Russian Academy of Science Chief Editor of "Frontiers in Earth Science (Atmospheric Science section)" Guest editor of Atmosphere: Special issue "Ozone evolution in the past and future"
Stylianos Kazantzis	Scientific Advisory Group Aerosol (WMO/GAW) Editor of Atmospheric Chemistry and Physics Editor Atmospheric Measurement and Techniques; special issue “SKYNET aerosol network” Swiss delegate to the Management Group of Cost 16202 International Network to Encourage the Use of Monitoring and Forecasting Dust Products Working Group, Leader of WG3 Swiss delegate to the Management Group of Cost CA18235 “PROfiling the atmospheric Boundary layer at European scale” Lecturer, “Fundamentals of remote sensing”, MSc in Space Science Technologies and Application, Univ. of Peloponnese, Greece GAW-CH Working Group (MeteoSwiss) Associate Researcher; National Observatory of Athens, Greece – Institute of Environmental Research and Sustainable Development
Luca Egli	Member IAMAS International Radiation Commission GAW-CH Working Group (MeteoSwiss)

Public Seminars

24.01.2019 Luca Zurmühle
Civilian Conscript
PMOD/WRC

Introduction to quantum computing

28.01.2019 Julian Koller
Civilian Conscript
PMOD/WRC

Behind the notes

25.04.2019 Danuch Phaisathit
Exchange Student
Thailand

A development of a low-cost pyranometer for measuring broadband solar radiation

24.05.2019 Joradol Jansawang
Exchange Student
Thailand

A variation of the field of view for calibrating of pyranometer

06.06.2019 Pascal Vecsei
Civilian Conscript
PMOD/WRC

Neural Network-based classification of crystal symmetries from X-ray powder diffraction patterns

17.06.2019 William Ball
Post-Doc
PMOD/WRC and IAC ETH Zurich

New insights into the recent lower stratospheric ozone decreases

17.06.2019 Yang Zhongdong
Chinese Meteorological Administration, Principal Scientist of FY-3E satellite application

Current Performance and Future Perspective of FY-3 Satellite Instruments

18.07.2019 Prof. Louise Harra
Director
PMOD/WRC

My research interests: solar flares and solar wind formation

28.08.2019 Hisashi Hayakawa
Osaka University
Japan

Reconstruction of the Carrington Event: Sunspot Group, Auroral Oval, and Storm Intensity

23.09.2019 David Morate
Instituto de Astrofisica de Canarias
Spain

The PRIMASS survey

11.10.2019 Arseniy Karagodin-Doyennel
PhD Student
PMOD/WRC

The first six months progress report

11.12.2019 Dr. Markus Suter
Davos Instruments AG
Davos

Davos Instruments & the PMO8

Meetings/Event Organisation

13.02.2019	INFO3RS Meeting
06 - 07.03.2019	3rd Swiss SCOSTEP workshop
12.04.2019	Meeting with representatives from the Chinese Embassy
13.06.2019	PMOD/WRC Supervisory Board, Spring Meeting in Arosa
15.06. - 23.06.2019	Meeting with visitors from CIOMP, China; 8 people
15.06. - 15.07.2019	Meeting with visitors from CIOMP, China; 2 people
21.06.2019	JTSIM-DARA hand-over ceremony with representatives from the Chinese Embassy
23.08.2019	METAS, internal meeting at PMOD/WRC
27.08.2019	SOCOL workshop at PMOD/WRC with IAC ETH Zürich
11.09.2019	ESA Lagrange mission - TM and Fee CCN, Kick-Off meeting
10.10.2019	Draft agenda of JOIM meeting
25.10.2019	1st Davos Science Olympics (PMOD/WRC, SIAF, SLF, WSL, AO, GRF)
01.11.2019	Supervisory Board followed by discussion-round with PMOD/WRC staff
14.11.2019	Extraordinary meeting of the SFI Board of Trustees
04.12.2019	Symposium in honour of the retirement of Prof. Werner Schmutz
05.12.2019	Extraordinary meeting of the SFI Board of Trustees

Karbacher Fonds

A contribution from Mr. Daniel Karbacher (from Küsnacht, ZH) made it again possible to cover expenses of the solar physics research project, 3D-SOLSPEC, dedicated to determine the uncertainty of the solar spectral irradiance obtained with different radiative transfer codes, including PMOD/WRC's COSI code. The benchmarking was conducted using 1D atmospheric structures of sunspots, plage and faculae, as well as 3D MHD simulations of different magnetic field strength. This study was part of an International Team effort of the International Space Science Institute in Berne, Switzerland.

In autumn 2019, we received funds from the Karbacher Fonds until the end of 2020 in the first instance. This covers operational aspects of the space missions that PMOD/WRC are involved in, which include NorSat-1 CLARA, SOHO-Virgo, JTSIM-DARA, Proba-3 DARA and Solar Orbiter EUI and SPICE instruments. We very much look forward to carrying on operations support for operational missions, and look forward to the new missions to the fleet. In addition, some funds were provided for outreach activities based around the space missions.

Bilanz per 2019 (inklusive Drittmittel) mit Vorjahresvergleich

Aktiven	31.12.2019 CHF	31.12.2018 CHF
Flüssige Mittel	1'170'707.10	1’302’099.33
Forderungen	125'049.60	130’608.65
Delkredere	-20'450.00	0.00
Warenvorräte	0.00	75'000.00
Aktive Rechnungsabgrenzungen	549'051.95	443’811.70
Total Aktiven	1'824'358.65	1’951’519.68

Passiven		
Verbindlichkeiten	78'049.25	163’311.65
Kontokorrent Stiftung	202.50	8’104.85
Passive Rechnungsabgrenzung	761'090.38	1’077’424.51
Rückstellungen	885'000.00	700’000.00
Eigenkapital	100'016.52	2’678.67
Total Passiven	1'824'358.65	1’951’519.68

Erfolgsrechnung 2019 (inklusive Drittmittel) mit Vorjahresvergleich

Ertrag	CHF	CHF
Beitrag Bund Betrieb WRC	1'460'000.00	1'460'000.00
Beitrag Bund (BBL), Unterhalt Gebäude	141'784.35	141’141.30
Beitrag Kanton Graubünden WRC	499'282.00	499'282.00
Beitrag Kanton Graubünden für ETH Prof.	140'000.00	0.00
Beitrag Gemeinde Davos	651'168.00	651'168.00
Beitrag Gemeinde Davos, Mieterlass	160'000.00	160'000.00
Dienstleistungsauftrag MeteoSchweiz OZON	265'136.70	0.00
Overhead SNF	30'980.50	47’117.00
Instrumentenverkäufe	225'722.50	165’770.65
Reparaturen und Kalibrationen	217'940.43	214’447.11
Ertrag Dienstleistungen	18'109.75	20’207.84
Übriger Ertrag	18'170.05	31’562.00
Erlösminderungen	-23'188.00	0.00
Finanzertrag	399.60	1.35
Ausserordentlicher Ertrag	1'106.30	27’254.96
Drittmittel	1'619'332.03	2’048’427.19
Total Ertrag	5'425'944.21	5’466’379.40

Aufwand		
Personalaufwand	3'876'687.05	3’813’869.50
Investitionen Observatorium	208'612.91	243’993.03
Investitionen Drittmittel	25'637.70	81’576.35
Unterhalt Gebäude (Beitrag Bund)	141'784.35	141’141.30
Unterhalt	65'030.50	45’021.74
Verbrauchsmaterial Observatorium	31'061.35	32’523.86
Verbrauchsmaterial Drittmittel	172'920.97	403’682.71
Verbrauch Commercial	107'338.95	150’332.60
Reisen, Kurse	110'178.79	129’222.94
Raumaufwand/Energieaufwand	210'153.40	213’775.05
Versicherungen, Verwaltungsaufwand	103'792.99	106’835.69
Finanzaufwand	2'208.14	1’937.00
Übriger Betriebsaufwand	72'499.75	138’940.75
Ausserordentlicher Aufwand	15'699.51	39’916.91
Total Aufwand	5'143'606.36	5’542’769.43
Jahresergebnis vor Auflösung Rückstellungen	**282'337.85**	**-76’390.03**
Auflösung Rückstellungen zur Defizitdeckung	0.00	72’789.75
Bildung Rückstellungen	185'000.00	0.00
Jahresergebnis	**97'337.85**	**-3’600.28**
	5'425'944.21	5’466’379.40

Abbreviations

AERONET	Aerosol Robotic Network, GSFC, USA
AOACCM	Atmosphere-Ocean-Aerosol-Chemistry-Climate Model
AOD	Aerosol Optical Depth
BIPM	Bureau International des Poids et Mesures, Paris, France
BSRN	Baseline Surface Radiation Network of the WCRP
CCM	Chemistry-Climate Model
CIMO	Commission for Instruments and Methods of Observation of WMO, Geneva, Switzerland
CIOMP	Changchun Institute of Optics, Fine Mechanics and Physics
CIPM	Comité International des Poids et Mesures
CLARA	Compact Light-weight Absolute Radiometer (PMOD/WRC experiment onboard the NorSat-1 micro-satellite mission)
CMA	Chinese Meteoroligical Administration
CMC	Calibration and Measurement Capabilities
CME	Coronal Mass Ejections
COSI	Code for Solar Irradiance (solar atmosphere radiation transport code developed at PMOD/WRC)
COST	European Cooperation in Science and Technology
CSAR	Cyrogenic Solar Absolute Radiometer (PMOD/WRC research instrument)
DARA	Digital Absolute Radiometer (PMOD/WRC experiment onboard the ESA PROBA-3 formation flying mission)
EAGLE	Entire Atmosphere Global Model
ECV	Essential Climate Variable
EMRP	European Metrology Research Programme
ESA	European Space Agency
EUI	Extreme Ultraviolet Imager (PMOD/WRC participation in EUI, onboard the Solar Orbiter mission)
EUV	Extreme Ultraviolet region of the light spectrum
FEE	Front-End Electronics
FM	Flight Model
FRC	Filter Radiometer Comparisons, held at PMOD/WRC every 5 years
FS	Flight Spare
FUPSOL	Future and Past Solar Influence on the Climate, SNF Sinergia Project
FY-3E	Chinese weather satellite, Fengyun-3, to be launched in the near future
GAW	Global Atmosphere Watch, a WMO Research Programme
GCM	General Circulation Model
GCR	Galactic Cosmic Rays
IACETH Zurich	Institute for Climate Research of the ETH Zurich, Switzerland
IPC	International Pyrheliometer Comparisons, held at PMOD/WRC every 5 years
IPgC	International Pyrgeometer Comparisons, held at PMOD/WRC every 5 years
IRCCAM	Infrared Cloud Camera (PMOD/WRC research instrument)
IRIS	Infrared Integrating Sphere Radiometer (PMOD/WRC research instrument)
IRS	Infrared Section of the WRC at PMOD/WRC
ISO/IEC	International Organisation for Standardisation/International Electrotechnical Commission
ISO 17025	General requirements for the competence of testing and calibration laboratories
JTSIM-DARA	Joint Total Solar Irradiance Monitor - DARA (experiment onboard the Chinese FY-3E mission)
LUCI	Lagrange EUV Coronal Imager (experiment onboard the ESA LAGRANGE mission)

→

METAS	Federal Office of Metrology, (Eidgenössisches Institut für Metrologie), Bern-Wabern, Switzerland
MITRA	Monitor to Determine the Integrated Transmittance (PMOD/WRC research instrument)
MRA	Mutual Recognition Arrangement
MWR	Microwave Radiometer
NASA	National Aeronautics and Space Administration, Washington DC, USA
NIST	National Institute of Standards and Technology, Gaithersburg, MD, USA
NorSat-1	Norwegian Satellite-1
NPL	National Physical Laboratory, Teddington, UK
NREL	National Renewable Energy Laboratory, Golden, CO, USA
PFR	Precision Filter Radiometer (manufactured by PMOD/WRC)
PMO6-cc	Type of absolute cavity radiometer (previously manufactured by PMOD/WRC)
POLE	Past and Future of the Ozone Layer Evolution
PROBA	ESA Satellite Missions (PROBA-1 to 3)
PRODEX	PROgramme de Développement d'Expériences scientifiques, ESA
PSR	Precision Spectroradiometer (manufactured by PMOD/WRC)
PTB	Physikalisch-Technische Bundesanstalt, Braunschweig and Berlin, Germany
QASUME	Quality Assurance of Spectral Ultraviolet Measurements in Europe
QMS	Quality Management System
SCNAT	Swiss Academy of Sciences
SIAF	Schweiz. Institut für Allergie- und Asthma-Forschung, Davos, Switzerland
SFI	Schweiz. Forschungsinstitut für Hochgebirgsklima und Medizin, Davos, Switzerland
SNSF	Swiss National Science Foundation
SOCOL - MPIOM	Combined GCM and CTM Computer Model developed at PMOD/WRC→
SoHO	Solar and Heliospheric Observatory (ESA/NASA space mission)
Solar Orbiter	SolO; An ESA mission to conduct solar research (PMOD/WRC are participating with the EUI and SPICE instruments)
SPE	Solar Proton Events
SPICE	Spectral Imaging of the Coronal Environment (PMOD/WRC participation in SPICE, onboard the Solar Orbiter mission)
SRS	Solar Radiometry Section of the WRC at PMOD/WRC
SSI	Solar Spectral Irradiance
TEC	Total Electron Content
TSI	Total Solar Irradiance
VHS	Ventilation Heating System (manufactured at PMOD/WRC)
VIRGO	Variability of Solar Irradiance and Gravity Oscillations (PMOD/WRC experiment onboard the SOHO mission)
WCC-UV	World Calibration Center for UV in the WRC of the PMOD/WRC
WDCA	World Data Centre for Aerosols, NILU, Norway
WISG	World Infrared Standard Group of pyrgeometers (maintained by WRC-IRS at PMOD/WRC)
WMO	World Meteorological Organisation, a United Nations Specialised Agency, Geneva, Switzerland
WORCC	World Optical depth Research and Calibration Center of the WRC at PMOD/WRC
WRC	World Radiation Center at PMOD/WRC, composed of the Sections: IRS, SRS, WCC-UV, and WORCC
WRR	World Radiometric Reference
WSG	World Standard Group of pyrheliometers (realises the WRR; maintained by WRC at PMOD/WRC)

Farewell to Werner Schmutz

Symposium on 4 Dec. 2019 at PMOD/WRC in honour of the retirement of Prof. Werner Schmutz (standing left of centre) and the handover of the PMOD/WRC directorship to Prof. Louise Harra (centre).

Many thanks Werner for your 20 years of dedication, support and leadership. We look forward to seeing you at PMOD/WRC whilst you continue working on the DARA project and others in the future!

Annual Report 2019

Editors: Louise Harra and Stephan Nyeki
Layout by Stephan Nyeki
Copy-editing by Stephan Nyeki and Monica Freeman

Publication by PMOD/WRC, Davos, Switzerland
Edition: 600, printed June 2020

Front cover: Liftoff! Atlas V Solar Orbiter. A United Launch Alliance (ULA) Atlas V rocket carrying Solar Orbiter lifts off from Space Launch Complex-41 at 05:03 CET on 10 February 2020. Solar Orbiter is an international cooperative mission between ESA and NASA to conduct solar research. Image Credit: United Launch Alliance.

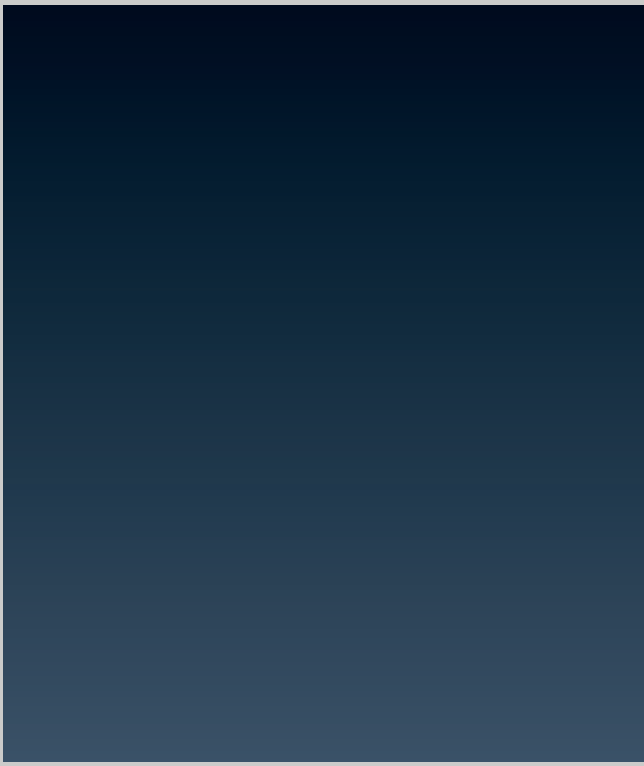

Dorfstrasse 33, 7260 Davos Dorf, Switzerland
Phone +41 81 417 51 11, Fax +41 81 417 51 00
www.pmodwrc.ch